NEUROMOTOR RESPONSE TO WHOLE BODY VIBRATION TRANSMISSIBILITY IN THE HORIZONTAL DIRECTION AND ITS MATHEMATICAL MODEL

By

Vinay Hanumanthareddygari

Submitted to graduate degree program in Mechanical Engineering and the Graduate Faculty of the University of Kansas School of Engineering in partial fulfillment of the requirements for the degree of Master of Science

Committee:

_____

Dr. Sara E. Wilson, Chairperson

_____

Dr. Terry N. Faddis, Committee Member

_____

Dr. Sarah L. Kieweg, Committee Member

Date Defended: _____

The Thesis Committee for Vinay Hanumanthareddygari certifies that this is the approved version of the fallowing thesis:

NEUROMOTOR RESPONSE TO WHOLE BODY VIBRATION TRANSMISSIBILITY IN THE HORIZONTAL DIRECTION AND ITS MATHEMATICAL MODEL

Committee:

_____

Dr. Sara E. Wilson, Chairperson

_____

Dr. Terry N. Faddis, Committee Member

_____

Dr. Sarah L. Kieweg, Committee Member

Date Approved: _____

Contents:

Abstract 1
1. Introduction 4
1.1 Lower Back Pain (LBP): 4
1.2 Risk Factors for Developing Lower Back Injury: 4
1.3 Posture: 5
1.4 Whole Body Vibrations and Lower Back Pain: 6
1.4.1 Whole Body Vibrations: Definition 6
1.5 Overview of Whole Body Vibration Research in General: 7
1.5.1 Vibration-Induced Muscular Fatigue: 8
1.5.2 Vibration-Induced Mechanical Creep: 9
1.5.3 Whole Body Vibration Effects on Proprioception: 10
1.6 Whole Body Vibration transmissibility: 11
1.6.1 Whole Body Vibration Transmissibility in Vertical Direction: 11
1.6.2 Whole Body Vibration Transmissibility in Horizontal Direction: 13
1.7 ISO 2631: 13
1.8 Studies from Human Motion Control Laboratory 14
1.9 Mathematical Modeling: 16
1.9.1 Validation of Models: 18
1.9.2 Need for Biodynamic Models of Whole Body Vibrations: 18
1.9.3 Discussion on Lumped Parameter Models: 20
1.10 Uniqueness about the Current Model: 29
1.11 Specific Aims of This Thesis 30
2. Methods: 31
2.1 Experimental Study: 32
2.1.1Subjects: 32
2.1.2 Vibration Simulator: 32
2.1.3 Equipment Used: 33
2.1.4 Experimental Protocol: 35
2.1.5 Running Average Method: 37
2.1.6 Transmission Functions: 38
Part 2: 40

2.2 Mathematical Model: 40
2.3 Muscle Model: 47
2.4 Input Data for the Models: 62
2.5 Validation of the models: 63
2.6 Parametric Analysis: 64
2.7 Evaluation of error between the model and experimental results: 64
3.0 Results: 66
3.1 Trunk Acceleration Transmissibility Function (TF1): 66
3.2 Vibration Induced Lumbar Rotations (TF 2): 69
3.3 Muscle Activity due to Input acceleration (TF3): 72
3.4 Lumbar Rotations induced Muscle Activity (TF4): 74
3.5 Parametric Analysis: 76
3.6 Evaluation of error between the model and experimental results: 79
3.6.1 Error between model and experimental results in TF1: 79
3.6.2 Error between model and experimental results in TF2: 80
3.6.3 Error between model and experimental results in TF3: 82
3.6.4 Error between model and experimental results in TF4: 83
3.7 Time Delay: 85
3.8 Inter subject variation of transmissibility functions: 88
4. Discussion: 92
4.1 Trunk Acceleration Transmissibility (TF1) 93
4.2 Vibration Induced Lumbar Rotations TF2: 94
4.3 Vibration Induced Muscle Activity TF3: 96
4.4 Muscle Activity due to Lumbar Rotations TF4: 97
4.5 Time Delay: 98
4.6 Limitations and Future Work: 99
4.7 Conclusions: 100
5. References: 101

List of Figures:

Figure 1: This figure illustrates the transmissibility functions to asses WBV transmission 15
Figure 2: Illustration a model approach to a real world problem 16
Figure 3 Coermann's 1962 model 21
Figure 4: Fairley and Griffin 1989 22
Figure 5: Wei and Griffin model 1998 22
Figure 6: Wei and Griffin 2 DOF model 23
Figure 7: Mertens 1978 model 24
Figure 8: Muksain and Nash 1976 25
Figure 9: Matsumoto and Griffin 1998 model 26
Figure 10 Vibration Simulator setup 33
Figure 11: Testing protocol with backrest condition 36
Figure 12: Testing protocol without backrest condition 37
Figure 13: Schematic of Running Average Method 38
Figure 14: Figure demonstrating the different transmissibility functions to assess the whole body vibration transmission 39
Figure 15: Mathematical model developed 40
Figure 16: Hill's 1938 model 48
Figure 17: Force and length response of Hills model for a constant tetanized muscle length 50
Figure 18 Force and length response of Hills model for a step varied tetanized muscle length .. 51
Figure 19: Muscle model based on Hill's model proposed by Winters 52
Figure 20: Muscle model with a single mass to demonstrate the effect of muscle group on the body 53
Figure 21: Mathematical model With the inclusion of Muscle Model. The Muscle Model is assumed to be Erector Spine muscle group. 55
Figure 22: Muscle model with controller and time delay element in feedback loop 62
Figure 23: Trunk acceleration transmissibility plot (Experimental) with and without backrest .. 67
Figure 24: Trunk acceleration transmissibility plot (Experimental) without backrest with K1=65000 N/m 68
Figure 25: Trunk acceleration transmissibility plot (Experimental and model) with and without backrest with K1=65000 N/m 68
Figure 26: Vibration induced lumbar rotations plot (experimental) 69
Figure 27: Vibration induced lumbar rotations plot (experimental and model) 70
Figure 28: Vibration induced lumbar rotations (basic model) using k'= 25KN/m. 71
Figure 29: Vibration induced lumbar rotations model and experimental. Model 1 is the basic model and model 2 is the muscle model incorporated model 72
Figure 30: Muscle activity due to input acceleration (experimental) 73
Figure 31: Vibration induced muscle activity model and experimental with k'=25 KNm/rad 74
Figure 32: Lumbar rotations induced muscle activity (experimental) 75

Figure 33: Lumbar rotations induced muscle activity model and experimental with k'=25KNm/rad 76
Figure 34: Trunk acceleration Transmissibility plot for varying spine stiffness (model) 77
Figure 35: Vibration induced lumbar rotations for varying spine stiffness (k') 77
Figure 36: Vibration induced muscle activity model with varying muscle stiffness 78
Figure 37: lumbar rotation induced muscle activity model with varying muscle stiffness 78
Figure 38: RMS Error for trunk acceleration transmissibility 79
Figure 39: Deviation of experimental values for TF1 80
Figure 40: RMS Error for lumbar rotations due to seat pan acceleration 81
Figure 41: Deviation of experimental values for TF2 81
Figure 42: RMS Error for muscle activity due to seat pan acceleration 82
Figure 43: Deviation of experimental results for TF3 83
Figure 44: RMS Error for muscle activity due to lumbar rotations 84
Figure 45: Deviation of experimental results for TF4 84
Figure 46: Time delay between lumbar rotations and input acceleration 85
Figure 47: Time delay between muscle activity (nEMG) and input acceleration 86
Figure 48: Time delay between lumbar rotations and muscle activity (nEMG) 87
Figure 49: Trunk acceleration transmissibility plot for individual subjects 88
Figure 50: acceleration induced lumbar rotations plot for individual subjects 89
Figure 51: Muscle activity due to input acceleration plot for individual subjects 90
Figure 52: Muscle activity due to lumbar rotations plot for individual subjects 91

Abstract

Recent studies of whole body vibration in seated postures have suggested that the neuromotor system may play a role in the etiology of low back disorders. A number of researchers have modeled whole body vibration transmission to the low back, spine and head. However, no model to our knowledge has examined the transmission of mechanical vibration to muscle shortening/lengthening, the neuromotor system and reflex muscle activation. In addition, only a few studies have examined biodynamic vibration transmission in the fore-aft (anterior-posterior) direction. In this work, transmission of fore-aft vibration to the spine rotation and erector spinae muscle activation was assessed and a model of the motion was created.

Ten healthy young subjects (5 male, 5 female, age 24±3 years, height 1.6 ± 0.04 m, weight 69 ± 4 kg) were assessed. Subjects were screened for low back pain and other neuromuscular disorders. The KU-L Human Subjects Committee approved this study and all subjects gave informed consent. A Ling 1512 electro-dynamic shaker was used to create fore-aft vibration. Data from tri-axial accelerometers on the seatpan and attached to the skin at the T10 spinous process, an electrogoniometer across the lumbar spine, electromyography (EMG) on the erector spinae (ES) muscles at L2/L3 were collected during vibration. EMG data were filtered, rectified, integrated and normalized to a maximum obtained prior to vibration exposure. A running average method was used to analyze and obtain a single ensemble average of the processed data for a vibration period. Responses to fore-aft seatpan vibration (3 Hz to 14 Hz, 1 m/s^2 RMS and 2 m/s^2 RMS) both with and without a backrest were measured. From the ensemble averages, trunk acceleration transmissibility (seatpan acceleration to T10 accelerometer), vibration transmitted to lumbar rotations (seatpan acceleration to electrogoniometer), vibration-

induced muscle activity (seatpan acceleration to ES EMG) and muscle activity relative to lumbar rotation (electrogoniometer to ES EMG) were calculated.

A lumped parameter model was created with two lumped masses representing head-arm-trunk (HAT) and the pelvis-legs connected with linear and rotational dampers and springs. Muscle dynamics were introduced to the model. The parameters for the model were based on weights of the experimental subjects and anthropometric data from literature. Using Lagrangian dynamics, a linearized state-space model was created. This model was used to compare the model to the experimental data. In addition, using Simulink in MATLAB, the vibration experiment was simulated.

The fore-aft trunk acceleration transmissibility declined with increasing frequency consistent with previous research and increased with the presence of a backrest. Transmissibility was found to be greater at 2 m/s^2 RMS compared to 1 m/s^2 RMS. It was observed that the vibration induced lumbar rotations declined with frequency similar to trunk acceleration transmissibility but with little change in the presence of a backrest. Examining the relationship between muscle activity and lumbar rotation, the magnitude of muscle activity was found to be mostly linearly related to the magnitude of lumbar rotation, suggesting that lumbar rotation is eliciting the muscle response. The peak muscle activity was delayed relative to peak trunk acceleration, with delays of 390ms at 3Hz to 43ms at 14Hz, suggesting a transition from voluntary to reflex muscle activation. The model was found to exhibit a similar pattern of fore-aft vibration transmissibility and lumbar rotation as found experimentally. It was also found to exhibit similar patterns of both fore-aft and vertical vibration transmissibility and lumbar rotation as previously reported in the literature.

In this work, transmissibility of fore-aft vibration to the low back was found to be consistent with previous literature. Muscle activity in fore-aft vibration was found to correspond to lumbar rotation with delays that suggest a transition from voluntary to reflex-modulated erector spinae muscle response. A mechanical model of trunk dynamics has been created and found to have similar transmissibility and lumbar rotations as were observed experimentally. A Hill-type model of muscle dynamics was added to the basic model to assess the model behavior relative to the muscle activity. The model results were compared and validated using experimental predictions. Future work will be to include multiple muscle groups into the model and develop a model for vertical vibration.

1. Introduction

1.1 Lower Back Pain (LBP):

One of the most severe and costly problems in public health is the occurrence of lower back pain (LBP) [1-5]. LBP and low back disorders (LBD) are considered as a leading cause of worker disability compensation and a common cause for loss of work hours [6]. In the United States alone, an estimated 80 billion dollars is associated annually with LBP and LBD [7]. The growth rate of LBP is much higher when compared to population growth [8]. 37% of the LBP worldwide is attributed to occupation with a twofold variation across the regions [9]. Chronic LBP is reported as a reason for early retirement in many countries [10]. Studies have shown that LBP affects men more than women because of higher participation in physical labor [9]. Workers compensation claims for the lower back (LBP and LBD) include injury classification ranging from general muscle pain to specific disorders such as strain, sprain, inflammation, rupture and hernia [11]. However, it is not uncommon for the source of pain in the lower back to remain unidentified. LBP and LBD are an increasing burden for the economy and a challenge for engineering and medicine.

1.2 Risk Factors for Developing Lower Back Injury:

Although LBP is the most commonly known disabling musculoskeletal symptom, there is still limited understanding regarding the different risk factors and mechanism of injury. Heavy lifting, lifting loads in awkward postures, repetitive work, prolonged static seating, and repetitive work

in whole body vibration environments, increased lumbar lordosis; pulling-pushing, mechanical stresses, sedentary/irregular lifestyle, obesity, personal habits, and psychological stresses have been identified as risk factors in the etiology of LBP [12-25]. Loading of soft tissues in prolonged static postures (either standing or sitting) is also associated with LBP [26]. Two prevailing theories exist for the mechanism of these injuries. The first is that injury is due to direct overloading of spine tissues (and intervertebral compression). The second suggests that the muscles around soft tissues do not respond quickly or strongly enough to perturbations in spine posture, leading to local dynamic instability [27].

1.3 Posture:

Standing and sitting postures have specific advantages and disadvantages for mobility, energy consumption, exertion of force, coordination and muscle control [26]. In sitting postures, the center of gravity is typically forward of the spine, requiring the muscles in spine to counterbalance it through a short lever arm and resulting in compression of the intervertebral discs [28]. The risk of LBP occurrence is higher in occupations requiring prolonged sitting. Prolonged sitting hours with a little freedom to change the posture may lead to occurrence of LBP and degeneration of the spine [2, 29-31].

1.4 Whole Body Vibrations and Lower Back Pain:

Whole body vibrations has been identified as a major risk factor for LBP and LBD [32]. Professional drivers of buses, trucks and heavy earth moving equipment are subjected to whole body vibration and this vibration has been associated with discomfort and pain in the lower back, spine and neck [2, 21, 30-31]. Literature reviews have concluded that there is a positive relationship between Lower Back Pain (LBP) and Whole Body Vibrations (WBV [26, 33-47]. Spinal damage risk may arise from forces acting on spine. These forces are the direct or indirect products of the vibration which alters dynamic control and motion of the lumbar spine [27, 48-49]. An understanding of mechanical response of the lumbar spine to whole body vibration may yield insight into possible mechanisms of lower back injury.

1.4.1 Whole Body Vibrations: Definition

Vibrations are present in many situations of everyday life. Sources of vibrations can be found in a wide range of transportation devices or working tools. Furthermore, in many sport activities significant vibration load occurs, such as inline-skating, surfing, skiing, horse riding or off-road biking. In day to day activities, the human body is exposed to various whole body vibrations from different sources. Whole body vibrations are defined as vibrations that occur when the subject is in contact with a vibrating surface. The contact can be in sitting, standing or lying postures. WBV refers to "mechanical energy oscillations which are transferred/transmitted to the body as a whole (in contrast to specific body regions such as the hand), usually through a supporting system such as a seat or platform" [50]. Such vibrations can occur in horizontal (fore-aft or anterior-posterior), vertical or lateral (left-right) directions relative to the body. Typical

exposures include: driving automobiles and trucks, piloting helicopters and other aircraft and operating industrial vehicles such as off-road construction vehicles and forklifts. Transmission of WBV to the human body in these various postures and exposures and the methods for evaluation of this transmission are important to assess.

1.5 Overview of Whole Body Vibration Research in General:

Experimental studies have used periodic, single frequency vibrations to investigate the human response to vibration because of the ease in producing such vibration signals [2, 31, 40-41, 48, 51-64]. In practice, on the other hand, vibration exposure in the workplace can be complicated combinations of multi-frequency, multi-directional vibration and impulse-like shocks. Vibrations with random characteristics are very often encountered in day to day vibration environments. It has been reported in the literature that the human body is more sensitive for random or stochastic vibration [31, 40, 46, 51-52, 56, 65-66]. As the vibrations are transmitted to the body, the effects of vibrations are influenced by factors such as body postures, type of seating, magnitude of vibration, and frequency of vibration [41]. Duration of exposure is also an important factor in injury risk [23, 67-68]. A study in the Netherlands by Bongers et al [67] using a retrospective follow up study of crane operators exposed to whole body vibrations, has found that the crane operators with more than five years of exposure to WBVs are almost three times more at risk of disability because of intervertebral disc disorders compared with a control group of fellow workers [68].

In summary, the literature advances the following conclusions based on the epidemiological evidence:

- Occupational exposure to WBV may contribute to an increased risk of injuries and disorders of lower back.
- Whole body vibrations in combination with prolonged seated posture may result in risk of injuries and disorders of lower back.
- Understanding the transmission of vibration to lumbar spine and trunk musculature is necessary to understand the possible mechanism for lower back injury.

While the association between WBV and LBP has been established the exact mechanism of injury is unknown. Suggested mechanisms include muscle fatigue, intervertebral creep and altered proprioception.

1.5.1 Vibration-Induced Muscular Fatigue:

Muscle fatigue has been suggested as one of the possible mechanisms for lower back injury [69-70]. Muscle fatigue and lack of recovery of fatigue are potential forerunners for lower back injury [71-72]. Muscle fatigue alters the dynamic stability of spine, potentially increasing the risk of lower back injury [49, 73-74]. It has been reported that neuronal and muscular components play a part in the mechanism of fatigue in vibration environments [75]. Muscle activity increases significantly with WBV, however the magnitude of increases in muscle activity was found to vary for different muscle groups. Electromyography sensors (EMG) are most commonly used for analyzing muscle fatigue due to Vibrations. Muscle fatigue is characterized by a shift in the power spectrum towards lower frequencies with simultaneous increase in EMG amplitude [27, 40]. Studies have shown an increased muscle activity during

vibration exposure with higher magnitudes than the ones observed during voluntary muscle activity [69, 76-77]. It was also observed that WBV increased motor neuron excitability because of more efficient use of reflex pathways [56, 76, 78]. It was also suggested that WBV provokes shortening and lengthening in muscles which stimulate sensory receptors which can activate alpha motor neurons leading to muscle contractions eliciting the tonic vibration reflex [56, 79-81]. Sensory motor response is therefore a likely contributor to increase in muscle contraction thus to develop muscle fatigue [71].

1.5.2 Vibration-Induced Mechanical Creep:

Creep is the tendency of the material to gradually deform under the influence of stresses. The extent of deformation can be an irreversible plastic phenomenon. Mechanical creep is a function of exposure time, load and magnitude of load. Creep after constant loading is rather extensive in soft muscles. Soft muscles or tissues which possess visco-elastic properties show creep and stress relaxation when subjected to repetitive loading [82-84]. Creep within visco-elastic tissues can cause desensitization of mechanoreceptors [85] and the mechanoreceptors response to CNS reduces greatly as the tissues underwent creep [85-88]. Adams [83] studies have observed a prolonged creep after a long period of driving, greatly reduced stress in anterior annulus and increased peak stress in posterior annulus [82-83]. Visco-elastic properties of the intervertebral disc allows the spine to undergo creep and studies have shown that mechanical response is different in degenerated discs which can be attributed to attenuated ability to absorb shocks[89]. WBV in seated postures increases the loss of height of spine [90] and the majority of this loss is a direct result of mechanical creep of the intervertebral disc [91-93].

1.5.3 Whole Body Vibration Effects on Proprioception:

Proprioception (our own perception) is our body sense or ability to sense stimuli arising within the body. It enables us to monitor the position of our body involuntarily depending on receptors in muscles, tendons and joints. Learning any new motor skill involves training our own proprioceptive sense. Proprioception coordinates the CNS and internal peripheral areas of the body that contribute to postural control, joint stability, and several conscious sensations [94]. Proprioception is also suggested as a possible mechanism for lower back injury [49]. Vibration induced changes in proprioception in the lower back due to exposure to paraspinal muscle vibrations were demonstrated by Brugmagne's studies [95]. Studies have shown that WBV can simulate proprioceptive system leading to increased errors in proprioception [49, 96-97]. Li's[49] investigation showed that the position sense error increased 1.58 fold on exposure to 5 Hz vertical seat pan vibration for 20 minutes. Studies by Roll [98] have suggested that exposure to vibration between frequencies 10 to 120 Hz results in altered proprioception. Li's study also observed that subjects with a history of LBP had a significantly lower proprioceptive keenness compared to a healthy volunteer. Studies have also revealed that proprioception modified during vibration exposure remains for certain time even after vibration is removed [99-100]. The computational model developed by Li to assess the effects of loss in proprioception on dynamic response indicated delays in muscle response which could lead to reduction of trunk stiffness and stability [49].

1.6 Whole Body Vibration transmissibility:

As discussed above WBV transmission normally occurs when a subject is in contact with the source (vibrating surface). These vibrations can occur in horizontal, vertical, lateral directions or their combinations. These vibrations depending on frequency combinations and magnitudes can have effects of lower back, soft muscles and the sensory system. Like every material and structure an engineer might encounter, the human body responds to vibration with its own natural frequency and dynamic response characteristics that depend on the direction of the vibration, posture of the body, and tone of the musculature. Transmissibility is the relationship of output vibration measurements to input vibration measurements and is a common way to assess the body's response to WBV. It can be separated into components including the ratio of the output vibration magnitude at a given frequency to the input vibration magnitude and the phase shift between the output and input vibrations for any given frequency.

1.6.1 Whole Body Vibration Transmissibility in Vertical Direction:

WBV transmissibility is measured as a ratio of accelerations measured on lumbar spine to the input acceleration. Numerous studies were conducted by different researchers to investigate the effect of seatpan trunk acceleration transmissibility in the vertical direction [40-41, 62, 64-65, 101-103] . The studies have consistently shown that the natural frequency in a seated human subject (resonance) exposed to vertical seat pan vibration occurs between 4Hz to 6Hz and a few studies have also observed a secondary resonance between 9Hz to 11 Hz [34, 104-105]. It is suggested that primary resonance in seated posture corresponds to the upper torso moving vertically with respect to the pelvis and the rotational movement of the lumbar spine [106].A

secondary peak can be correlated to flexion-extension motion of the lumbar spine[48]. Resonance is a phenomenon where a system oscillates at greater amplitudes at certain frequencies. Resonance occurs when the frequency at which the system is oscillating matches with the natural frequency of the system. Seating postures or seating conditions are also found to influence the resonance.

Griffin and Matsumoto [103] examined (through experimental studies and mathematical model) the movement of the upper body of the seated subjects exposed to vertical whole body vibrations The motions were measured on body at T1, T5, T10 (thoracic spine 1, 5, and 10), L1, L3, L5 (lumbar spine 1,3 and 5) and pelvis. Correction factor was also added to estimate the motions at the skin. The subjects were exposed to vertical vibration in the frequency range from .5 Hz to 20 Hz at a magnitude of 1 rms (m/s^2). It was observed that the apparent mass of the subjects (ratio of force transmitted at the subject and source (seat) interface and the acceleration measured between subject and source (seat)) showed a principal resonance in the frequency range between 4.75 Hz and 5.75 Hz. The transmissibility of vertical seat pan vibration to the pelvis pitch vibration was found to increase with increase in frequency with a local peak between 5.75Hz and 7.25 Hz. The study also indicated that combination of bending (in the lumbar spine) and rocking motions of spine are involved in principal resonance in apparent mass of a seated subject. Abraham's [107-108] study where subjects were exposed to frequencies for 3Hz to 20 Hz at magnitudes of 1, 1.5 and 2 rms (m/s^2) showed that the trunk seat acceleration transmissibility declined with increase in frequency with a primary peak at 4 Hz and secondary peak at 6Hz. The magnitude of transmissibility was found to be highest at 2 rms (m/s^2) and least at 1 rms (m/s^2). The vibrations transmitted to the lumbar rotations also followed the similar pattern.

1.6.2 Whole Body Vibration Transmissibility in Horizontal Direction:

Many studies have investigated the WBV transmissibility in the vertical direction. However, there are very few or very limited studies on WBV transmissibility in the horizontal direction. In vehicles, the highest loading was found to be in the vertical direction and lowest in the lateral direction. Also, substantial fore-aft (horizontal) vibrations have been recorded in off road vehicles, tractors, trucks [41, 62]. Understanding the behavior of the human body under the influence of fore-aft vibrations is important to optimal design of motor vehicles.

Studies by Demic and Lukic [109], where human subjects were analyzed under the influence of fore-aft vibrations (.3 to 30 Hz) at magnitudes of 1.75 rms (m/s^2) and 2.25 rms (m/s^2), with and without back rest conditions, have concluded that the parameters of resonance points depend on the position of seat backrest position and rms excitation, which is characteristic for non-linear dynamic systems. Paddan and Griffin [44] measured the amount of vibration transmitted to the head with and without the presence of backrest, when the subjects were exposed to random vibrations between 0.2 Hz and 16 Hz at a magnitude of 1.75±.05 rms (m/s^2). The transmissibility curves were shown to decline gradually with increase in frequency. A peak at 2 Hz was observed without the back rest condition. A peak was observed at 1.5 Hz in the presence of a backrest condition and a minor peak was observed at 8 Hz which was attributed to the presence of a back rest. The primary peak is found to vary between .5 Hz and 3 Hz depending on factors like sitting posture, magnitude of vibration, time of exposure etc.

1.7 ISO 2631:

The international organization for standardization (ISO) [41, 110] defines methods for

quantifying WBV in relation to human health and comfort, the likelihood of vibration perception, the incidence of motion sickness. ISO 2631 specifies that the vibration evaluation in work place should include measurements of the root mean square (rms) acceleration. The weighed r.m.s. acceleration or vibration dose is expressed in meters per second (m/s^2) for translational vibration and radians per second (rad/s^2) for rotational vibration [41, 110]. The mathematical representation is

$$WDV = \int_{t=0}^{t=T} a^4(t)dt$$

Where a is the frequency weighed acceleration over a exposure time period t.

To obtain this value acceleration is first weighed by frequency dependent functions that reflect vibration transmissibility. This measure is useful to get a consolidated number that reflects overall vibration exposure but is limited for use in understanding vibration transmission or mechanism of injury. As such, it was not used in this study.

1.8 Studies from Human Motion Control Laboratory

Previous studies in our laboratory have examined this transmissibility of vibration from vertical vibration of the seat pan (measured using an accelerometer) to vertical vibration of the torso (measured using an accelerometer), trunk flexion-extension motions (measured using an electrogoniometer) and muscle activation (measured using electromyography (EMG) [111]). In the current study, this work has been continued by examining this transmission for horizontal vibration.

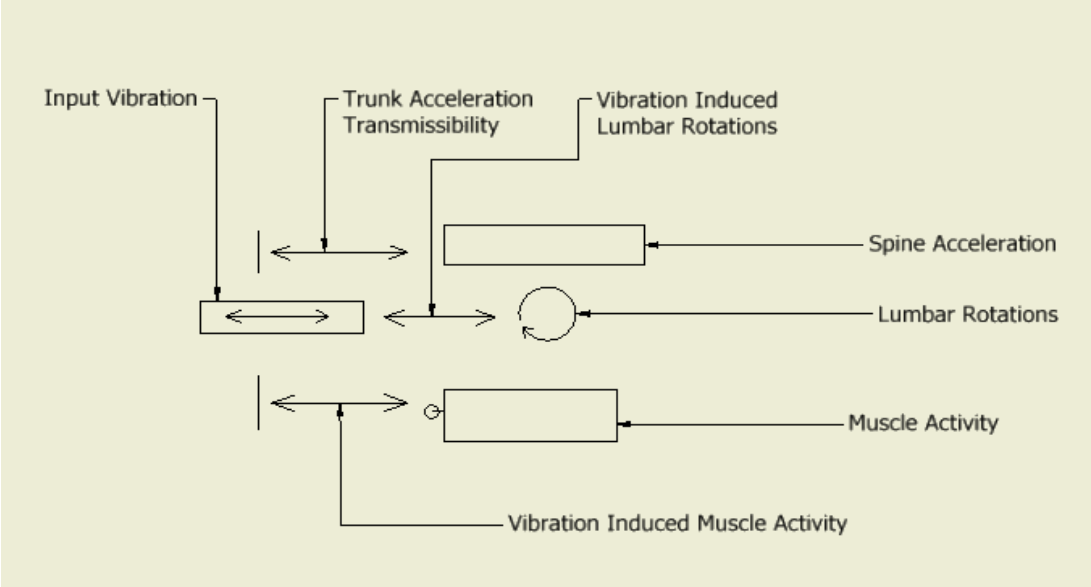

Figure 1: This figure illustrates the transmissibility functions to asses WBV transmission

Figure 1 illustrates the transmissibility functions to assess the whole body vibration transmission. Trunk acceleration transmissibility is the ratio of spine acceleration (measured at the T10 spinous process) to the input seat pan vibration. Vibration induced lumbar rotations is the measure of lumbar rotations relative to input seat pan vibrations. Vibration induced muscle activity is the ratio of muscle activity (generally measured in terms of electrical signal using a electromyography) due to input seat pan vibration. It has been theorized by authors from our laboratory [111] that the seat pan vibration leads to a rocking of the torso (lumbar rotation) that in turn leads to lengthening and shortening of the extensor muscles of the spine such as the erector spinae muscles [111]. To assess this link, mechanoneuromotor transmission has been defined as the muscle activity (measured in terms of electrical signal using an EMG) relative to lumbar rotations. The first aim of this study is to establish the above described transmissibility functions for horizontal seatpan vibration with and without the presence of the back rest.

1.9 Mathematical Modeling:

Mathematical Modeling of a system illustrates the more theoretical and intellectual aspects of the system in practice. In a general way, a model of the system can be defined as a tool that can be used to answer the questions about the system or understand the system without doing experimentation. The aim of the system modeler is to obtain in mathematical form, the description of a system in terms of some physically significant variables. A model can be a simpler or idealized realization of some more complex reality. A well-defined model may well provide improved understanding and, better yet, new information about the real world system (phenomenon). It may be more feasible to investigate the model rather than the more complex reality itself. For many reasons, experiments cannot be carried out under all conditions, but a well defined model of the system can be used to examine these conditions. It can be used to predict how the system would behave under all different conditions. With effective computer power, a numerical experiment called a simulation can be performed on the model. However, it should be noted the simulation results depend completely on the quality of the model [112].

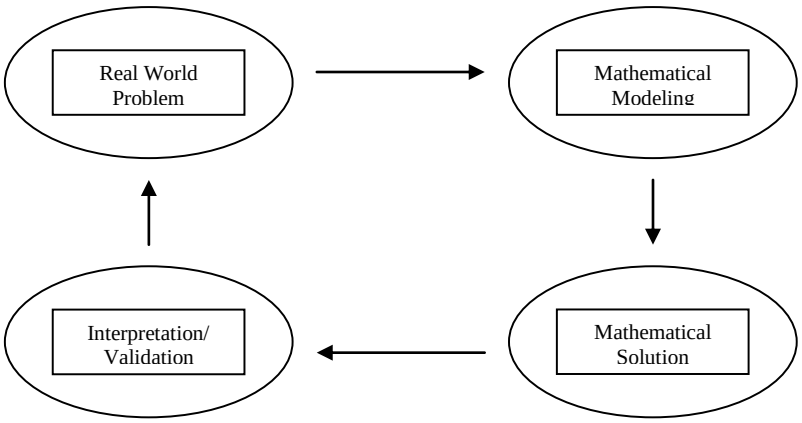

Figure 2: Illustration a model approach to a real world problem

The process of modeling is illustrated in Figure 2 above. The top arrow corresponds to the initial part of the modeling. One has a real world problem, which is replaced by an abstract model for the purpose of employing tools of mathematical analysis. This model typically takes a mathematical formulation involving basic variables and physical relationships corresponding to the a laws of nature or behavior being observed. The right-hand arrow represents the solving of some resulting well-defined mathematical problem. The subsequent solution is usually in a mathematical form and must in turn be reinterpreted back in the original real world setting. The left-hand arrow, the interpretation must be checked against the original reality. It is essential for one to maintain the critical ingredients while filtering out the non-crucial elements in order to arrive at a realistic and still tractable mathematical problem. One must clearly identify the basic variables and characterize the fundamental laws or constraints involved. If this process does not result in the additional knowledge desired, then one may repeat the full cycle over and over again with alternate assumptions and tools. One often must forego excessive details to keep the model manageable [112].

In practice, it is common to proceed around this modeling cycle many times. One repeatedly attempts to refine the model. One also goes back and forth between different aspects of the cycles before arriving at a satisfactory "solution" to the original problem. It is very important that we relate the mathematical solution of the model to the real world problem. Also, it is essential that one must check the model is reasonable or does it agree with previously known aspects of the original problem. Experimental validation will play an important role in authenticating the model [112].

1.9.1 Validation of Models:

At times it is not difficult to build the model. The real difficulty lies in making the model accurate, reliable and reasonable. For the model to be considered reliable, the results and outputs from it should be valid. Comparing the model results with the experimental results could validate this [113-114]. It should be noted that it is rarely possible to match the experimental results with the model results because of many varying parameters (specifically in human body modeling), but models models will have a domain of validity, which defines ability of model to represent the real-world conditions. The better the model limited and well defined is the domain of variability. It should always be noted that observations of the system and experimental properties on the system often are the basis for descriptions of the system, which are handy for modeling but can be influenced by error and inaccuracy in the data.

1.9.2 Need for Biodynamic Models of Whole Body Vibrations:

Experimental studies play a very important role in understanding the effects of WBV's on the human body. However, it is not possible to conduct tests with all varied inputs. A well defined, biodynamic model can come in handy under many conditions. The biodynamic models of the human body in WBV's are developed with the aid of experimental results. Such models are used to predict the forces and movements in the body for a number of purposes [42, 64, 102, 114].

Advantages of developing good biodynamic models:

1. Predict the influence of different variables on biodynamic response of the system
2. Understand the nature of human body moments under different conditions
3. Make predictions which cannot be determined by experiments due to experimental limitations
4. Make predictions without the biological variability inherent in human experimentation
5. Provide a standard convenient protocol for experimentation
6. Determine standard impedance conditions for vibration testing of systems used
7. Give the necessary information for optimization of isolation systems and dynamics of other systems coupled to the system.

Biodynamic models are more than useful in finding the risk zones based on its characteristics. Biodynamic models are categorized based on what they try to predict. The models can be summarized into three categories as mechanistic models, quantitative models and effect models. Mechanistic models are the ones which focus on the mechanisms that govern the movement of body. Quantitative models are the ones which focus on input output relation between the input simulation source and resultant output. Effect models focus on injury risk, discomfort in humans and response to particular input simulation. Each of the categorized models has its own specific advantages. A mechanistic model is represented as group lumped parameters with each lumped mass representing a anatomical section of the body. Groups of lumped parameters represent the apparent transmissibility and apparent mass at more than one location and in more than one orientation. Lumped parameters are discrete masses connected with springs and dampers. More complex finite element models are used as mechanistic models to predict/describe the forces

acting/transmitted through the spine. Quantitative models can be used to characterize the typical apparent masses or mechanical impedances so as to predict the seat transmissibility based on experiments results. Quantitative models, however, do not necessarily have any anatomical representation of the body. Both mechanistic models and quantitative models often adapt lumped parameter method because of advantages to simplify and quantify the complex biodynamic response in terms of relatively small parameters. The number of lumped parameters and the degrees of freedom varies based on purpose and application of the model.

1.9.3 Discussion on Lumped Parameter Models:

A mass-spring-damper system with single-degree-of-freedom is the simplest form to represent the apparent mass of the seated human body and to predict biodynamic responses of seated human subjects. Limitations with this model are because of the models inability to properly simulate the human response due to its limited mass segments. Coermann [105] developed a model, which was constructed with one mass segment of 56.8 kg. Human seat interface is modulated by a set of linear springs and dampers to represent the physical properties of a seated human (see figure 2). Fairley and Griffin [104] constructed a single-degree-of-freedom model to describe the mean apparent mass and phase with feet moving with the seat (figure 3). The mass M1 represented moving body mass relative to platform; mass M2 represented the body mass and legs that did not move relative to platform. Mass M3 represented the effect of a stationary footrest. The model was not developed to accommodate effect of change in muscle tension, contact with backrest or vibration magnitude. Wei and Griffin [115] developed a model similar to Coermann's [105] model with two mass segments attached with a spring-damper (figure 4). In analysis the bottom mass segmen,t considered as legs and buttocks, was assumed connected to

the seat pan. Similar to the 1 DOF model developed earlier [115] Wei and Griffin, they developed a 2 DOF freedom model for better fitting of the experimental results. The excitation input was assumed to be from the bottom mass, which represented buttocks and legs. This model provided better fit for both phase and magnitude. It was observed that to provide optimum models at different vibration magnitudes different vibration parameters would be needed.

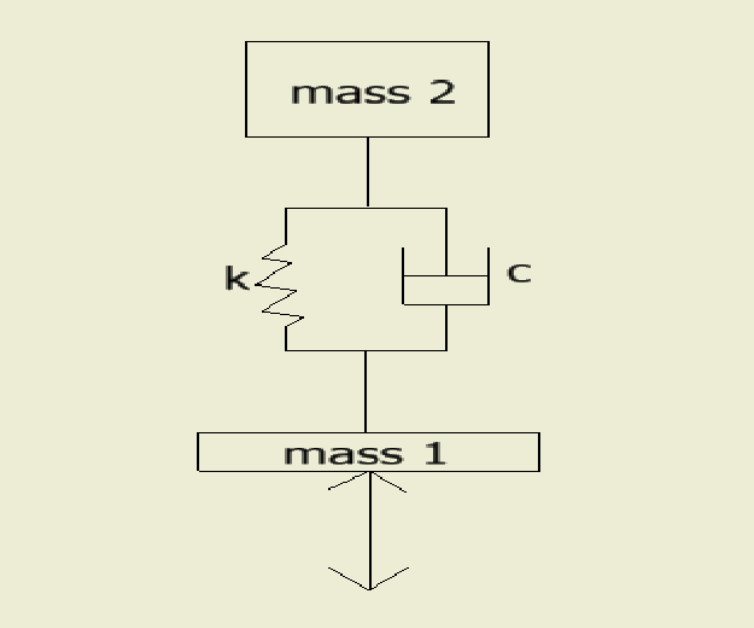

Figure 3 Coermann's 1962 model

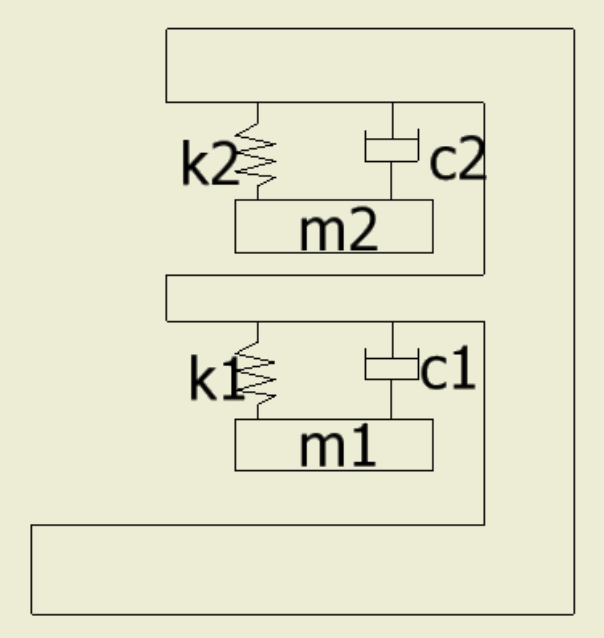

Figure 4: Fairley and Griffin 1989

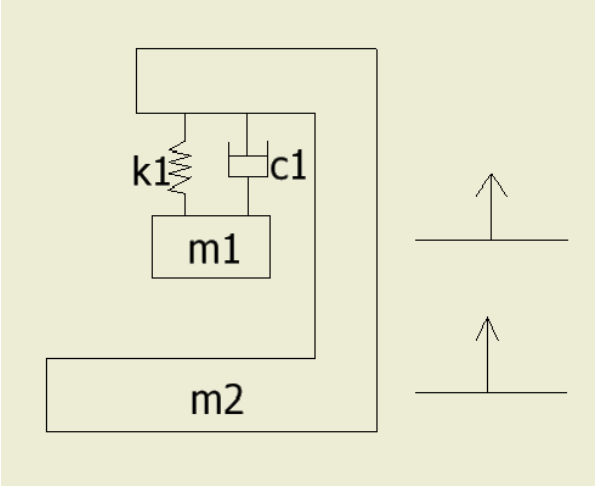

Figure 5: Wei and Griffin model 1998

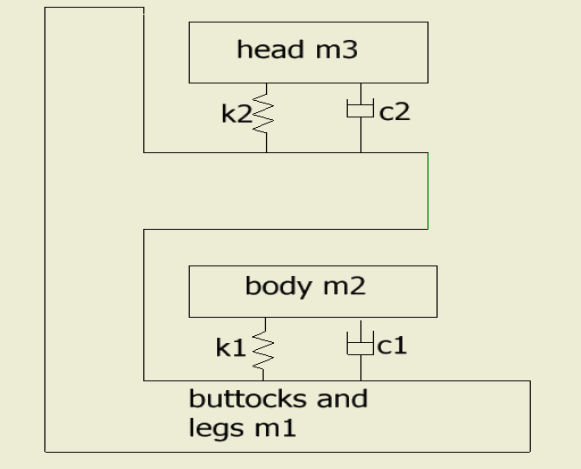

Figure 6: Wei and Griffin 2 DOF model

An Anatomically detailed model was developed by Mertens and Vogt [116] to predict human response to shocks concerning injury risks. A five-degree model with 5 masses connected by 7 sets of spring-dampers represented the models. Legs, buttocks, abdominal components, head and chest were represented in detail in the model. The key factor is the spinal cord which was represented as a set of 3 serial spring-dampers. The segmental masses were determined from experiments and previous literature. Stiffness and damping parameters were determined by comparing the transmissibility and mechanical impedance from experiments. With more detailed anatomical representation, the model considered into account the change in modulus and phase with change in magnitude of vibration. It was absorbed that as the magnitude of vibration increased the first peak shifted to left and later peaks tended to be unclear. These changes implied that nonlinearity with vibration magnitude arises from a combination of different modes of the body.

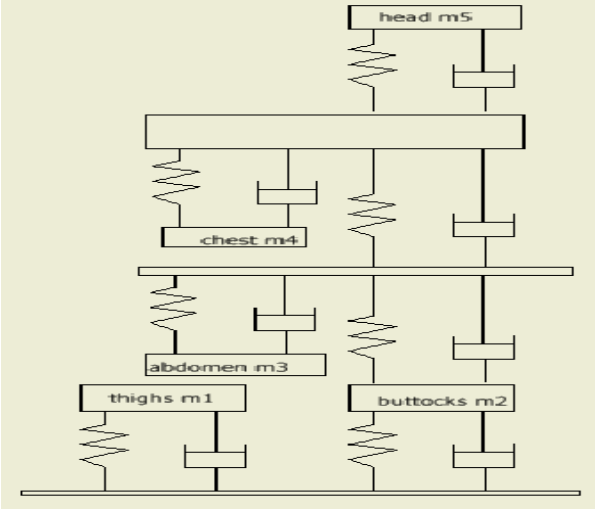

Figure 7: Mertens 1978 model

A six-DOF model with total mass of 80 kg was developed by Muksain and Nash [117], to represent the anatomical description of the human body in sitting posture. The spring and viscous damping forces were considered as due to relative displacements and velocities and their cubic terms, respectively, between two coupled masses except for the neck and back springs and dampers which are linear. Coulomb friction forces were included in the model in addition to the sliding surfaces between back and torso, muscle contraction and ballistocardiographic and diaphragm muscle forces. The motions were restricted to the vertical direction and pelvic stiffness and damping coefficient included in back, the input sinusoidal excitation of seat was effectively taken from the pelvis. The seat-to-head transmissibility is in good agreement with test results.

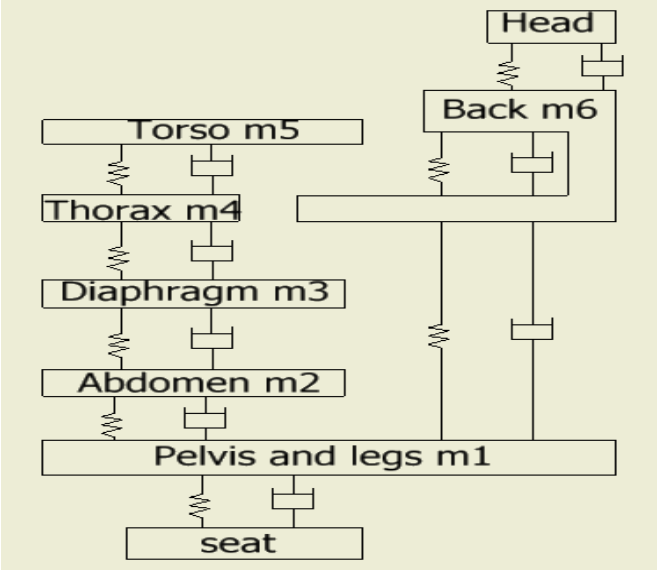

Figure 8: Muksain and Nash 1976

Matsumoto and Griffin[43] developed 2 models of 4 DOF and 5 DOF in order to study the mechanisms involved with point of resonance in apparent mass at around 5 Hz. The models (figure 9) used spring-dampers of transitional and rotational stiffness to represent two-dimensional movement of upper body in mid-sigittal plane. The 4 DOF model consisted of four segmented masses representing legs, pelvis viscera and upper body. 5 DOF model was similar to the 4 DOF model with the upper body divided into 2 masses connected by rotational spring damper pair. The masses and geometrical parameters were determined from literature review. The spring dampers in the model were used to represent buttock tissues, pitching of the pelvis, bending of the spine which was not considered in many previous models. The study suggested that vertical motions due to deformation at the buttocks and viscera made a dominant contribution to the apparent mass resonance, but the contribution of the spinal bending motion was small. This modeling study conforms to the transmissibility measured at a series of locations on the spine column [103] .

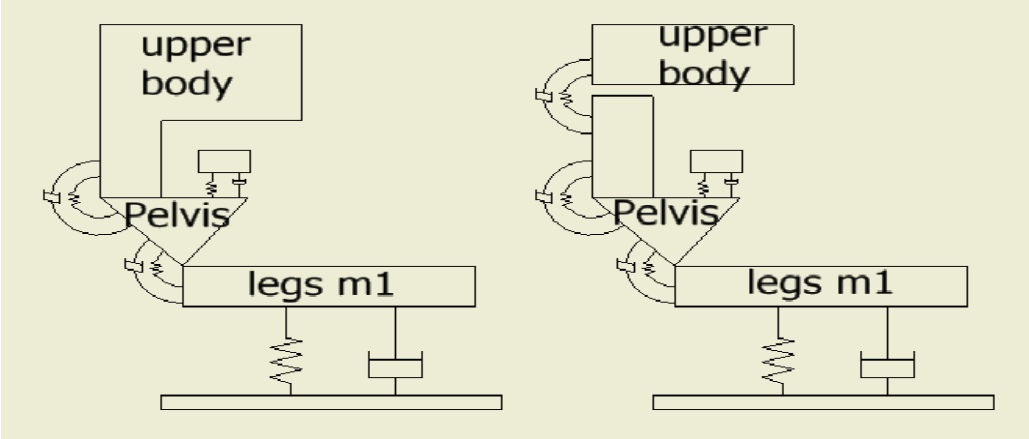

Figure 9: Matsumoto and Griffin 1998 model

Based on the rotational and translational spring damper mechanisms adapted by Matsumoto and Griffin[103], Nawayseh [118] formulated a set of models to represent the vertical and cross axis fore and aft forces at the seat during vertical random excitation. In model 1, masses m1 and m2 represented mass of the lower body carried by seat and the mass of the upper body with inclusion of pelvis respectively. The translational springs-dampers represented the stiffness and damping of the thighs and buttocks. Rotational degree of freedom included in the model reflected on pitching of pelvis and bending of spine. The mass m1 and geometric parameters were based on previous literature and experimental studies. All other parameters were optimized by minimizing the squared error of modulus and phase between the apparent mass and model response. Adding a vertical translational degree of freedom (i.e. Mass 3) to mass 2 (figure) improved the fittings in the phases of both the vertical and the fore-and-aft cross-axis apparent mass. Modifying model 1 to model 3 showed improved fittings in the phase of vertical apparent mass. Combination of model 2 and model 3 (model 4) showed more improved fittings in fore and aft cross axis apparent mass. It was also observed that mass m1 was not needed to produce the resonance

behaviors of (optimizing model 5 from model 4) seated body in both axis. It was also observed that stiffness of the vertical translational spring decreased with the increase in vibration magnitude, implying that the tissues beneath the ischial tuberosities primarily contribute to the nonlinearity, which is consistent with the findings by Matsumoto and Griffin [43] who had concluded that buttocks tensed sitting condition was a factor for nonlinearity.

Nonlinear geometric parameters are added to a model to represent the nonlinear behaviors of the human body. Nonlinear refers to the behavior of the system that does not obey superposition. A linear spring shall maintain a constant stiffness at different ranges of stiffness. But the stiffness of a nonlinear spring is not a direct function of the displacement. Nonlinear dynamic arrangements will also result in nonlinear responses. In such systems, the effective stiffness, damping and masses vary with varied vibration magnitude. The review of models with nonlinear arrangements or components is to identify any possible mechanism that could represent the characteristic nonlinearity. Muskin and Nash [117] used a nonlinear cubic spring and damper between back and torso to represent the ligaments attaching the ribs to vertebrae. Coulomb friction forces were to represent the sliding surfaces between back and torso. The 'ballistocardiographic' muscle forces were modeled as a frequency dependent function acting on the thorax. The model was calibrated to produce the transmissibilities to the head, back, torso, thorax, diaphragm, and abdomen during vertical sinusoidal vibration. It was observed that the fittings for 1Hz to 7 Hz were better than the 7 to 30Hz ones. The authors neither established nor quantified a relationship between nonlinear behaviors and transmissibilities. Muskin and Nash[119] modified the previously developed model with dual transmission path from the pelvis to the head. The model incorporated linear damping and stiffness parameters at frequencies

smaller than 10Hz. nonlinear parabolic damping was used in between pelvis and the body at frequencies larger than 10Hz. Based on the findings that a passive linear model could not represent the response of human body at a full range of frequencies (1 to 30 Hz), frequency dependent active components should be included in the biodynamic models.

Based on their studies, Fairley and Griffin [104] explained that the reason for nonlinearity may be the combination of muscle activity or the dynamic properties of human skeletal structure. They also reported that greater the movement with high magnitudes of vibration, the stiffness of musko-skeletal structure reduces. Mansfield and Griffin [64] observed a nonlinearity along a transmission path common to the spine and the abdomen. The nonlinearity was suggested to be caused by a combination of many factors including softening response of the buttocks tissue, bending or buckling response of the spine, inconsistency in muscular forces at different magnitude of vibration. The findings also contradicted their previous observations that geometric nonlinearity was not a primary factor for nonlinearity[120]. It was concluded that the nonlinearity was not solely caused by the nonlinear geometric arrangements of the body. Softening characteristics on the passive soft tissues and voluntary or involuntary muscle activity could primarily contribute to the nonlinearity [43]. Matsumoto and Griffin [43] also observed a slightly reduced degree of nonlinearity with increases muscle tension in buttocks and abdomen when exposed to broad random vertical vibration. The increased muscle tension was expected to reduce involuntary changes in tension during vibration exposure. This suggested that involuntary changes in muscle activity could alter nonlinearity. It was also observed that an increase in muscle tension at buttocks showed slightly less nonlinearity during sinusoidal vibration exposures, suggesting the dynamics of buttocks tissues contributed to nonlinearity. Nawayseh

and Griffin [118] observed that minimum thigh contact posture gave less degrees of nonlinearity than the maximum thigh contact and the feet hanging postures at the two highest magnitudes. Varying the thigh contact area controlled the pressure of the tissues beneath the ischial tuberosities. Changing the pressure in the buttocks did not affect the nonlinearity in the cross-axis apparent mass resonance frequency, consistent with the findings of Matsumoto and Griffin [43, 103]. Based on Matsumoto and Griffin's [43, 103] studies nonlinearity could originate in the transmission path common to the spine and the knee. It was suggested that the dynamics of the tissues beneath the foot and dynamics of the lower legs might have contributed to the nonlinearity found at the spine and the knee. From the literature reviewed above, it can be observed that the explanations for nonlinearity may be voluntary or involuntary muscle activity and softening characteristic of the passive soft tissues. While these findings are important they predominantly represent vertical vibration response and do not consider neuromotor response.

1.10 Uniqueness about the Current Model:

Not many models have been developed to investigate biodynamic vibration transmission in the horizontal direction. No model has investigated muscle lengthening shortening, neuromotor transmission and reflex muscle activation with the help of a mathematical model. Muscle fatigue and neuromuscular dynamics are expected to be dependent on transmission of vibration to lumbar rotations. Due to limitations in existing biomechanical models of spinal loading, it has been difficult to predict the health effects to the spine associated with exposure to WBV. Therefore there is a need to investigate vibration transmission to the spine and in particular to lumbar rotations. This can help us understand the possible mechanism for lower back injury.

1.11 Specific Aims of This Thesis

- Define and experimentally measure the transmissibility functions (TF1-TF4) for horizontal seat pan vibration with and without the presence of the back rest.
- Assess transmission of fore-aft vibration to the spine rotation and erector spinae muscle activation.
- Create a mathematical model of trunk motion, including flexion and extension in response to seatpan vibration.
- Incorporate the muscle and reflex dynamics into the trunk motion in order to examine transmissibility of vibration to neuromotor system.
- Study the relation between muscle activity and lumbar rotations in vibration environments.
- Use the experimental data to validate the models of trunk motion and muscle activation.

2. Methods:

In this chapter, the methods used to develop trunk transmissibility model and experimental setup are described. These methods consist of several parts:

1. Collection of experimental data on vibration transmission in fore-aft direction
    - Description of the equipment used
    - Experimental setup and protocol
    - Data processing procedures
    - Transmissibility functions
2. Development of a mathematical model
    - Development of the basic model
    - Muscle model
    - Incorporation of the muscle model into basic model
    - Selection of parameters for the models
3. Validation of the model and parametric study
4. Evaluation of error between the experimental values and model predicted values.

Part 1:

2.1 Experimental Study:

2.1.1Subjects:

Ten healthy young subjects (5 male, 5 female, age 24±3 years, height 1.6 ± 0.04 m, weight 69 ± 4 kg) were assessed. Subjects were screened for low back pain and other neuromuscular disorders. The KU-L Human Subjects Committee approved this study and all subjects gave informed consent.

2.1.2 Vibration Simulator:

The Ling Electronics model 1512 electrodynamic shaker (Ling Dynamic Systems, Royston, Hertfordshire, UK) that can operate in the horizontal axis as well as the vertical axis was used to simulate vibrations. The shaker operates in the frequency range of 3 Hz to 2000 Hz from either a sine wave or random noise source. The shaker was powered by 5 kVA Ling Electronics DMA 2/X solid state power amplifier. The control for the shaker was provided by DAKTRON shaker control system (Daktron Electronics, East Boldon, Tyne & Wear, UK). The subjects were assessed for their response to frequencies ranging from 3 Hz to 14 Hz at magnitudes of 1 RMS (m/s^2) and 2 RMS (m/s^2).

A firm wooden seat was installed on the shaker as illustrated in **Figure *10***. The seat had a wooden backrest to provide trunk support for the subjects. Each frequency and magnitude at which the subjects were assessed was specified on DAKTRON control software. The vibration profile was set for constant acceleration sine vibration test. All data was collected at 1500 Hz on

a 16 channel analog to digital board using with data acquisition software (LabVIEW, National Instruments, Austin, TX).

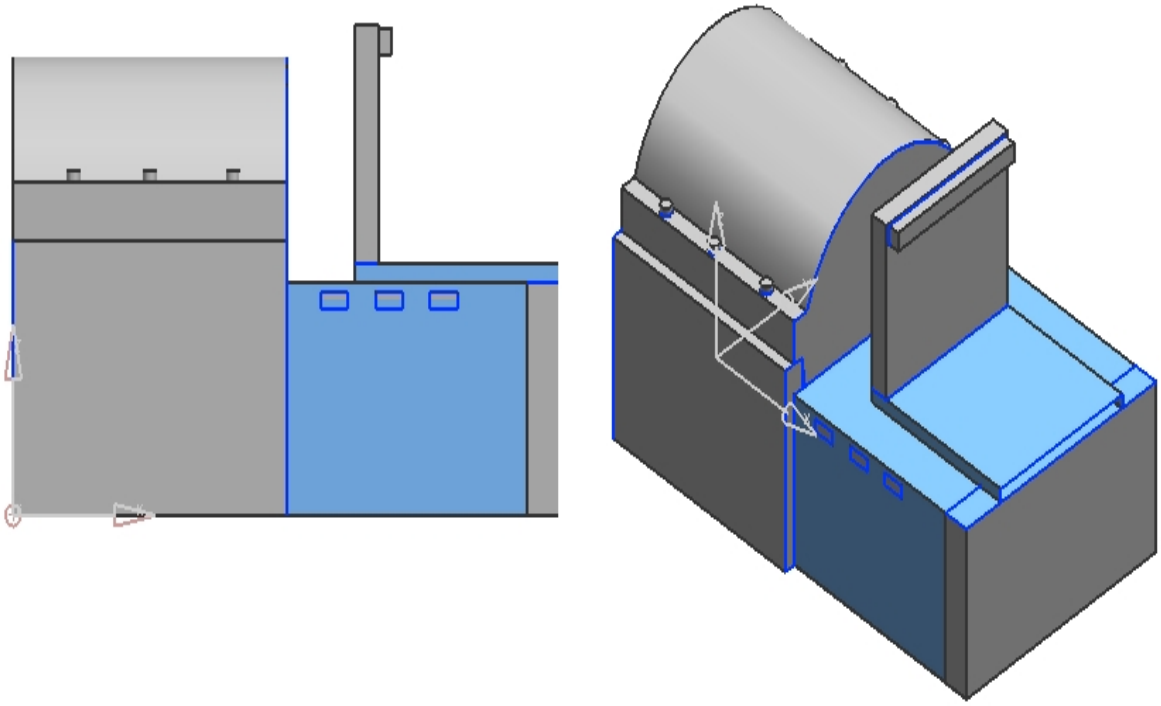

Figure 10 Vibration Simulator setup

2.1.3 Equipment Used:

Two piezoelectric-axial accelerometers 356A17 (PCB Electronics, Buffalo, NY) were used to measure acceleration at seat pan and torso. The accelerometer mounted on the seat pan was used to record the input vibration. The second accelerometer was mounted on the skin at thoracic 10 spinous or the T-10. All the data was collected at a frequency of 1500 Hz using the motion monitor software interface. The output from the accelerometers was in millivolts which were converted to the units of gravity g ($9.8\,ms^{-2}$) using the factory specified calibration tables. Noise

in the accelerometer data was removed using notch filters at multiples of 60 Hz and a low pass filter at 240 Hz.

	X-axis	Y-axis	Z-axis
Accelerometer 1 Sensitivity $\left[mV/ms^{-2} \right]$	496	491	508
Accelerometer 2 Sensitivity $\left[mV/ms^{-2} \right]$	517	524	505

Table 1: Table specifying the calibration specifications for the accelerometers as specified by manufacturer

The flexion and extension movements of the back were measured using a SG 150B twin axis electrogoniometer (Biometrics, Cwmfelinfach, Gwent, United Kingdom). The electrogoniometer was attached to the skin with double-sided tape at T-12 and s1 spinous processes. The subjects were instructed to maintain a constant seating posture throughout the experimental run using visual feedback from ADU301 angle display unit of the electrogoniometer. The output of the electrogoniometer was an electrical signal in voltage which was converted to degrees using the corresponding calibration specifications. The raw electrogoniometer data was also filtered using a notch filter at 60Hz and a low pass filter at 240 Hz[121].

Non-invasive surface electromyography (EMG) sensors were used to record the muscle activity (Delesys, Boston, MA). The placement of EMG sensors were based on the protocol established bt Mikra (Mikra 1991)[122] .Eight bipolar surface electromyographic electrodes were attached to the skin at left side and right side of erector spinae (electrodes were placed at the L2/L3 level

of the spine with a spacing of about 4 centimeters between the electrodes), rectus abdominus (electrodes were places 1 to 2 centimeters superior to umbilicus with a spacing of about 4 centimeters between the electrodes), external obliques (electrodes were placed lateral to the umbilicus at an orientation of 45 degrees to the spine, with a spacing of about 8 to 10 centimeters between the electrodes) and internal obliques.(electrodes were placed 8 to10 centimeters apart lateral to the midline within the lumbar triangle at a 45° orientation to the spine)[122]. The EMG data was recorded at a sampling frequency of 1500 Hz. The EMG data was amplified with a gain of 1000 prior to acquisition. The useable energy of the EMG signals is between 0 Hz to 500 Hz and is most dominant in the range of 50 Hz and 150 Hz [107]. To eliminate the noise and other disturbance from the raw EMG data notch filters were set up at multiples of 60 Hz. Forward and inverse butterworth filters were used to band pass filter the EMG data between 30 Hz and 250 Hz. The EMG data was further demeaned, rectified and integrated using a 100 point Hanning window. The EMG data was normalized to the maximum value obtained prior to the vibration exposure. This was done to minimize the inter-subject variability. The EMG data was normalized with respect to maximal activity exhibited by the subjects corresponding to each muscle group.

2.1.4 Experimental Protocol:

The subjects were made to sit on an unpadded wooden seat mounted on the shaker with EMG electrodes, electrogoniometer and accelerometer attached as described above. Once the subject assumed a comfortable sitting posture, the angle display unit in of the electrogoniometer in the hands of the subject was zeroed. The subjects were asked to maintain the same (zeroed) posture

for the entire experimental procedure (feedback to maintain the same posture was through the angle display unit of the electrogoniometer.

The subjects were tested under two seating conditions, with backrest and without backrest. During with the backrest condition the subjects were asked to rest their thoracic back against the wooden backrest provided to the seat. During the without backrest condition subjects were seated with their trunk not touching any backrest. The subjects were instructed to maintain constant seating posture with the help of feedback from angle display unit of the electrogoniometer during the assessment with and without backrest condition.

The subjects were exposed to vibrations at frequencies of 3, 4, 5, 6, 8, 10, 11, 12 and 14 Hz and at the magnitudes of 1 RMS (ms^{-2}) and 2 RMS (ms^{-2}). The sampling frequency was set to 1500 Hz and the testing period at each trial was 40 seconds. (9 different frequencies at 2 magnitude levels and 2 seating conditions totaled to 36 trails). A rest time of about 2 minutes was given between different seating conditions to avoid fatigue in subjects. The subjects were instructed to resume their prior seating posture after every interval.

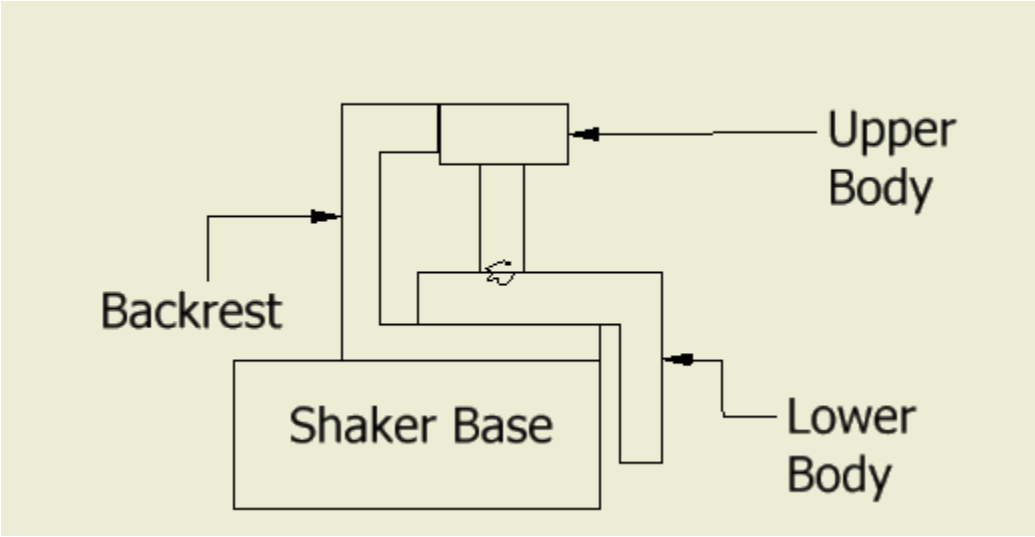

Figure 11: Testing protocol with backrest condition

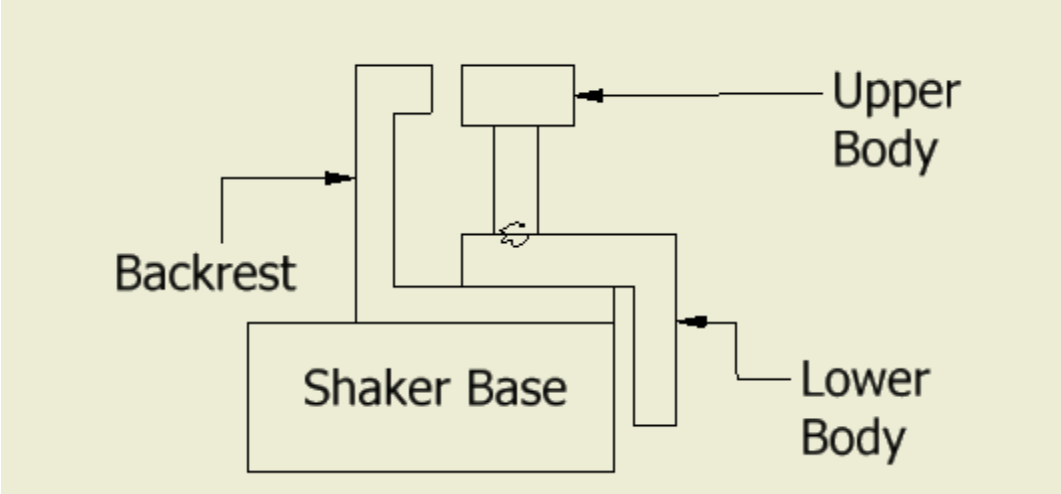

Figure 12: Testing protocol without backrest condition

2.1.5 Running Average Method:

A running average method was used to obtain a single ensemble average of the processed data signals (seatpan acceleration, spine acceleration, electrogoniometer and electromyography data) for a vibration period. The phase losses were avoided by averaging the input and output data at the same time point during each seatpan acceleration sinusoid. The maximum point in the first cycle was set as the start point and the length of the cycle was based on sampling frequency and the vibration test frequency. (Ex: Data was collected by exposing the subject to a frequency of 3 Hz for a period of 40 seconds at a sampling rate of 1500 Hz. The starting point here was the maximum in the first cycle of the seatpan acceleration data and the length of the cycle was $\frac{1500}{3} = 500$ points. Data was separated into 500 point segments starting from the maximum point in the first cycle of seatpan acceleration). Ensemble average was the mean signal for one cycle of a sinusoid of input data. Once the ensemble averages were obtained the magnitude of the signal based on ensemble average were calculated which was the difference between the

crest and trough of the ensemble signal. The magnitudes of the transfer functions were calculated as the ratio of the magnitude of the ensemble average output signal to input signal. It was also observed that there was a delay in occurrence of the peak in output and input signals. This delay corresponded to the time delay between the input and output signal.

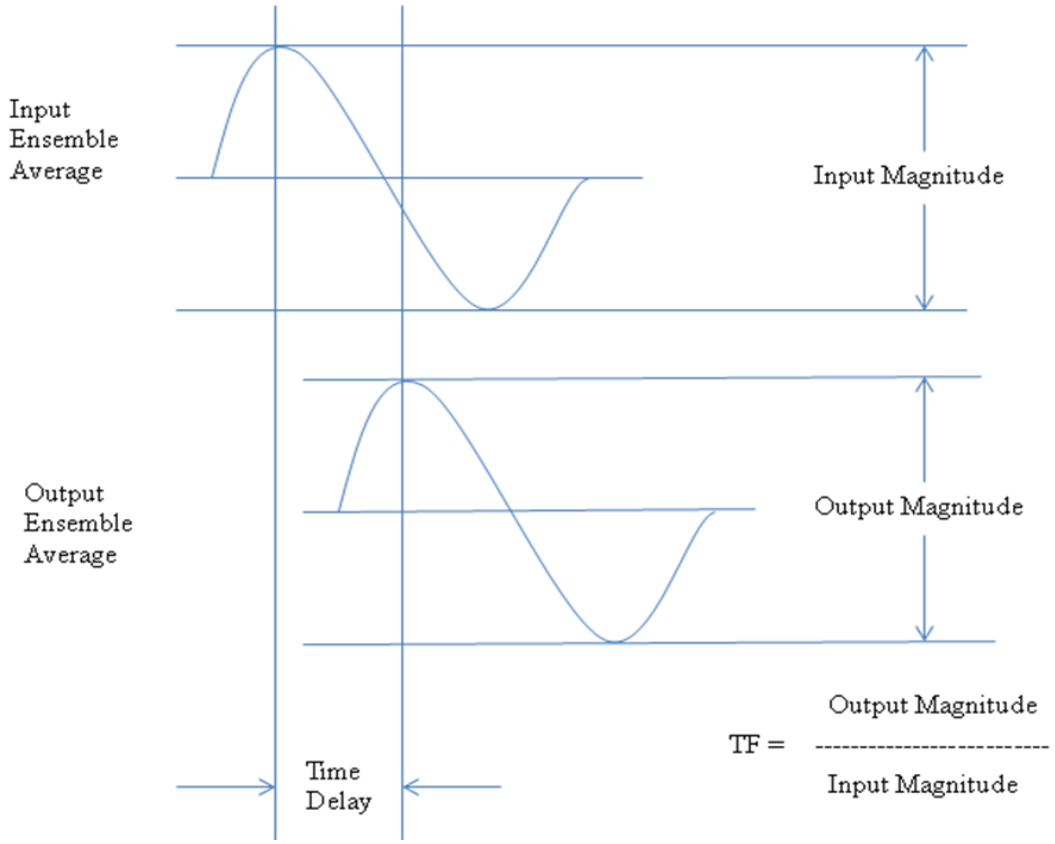

Figure 13: Schematic of Running Average Method

2.1.6 Transmission Functions:

Four transmission functions were determined using the data from the seat pan accelerometer, the spine accelerometer, the electrogoniometer and the EMG electrodes to assess the WBV transmissibility in seated humans subjected to horizontal vibrations. The transmission of

acceleration from seat pan to spine (TF_1) was quantified as ratio (in magnitude) of acceleration measured at spine to acceleration measured at seat pan. The transmission of horizontal vibration to lumbar rotation (TF_2) was quantified as the ratio (in magnitude) between the lumbar rotations and seat pan acceleration. The vibration induced muscle activity (TF_3) was the ration of normalized EMG to seat pan vibrations. The muscle activity relative to lumbar rotations or the mechano neuromotor transmission (TF_4) was the ratio of normalized EMG to lumbar rotations.

$$TF_1 = \frac{acceleration_{spine}}{acceleration_{seatpan}} \quad \textbf{Equation 1}$$

$$TF_2 = \frac{lumbarrotation}{acceleration_{seatpan}} \quad \textbf{Equation 2}$$

$$TF_3 = \frac{nEMG}{acceleration_{seatpan}} \quad \textbf{Equation 3}$$

$$TF_4 = \frac{nEMG}{lumbarrotation} \quad \textbf{Equation 4}$$

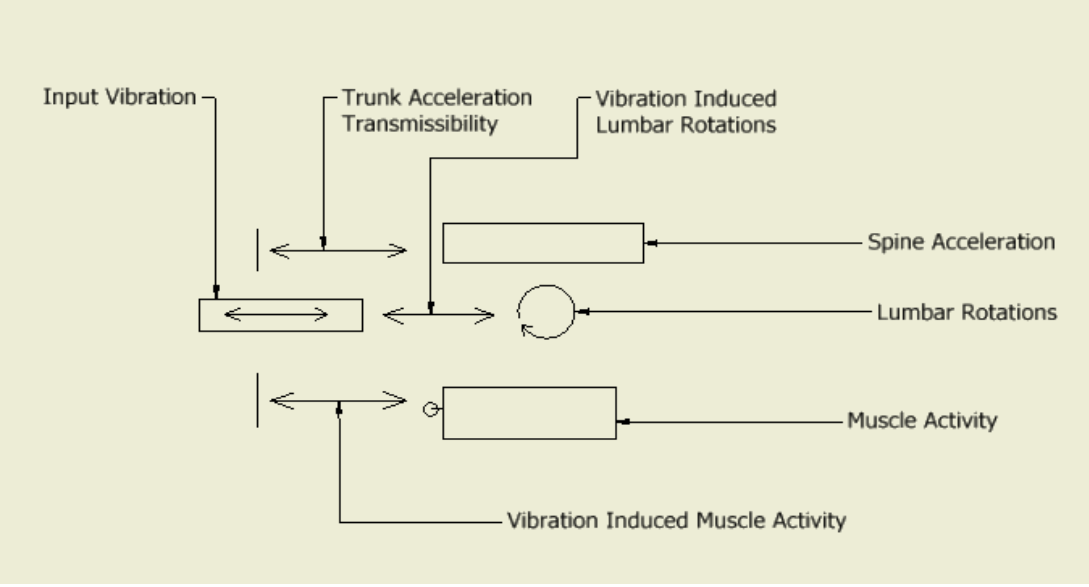

Figure 14: Figure demonstrating the different transmissibility functions to assess the whole body vibration transmission

Part 2:

2.2 Mathematical Model:

A lumped parameter model was created with two lumped masses representing head-arm-trunk (HAT) and the pelvis-legs connected with linear and rotational dampers and springs. The parameters for the model were based on weights of the experimental subjects and anthropometric data from literature (**Table 2**). Using Lagrangian dynamics, a linearized state-space model was created. This model was used to compare the model to the experimental data. In addition, using Simulink in MATLAB, the vibration experiment was simulated.

Mathematical Model: deriving equations of motion using Lagrangian dynamics.

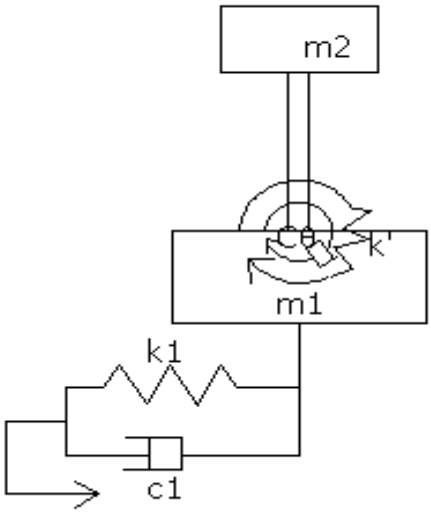

Figure 15: Mathematical model developed

Assuming the system to be holomonic using a Lagrangian equation:

$\frac{d}{dt}(\frac{\partial L}{\partial \dot{q}})-\frac{\delta L}{\delta q}=NCF$ ***(Non Conservative Forces)*** **Equation 1**

L is the difference between Kinetic Energy (K.E) and Potential Energy (P.E) of the system and q is the generalized coefficients. We also make an assumption that the length 'l' is constant in the process. The spring k' is assumed as a rotational spring representing the combined stiffness of the spine and the linear musculature acting around a moment arm.

Total kinetic energy of the system is the sum of kinetic energy of mass 1 and mass 2.

$$T.K.E.=(K.E)_{m_1}+(K.E)_{m_2}$$ **Equation 2**

Total potential energy of the system is the sum of potential energy of mass 2 height changes and energy storage in the two springs k_1 and k'.

$$T.P.E. = (P.E)_{k_1} + (P.E)_{m_2} + (P.E)_{k'}$$ **Equation 3**

To find the kinetic energy of mass 2:

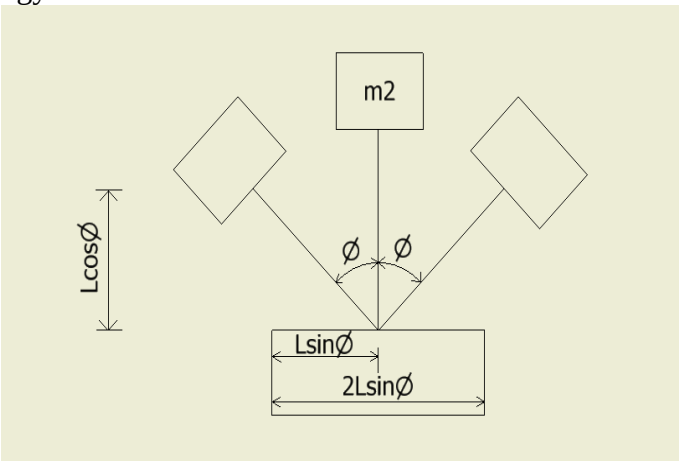

Referring to the above figure, position of mass 2 (m_2) is:

$$[(x-l\sin\theta),l\cos\theta]$$

And the velocity of m_2 is represented by

$$v_{m2}=\sqrt{\dot{x}^2+\dot{y}^2},$$

Where

$$\dot{x} = \dot{x} - l\dot{\theta}\cos\theta$$

$$\dot{y} = -l\dot{\theta}\sin\theta$$

Therefore, combining these equations, we can obtain the equation:

$$v_{m2} = sqrt[(\dot{x} - l\dot{\theta}\cos\theta)^2 + (-l\dot{\theta}\sin\theta)^2] \qquad \textbf{Equation 4}$$

Expanding and simplifying the above equation, we can obtain the equation:

$$v_{m_2} = sqrt[\dot{x}^2 + l^2\dot{\theta}^2\cos^2\theta + l^2\dot{\theta}^2\sin^2\theta - 2\dot{x}l\dot{\theta}\cos\theta] \qquad \textbf{Equation 5}$$

$$v_{m_2} = sqrt[\dot{x}^2 + l^2\dot{\theta}^2 - 2\dot{x}l\dot{\theta}\cos\theta]$$

Kinetic energy is:

$$K.E = \frac{1}{2}mv^2 + \frac{1}{2}I\dot{\theta}^2$$

Substituting v_{m_2} in the kinetic energy equation , kinetic energy of mass 2 will be:

$$\frac{1}{2}m_2(\dot{x}^2 + l^2\dot{\theta}^2 - 2\dot{x}l\dot{\theta}\cos\theta) + \frac{1}{2}I\dot{\theta}^2 \qquad \textbf{Equation 6}$$

To find the kinetic energy of mass 1:

Velocity of m_1 is:

$$v_{m_1} = \dot{x}$$

Kinetic energy of mass 1 is:

$$\frac{1}{2}m_1\dot{x}^2$$

Total kinetic energy is the sum of kinetic energy of mass 1 and mass 2:

$$T.K.E. = (K.E)_{m_1} + (K.E)_{m_2}$$

Substituting for kinetic energy of mass 1 and mass 2 and expanding the terms, we can obtain the equations:

$$K.E = \frac{1}{2} m_1 \dot{x}^2 + \frac{1}{2} m_2 (\dot{x}^2 + l^2 \dot{\theta}^2 - 2 \dot{x} l \dot{\theta} \cos\theta) + \frac{1}{2} I \dot{\theta}^2$$

Equation 7

$$K.E = \frac{(m_1+m_2)}{2} \dot{x}^2 + \frac{(m_2 l^2 + I)\dot{\theta}^2}{2} - m_2 \dot{x} l \dot{\theta} \cos\theta$$

Total potential energy is the sum of potential energies of spring k1, mass m2 and spring k'

$$T.P.E. = (P.E)_{k_1} + (P.E)_{m_2} + (P.E)_{k'}$$

Potential energy due to k1 is given by

$$(P.E)_{k1} = \frac{1}{2} k_1 (x - w)^2$$

Equation 8

Potential energy due to k1 is given by

$$(P.E)_{m_2} = m_2 gl\cos\theta + \frac{1}{2}(k')\theta^2$$

Equation 9

Total potential energy is

$$T.P.E. = \frac{1}{2} k_1 (x - w)^2 + m_2 gl\cos\theta + \frac{1}{2}(k')\theta^2$$

Equation 10

L, the Lagrangian, which is the difference between kinetic energy and potential energy of the system will be:

$$L = \frac{(m_1+m_2)}{2} \dot{x}^2 + \frac{(m_2 l^2 + I)\dot{\theta}^2}{2} - m_2 \dot{x} l \dot{\theta} \cos\theta - \frac{1}{2} k_1 (x - w)^2 - \frac{1}{2}(k')\theta^2 - m_2 gl\cos\theta$$

Equation 11

The original Lagrangian equation (Equation 1**)** has a generalized coordinates terms q. The generalized coordinates here are x and θ. Finding the partial derivative with respect to generalized co-ordinate θ:

$$\frac{\delta L}{\delta \theta} = m_2 \dot{x} l \dot{\theta} \sin\theta + m_2 g l \sin\theta - (k')\theta$$ **Equation 12**

$$\frac{\delta L}{\delta \dot{\theta}} = (m_2 l^2 + I)\dot{\theta} - m_2 \dot{x} l \cos\theta$$ **Equation 13**

Non Conservative forces in θ will be due to the damper c_θ **Equation 14**

Now finding the derivative of the above equation (**Equation 13**) and substituting it back in the Lagrangian equation we can obtain the equation:

$$\frac{d}{dt}\left(\frac{\delta L}{\delta \dot{\theta}}\right) = (m_2 l^2 + I)\ddot{\theta} - m_2 \ddot{x} l \cos\theta + m_2 \dot{x} l \dot{\theta} \sin\theta$$ **Equation 15**

Substituting this equation (**Equation 12**) back in Lagrangian equation (**Equation 1**) we can obtain the equation:

$$(m_2 l^2 + I)\ddot{\theta} - m_2 \ddot{x} l \cos\theta + m_2 \dot{x} l \dot{\theta} \sin\theta - m_2 \dot{x} l \dot{\theta} \sin\theta - m_2 g l \sin\theta + (k')\theta + c_\theta \dot{\theta}$$ **Equation 16**

Similarly, one can find the partial derivatives with respect to the other generalized co-ordinate x:

$$\frac{\delta L}{\delta \dot{x}} = (m_1 + m_2)\dot{x} - m_2 l \dot{\theta} \cos\theta$$

$$\frac{d}{dt}\left(\frac{\delta L}{\delta \ddot{x}}\right) = (m_1 + m_2)\ddot{x} + m_2 l \dot{\theta}^2 \sin\theta - m_2 l \ddot{\theta} \cos\theta$$ **Equation 17**

$$\frac{\delta L}{\delta x} = -k_1 (x - w)$$

Non Conservative Forces in x will be:

$$NCF = -c_1(\dot{x} - \dot{w})$$

Substituting the above values in equation 1, we can obtain the equation:

$$(m_1 + m_2)\ddot{x} + m_2 l \dot{\theta}^2 \sin\theta - m_2 l \ddot{\theta} \cos\theta + k_1(x - w) + c_1(\dot{x} - \dot{w}) = 0$$ **Equation 18**

In order to make equation 18 and equation 16 linear, we assumed smaller θ oscillations to simplify the following terms:

$\cos\theta \approx 1$ and $\sin\theta \approx \theta$

Neglecting the higher order terms, equation 18 and equation 16 can be reduced to:

$$(m_2 + I)l^2 \ddot{\theta} - m_2 \ddot{x} l - m_2 g l\theta + (k')\theta + (c_\theta)\dot{\theta} = 0$$ **Equation 19**

$$(m_1 + m_2)\ddot{x} - m_2 l \ddot{\theta} + k_1(x - w) + c_1(\dot{x} - \dot{w}) = 0$$ **Equation 20**

To make simplifications consider,

$\theta_1 = \dot{\theta}$

$\theta_2 = \ddot{\theta}$

$x_1 = \dot{x}$

$x_2 = \ddot{x}$

Where,

θ is the angular displacement

$\dot{\theta}$ is the angular velocity

$\ddot{\theta}$ is the angular acceleration

x is the linear displacement

$\dot{x}$ is the linear velocity

$\ddot{x}$ is the linear acceleration

Rewriting equations 19 and 20, using above notations to make simplifications easier, we obtain:

$$(m_2 l^2 + I)\theta_2 - m_2 x_2 l - m_2 g l\theta + (k')\theta + (c_\theta)\theta_1 = 0$$ **Equation 21**

$$(m_1 + m_2)x_2 - m_2 l\theta_2 + k_1(x - w) + c_1(x_1 - \dot{w}) = 0$$ **Equation 22**

To obtain a state space representation or the transfer functions from the above equations, we perform some algebraic simplifications. Performing the operation (*equation 21+ l*equation 22*) and further simplification gives the equations:

$$lm_1 x_2 - m_2 gl\theta + k_1 l(x - w) + c_1 l(x_1 - \dot{w}) + (k')\theta + (c_\theta)\theta_2 + I\theta_2 = 0$$ **Equation 23**

On further simplification the equation reduces as

$$x_2 = \frac{-k_1}{m_1} x - \frac{c_1}{m_1} x_1 - \frac{(k' - m_2 gl)}{lm_1}\theta - \frac{(c\theta)}{lm_1}\theta_1 - \frac{I}{m_1 l}\theta_2 + \frac{k_1}{m_1} w - \frac{c_1}{m_1}\dot{w}$$ **Equation 24**

Substituting equation 24 back in equation 21, we obtain:

$$m_2 l^2 \theta_2 - m_2 l(\frac{-k_1}{m_1} x - \frac{c_1}{m_1} x_1 - \frac{(k' - m_2 gl)}{lm_1}\theta - \frac{(c\theta)}{lm_1}\theta_1 + \frac{k_1}{m_1} w - \frac{c_1}{m_1}\dot{w} - \frac{I}{m_1 l}) - m_2 gl\theta + (k_1 + k_\theta)\theta + (c_\theta)\theta_1 = 0$$

Equation 25

On further simplification, the equations become:

$$\dot{\theta}_2 \left[m_2 l^2 + I(1 - \frac{m_2}{m_1}) \right] = -(\frac{k_1}{m_1} m_2 lx + \frac{c_1}{m_1} m_2 lx_1 + (\frac{m_2}{m_1} - 1)(k' - m_2 gl)\theta - (\frac{m_2}{m_1} - 1)(c_\theta)\theta_1 - \frac{k_1}{m_1} m_2 lw + \frac{c_1}{m_1 l} m_2 l\dot{w}$$

Equation 26

Representing equation 26 and equation 24 in the state space form:

$$\begin{bmatrix} x_1 \\ x2 \\ \theta 1 \\ \theta_2 \end{bmatrix} = \begin{bmatrix} 0 & 1 & 0 & 0 & 0 \\ \frac{-k_1}{m_1} & \frac{-c_1}{m_1} & \frac{-(k' - m_2 gl)}{lm_1} & \frac{-(c\theta)}{lm_1} & -\frac{I}{m_1 l} \\ 0 & 1 & 0 & 1 & 0 \\ \frac{-\frac{k_1}{m_1} m_2 l}{\left[m_2 l^2 + I(1 - \frac{m_2}{m_1}) \right]} & \frac{-\frac{c_1}{m_1} m_2 l}{\left[m_2 l^2 + I(1 - \frac{m_2}{m_1}) \right]} & \frac{-(\frac{m_2}{m_1} - 1)(k' - m_2 gl)}{\left[m_2 l^2 + I(1 - \frac{m_2}{m_1}) \right]} & \frac{-(\frac{m_2}{m_1} - 1)(c\theta)}{\left[m_2 l^2 + I(1 - \frac{m_2}{m_1}) \right]} & 0 \end{bmatrix} \begin{bmatrix} x \\ x_1 \\ \theta \\ \theta 1 \\ \theta_2 \end{bmatrix} + \begin{bmatrix} 0 & 0 \\ \frac{k_1}{m_1} & \frac{-c_1}{m_1} \\ 0 & 0 \\ \frac{k_1}{m_1 l} & \frac{c_1}{m_1 l} \end{bmatrix} \begin{bmatrix} w \\ \dot{w} \end{bmatrix}$$

Equation 27

A detailed table showing the range of values for each parameter in the model is described in a later section. The Inertia term I added in the model is relatively small compared to the other terms and neglecting the inertia term will not affect the performance of the model [123-125]. As you can observe in the above state space matrix the inertia term is adding up to $m_2 l^2$ and $m_2 l^2 <<$ I$<<$ $\frac{I}{m_1 l}$. So neglecting the inertia term in the state space matrix, we get

$$\begin{bmatrix} x_1 \\ x2 \\ \theta 1 \\ \theta_2 \end{bmatrix} = \begin{bmatrix} 0 & 1 & 0 & 0 \\ \frac{-k_1}{m_1} & \frac{-c_1}{m_1} & \frac{-(k'-m_2gl)}{lm_1} & \frac{-(c_\theta)}{lm_1} \\ 0 & 1 & 0 & 1 \\ \frac{-\frac{k_1}{m_1}m_2l}{\left[m_2l^2+I(1-\frac{m_2}{m_1})\right]} & \frac{-\frac{c_1}{m_1}m_2l}{\left[m_2l^2+I(1-\frac{m_2}{m_1})\right]} & \frac{-(\frac{m_2}{m_1}-1)(k'-m_2gl)}{\left[m_2l^2+I(1-\frac{m_2}{m_1})\right]} & \frac{-(\frac{m_2}{m_1}-1)(c_\theta)}{\left[m_2l^2+I(1-\frac{m_2}{m_1})\right]} \end{bmatrix} \begin{bmatrix} x \\ x_1 \\ \theta \\ \theta 1 \end{bmatrix} + \begin{bmatrix} 0 & 0 \\ \frac{k_1}{m_1} & \frac{-c_1}{m_1} \\ 0 & 0 \\ \frac{k_1}{m_1 l} & \frac{c_1}{m_1 l} \end{bmatrix} \begin{bmatrix} w \\ \dot{w} \end{bmatrix}$$

Equation 28

The above state space representation can be used to used to obtain the transfer functions needed for evaluation using MATLAB or equations 22 and 24 can be used directly to obtain the transfer functions x(s)/w(s) and θ(s)/w(s). Time delays can be added to the transfer function based on experimental data.

2.3 Muscle Model:

A.V.Hill[126], in 1938, proposed a muscle model based on his previous experimental work. Several models have been developed based on the ideas of the initial hill's model. A Hill based muscle model consists of typically 3 elements, a contractile component, an elastic component parallel to the series contractile element and another elastic element in series with the contractile element.

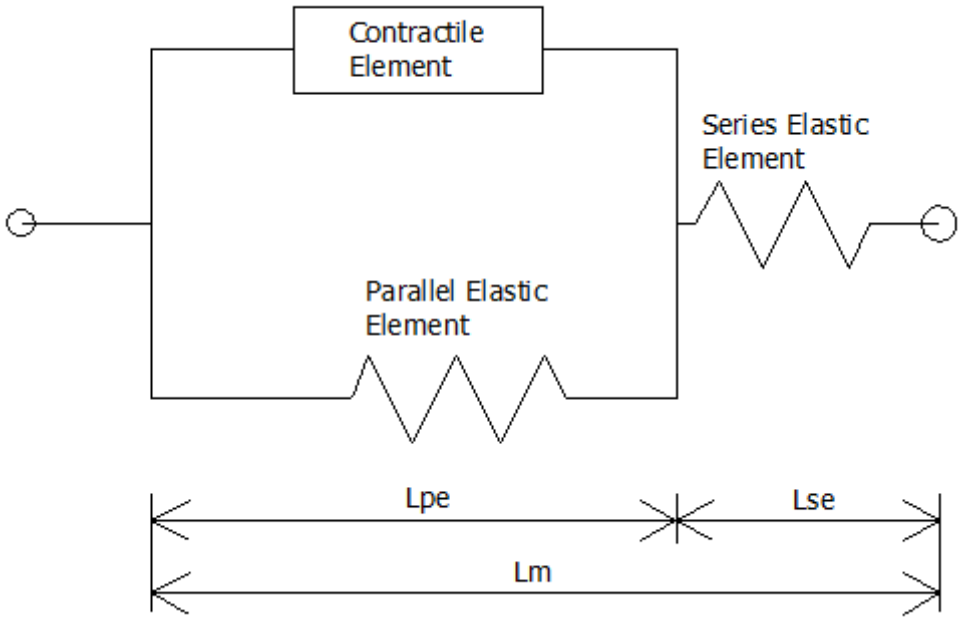

Figure 16: Hill's 1938 model

The above figure shows the Hill's 1938 model with a contractile element (CE), parallel elastic element of length Lpe and a series elastic element Lse and a total muscle length Lm. The series elastic element and parallel elastic element are simple nonlinear elastic elements and the contractile element is described by force-length and force-velocity relationships of the whole muscle. Hill also suggested that contractile element can be represented as a pure force generator in parallel to a nonlinear dashpot element. The plots below shows the Power and length response of the classical Hill's model for a constant muscle length and a step decrease in muscle length. The muscle was assumed to be in tetanus state of fully activated state. Hill also proposed an empirical formula relating the force generated by an isotonic contraction T_0, steady state force T and contraction velocity v given by

$$(T+a)(v+b)=(T_0+a)b$$

Which describes the classical hyperbolic form force velocity relationship of the muscle (a and b are constants).

Further studies have shown that extrapolation of Hill's muscle model to complex contractile conditions may be unreliable. This is because the contractile element in the Hill's model is described by a black box mathematical model and the equations cannot reproduce the known relationship between input and output characteristics without making any attempt to clarify the mechanism of muscle force production [124, 127].

Estimation of muscle properties is also a challenge in development or use of any existing muscle models. The muscle parameters vary for different muscles and there is an inter-subject variability as well as the change of muscle parameters with age. The parameters based on experimental studies are also not always accurate.

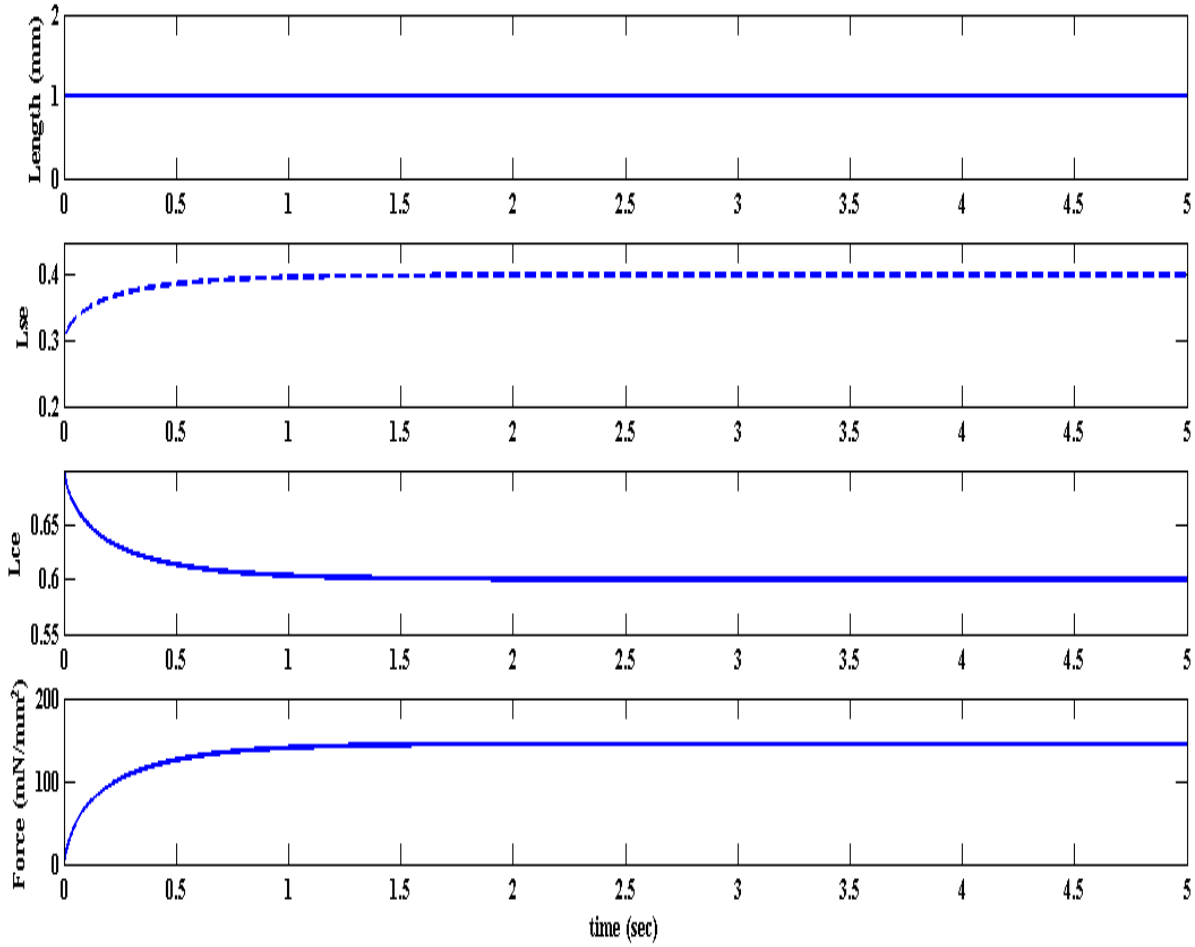

Figure 17: Force and length response of Hills model for a constant tetanized muscle length

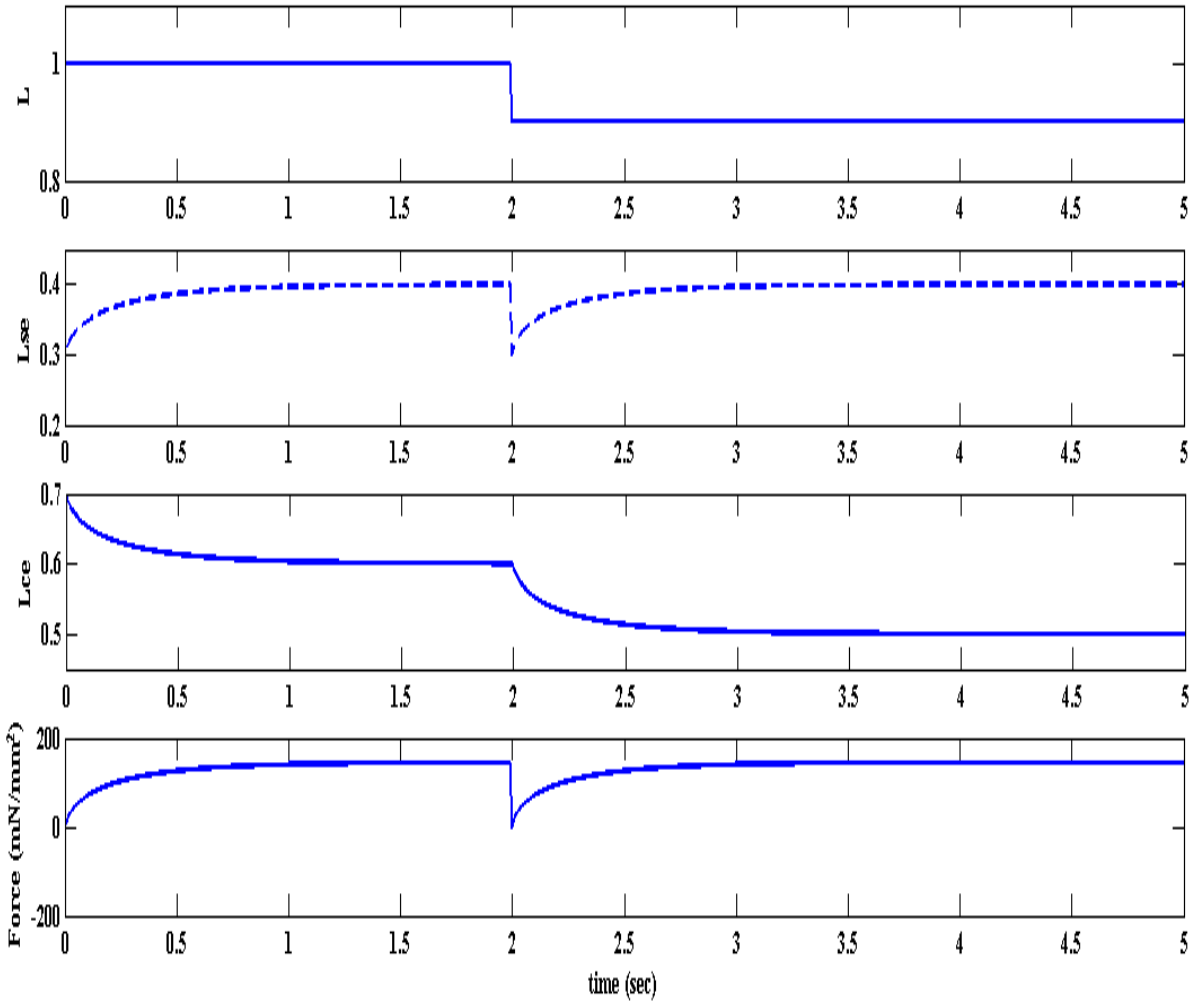

Figure 18: **Force and length response of Hills model for a step varied tetanized muscle length**

Several models have been developed based on Hill's models to predict the output forces from EMG inputs for specific joints or specific tasks [128-129]. There are benefits as well as limitations of using Hill's based muscle models. The muscle model used in the present study is based on Hill's model.

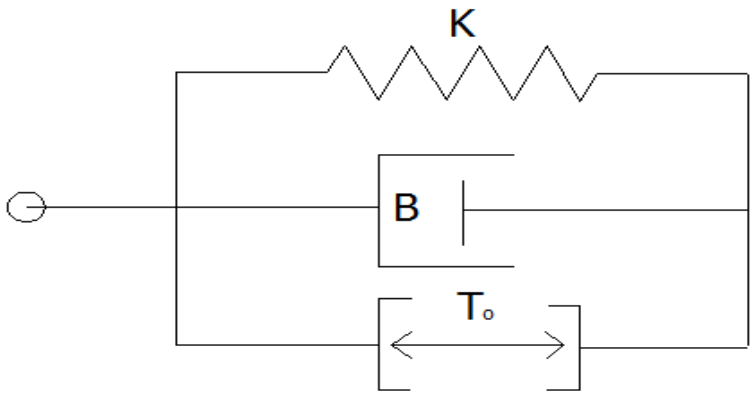

Figure 19: Muscle model based on Hill's model proposed by Winters

The above figure shows a muscle model based on model proposed by Winters [124]. This model does not include the series elastic element present in the hills model. This assumption considerably reduces the computational complexity of the model. Studies have shown that this model can effectively approximate the linear behavior on the nonlinear muscle about equilibrium. The model has a parallel stiffness element K, which is the intrinsic stiffness of the muscle, a damper B, which represents the intrinsic dampening and a force or inertia element. The muscle force f is a function of all the above components and is given by the below equation.

$$f(x_m) = F + K(x_m - x_{m_0}) + Bx'_m$$ **Equation 29**

The muscle stiffness and damping are considered as functions of the force element and length of the muscle. The muscle force can be represented[130] as

$$K = q\frac{T_0}{L}$$

Where K is the muscle stiffness, T_0 is the balanced muscle force and L is the muscle length. q is the muscle stiffness constant and the magnitude of q can vary from .5 to 40. The muscle force can be represented as

$$B = a\frac{T_0}{L}$$

Where K is the muscle stiffness, T_0 is the balanced muscle force and L is the muscle length. ‘a’ is the muscle damping constant. The muscle model was used to represent erector spine muscle group. The muscle was at a distance of 6 cms from the spine.

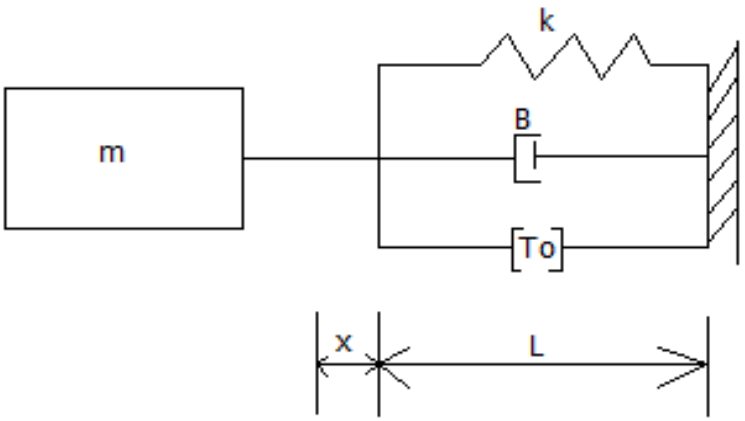

Figure 20: Muscle model with a single mass to demonstrate the effect of muscle group on the body

A modified Hill’s muscle model is shown in the above figure. The muscle model comprises of a force generating member and has an inherent stiffness. For the muscle to support a mass ‘m’ (shown at the left end), the tension within the muscle should overcome its internal stiffness and damping within. Hence the T_0 should be at least equal to the sum of the force drop across the stiffness and the damping.

The force provided by the muscle to support the mass ‘m’ is to be provided in the form of acceleration across the mass. Let the muscle could able to provide an extension ‘x’ across the mass ‘m’. Hence by Lagrangian Dynamics, the total kinetic energy of the system is contributed by the mass ‘m’ while the potential energy within the system is contained within the muscle stiffness. The Lagrangian of the system is calculated as given below:

The kinetic energy of the system is given by

$$KE=\frac{1}{2}m\dot{x}^2$$ **Equation 30**

The potential energy of the system is given by

$$PE=\frac{1}{2}k\dot{x}^2$$ **Equation 31**

Lagrangian L, is the difference between kinetic and potential energies of the system

$$L=KE-PE$$ **Equation 32**

The original Lagrangian equation (Equation 1**)** has a generalized coordinates terms q. The generalized coordinates here is x. Finding the partial derivative with respect to generalized co-ordinate x

$$\frac{\partial L}{\partial \dot{x}}=m\dot{x}$$
$$\frac{\partial L}{\partial x}=-kx$$
$$\frac{d}{dt}\left(\frac{\partial L}{\partial \dot{x}}\right)=m\ddot{x}$$ **Equation 33**

The non-conservative force includes the force being generated within the muscle and the force drop across the damper.

$$NCF=T_O-B\dot{x}$$ **Equation 34**

Hence the dynamics of the given system is given below:

$$m\ddot{x}+kx=T_O-B\dot{x}$$ **Equation 35**

Hence this result can be scaled up to include the dynamics of the seatpan and the upper body to model the upper body dynamics when subjected to a vibration.

Mathematical Model with the inclusion of the muscle model: deriving equations of motion using Lagrangian dynamics.

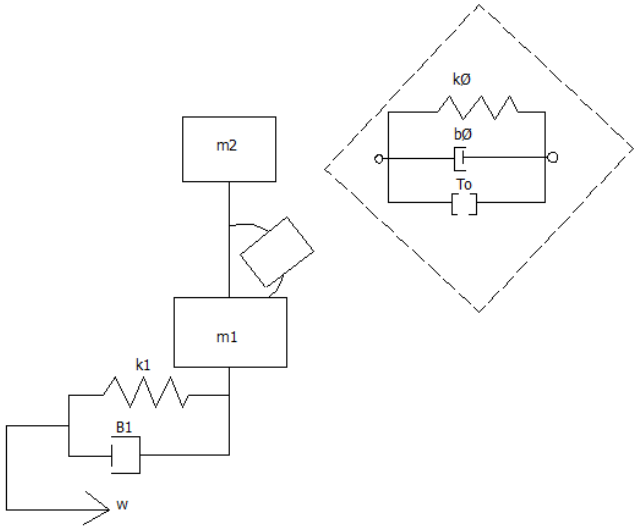

Figure 21: Mathematical model With the inclusion of Muscle Model. The Muscle Model is assumed to be Erector Spine muscle group.

If the system is holomonic, one can use the Lagrangian equation:

$$\frac{d}{dt}\left(\frac{\partial L}{\partial \dot{q}}\right)-\frac{\delta L}{\delta q}=NCF$$

Equation 36

(Non Conservative Forces)

Where L is the difference between Kinetic Energy (K.E) and Potential Energy (P.E) of the system and q is the generalized coefficients. We can make the assumption that the length 'l' between m1 and m2 is constant in the process.

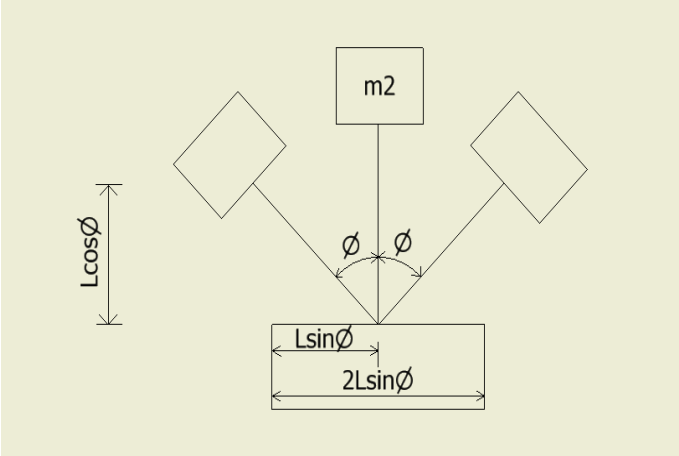

Referring to the above figure, position of mass 2 (m_2) is

$$[(x - l\sin\theta), l\cos\theta]_{/}$$

And the velocity of m_2 is represented by

$$v_{m2} = \sqrt{\dot{x}^2 + \dot{y}^2},$$

Where

$$\dot{x} = \dot{x} - l\dot{\theta}\cos\theta$$

$$\dot{y} = -l\dot{\theta}\sin\theta$$

Combining these, we obtain:

$$v_{m2} = sqrt[(\dot{x} - l\dot{\theta}\cos\theta)^2 + (-l\dot{\theta}\sin\theta)^2] \qquad \textbf{Equation 37}$$

Expanding and simplifying the above equation,

$$v_{m_2} = sqrt[\dot{x}^2 + l^2\dot{\theta}^2\cos^2\theta + l^2\dot{\theta}^2\sin^2\theta - 2\dot{x}l\dot{\theta}\cos\theta] \qquad \textbf{Equation 38}$$

$$v_{m_2} = sqrt[\dot{x}^2 + l^2\dot{\theta}^2 - 2\dot{x}l\dot{\theta}\cos\theta]$$

Kinetic energy of mass 2 is $K.E = \frac{1}{2}mv^2 + \frac{1}{2}I\dot{\theta}^2$

Substituting v_{m_2} in the kinetic energy equation above, we can obtain:

Kinetic energy of mass 2 will be:

$$K.E. = \frac{1}{2} m_2 (\dot{x}^2 + l^2 \dot{\theta}^2 - 2 \dot{x} l \dot{\theta} \cos\theta) + \frac{1}{2} I \dot{\theta}^2$$ **Equation 39**

Potential energy of mass 2 is:

$$(P.E)_{m2} = m_2 gl \cos\theta$$ **Equation 40**

Potential energy due to spring k1 is given by:

$$(P.E)_{k1} = \frac{1}{2} k_1 (x - w)^2$$ **Equation 41**

Potential energy due to spring k' is given by:

$$(P.E)_{k2} = \frac{1}{2} k' \theta^2$$ **Equation 42**

Kinetic energy of mass 1 will be:

$$\frac{1}{2} m_1 \dot{x}^2$$ **Equation 43**

Total kinetic energy is, therefore:

$$T.K.E. = (K.E)_{m1} + (K.E)_{m2}$$

$$T.K.E = \frac{1}{2} m_2 (\dot{x}^2 + l^2 \dot{\theta}^2 - 2 \dot{x} l \dot{\theta} \cos\theta) + \frac{1}{2} I \dot{\theta}^2 + \frac{1}{2} m_1 \dot{x}^2$$ **Equation 44**

Total potential energy is given by the equation:

$$T.P.E. = (P.E)_{k1} + (P.E)_{m2} + (P.E)_{k2}$$

$$T.P.E = \frac{1}{2} k_1 (x - w)^2 + m_2 gl \cos\theta + \frac{1}{2} k_\theta \theta^2$$ **Equation 45**

The Lagrangian of the system is calculated as the difference between kinetic and potential energy:

$$L = KE - PE$$

$$L = \frac{1}{2} m_2 (\dot{x}^2 + l^2 \dot{\theta}^2 - 2 \dot{x} l \dot{\theta} \cos\theta) + \frac{1}{2} I \dot{\theta}^2 + \frac{1}{2} m_1 \dot{x}^2 - \frac{1}{2} k_1 (x - w)^2 - m_2 g l \cos\theta - \frac{1}{2} k_\theta \theta^2$$ **Equation 46**

$$L = \frac{1}{2} (m_2 + m_1) \dot{x}^2 + \frac{1}{2} m_2 l^2 \dot{\theta}^2 - m_2 \dot{x} l \dot{\theta} \cos\theta + \frac{1}{2} I \dot{\theta}^2 - \frac{1}{2} k_1 (x - w)^2 - m_2 g l \cos\theta - \frac{1}{2} k_\theta \theta^2$$ **Equation 47**

Now the dynamics of the system can be derived using Lagrangian dynamics of the system with respect to the independent variable 'x' as follows:

$$\frac{\partial L}{\partial \dot{x}} = (m_2 + m_1) \dot{x} - m_2 l \dot{\theta} \cos\theta$$

$$\frac{\partial L}{\partial x} = -k_1 (x - w)$$ **Equation 48**

$$\frac{d}{dt}\left(\frac{\partial L}{\partial \dot{x}}\right) - \frac{\partial L}{\partial x} = (m_2 + m_1) \ddot{x} - m_2 l (\ddot{\theta} \cos\theta - \dot{\theta}^2 \sin\theta) + k_1 (x - w)$$

The force generation within the muscles model along with the force drops across the two dampers contributes the non-conservative forces in the system. The sum of all non-conservative forces is provided in the following equation.

$$NCF = -B_1 (\dot{x} - \dot{w})$$ **Equation 49**

$$\frac{d}{dt}\left(\frac{\partial L}{\partial \dot{q}}\right) - \frac{\delta L}{\delta q} = NCF$$ **Equation 50**

Now the dynamics of the system can be derived using Lagrangian dynamics of the system with respect to the independent variable 'θ' is given as following:

$$(m_2 + m_1) \ddot{x} - m_2 l (\ddot{\theta} \cos\theta - \dot{\theta}^2 \sin\theta) + k_1 (x - w) = B_1 (\dot{x} - \dot{w})$$ **Equation 51**

$$\frac{\partial L}{\partial \dot{\theta}} = -m_2 \dot{x} l \cos\theta + m_2 l^2 \dot{\theta} + I \dot{\theta}$$

$$\frac{\partial L}{\partial \theta} = m_2 \dot{x} l \dot{\theta} \sin\theta + m_2 g l \sin\theta - k_\theta \theta$$ **Equation 52**

$$\frac{d}{dt}\left(\frac{\partial L}{\partial \dot{\theta}}\right) - \frac{\partial L}{\partial \theta} = -m_2 l (\ddot{x} \cos\theta - \dot{x} \dot{\theta} \sin\theta) + m_2 l^2 \ddot{\theta} + I \ddot{\theta} - m_2 \dot{x} l \dot{\theta} \sin\theta - m_2 g l \sin\theta + k_\theta \theta$$

$$NCF = T_0 - B_2 \dot{\theta}$$ **Equation 53**

$$\frac{d}{dt}\left(\frac{\partial L}{\partial \dot{q}}\right) - \frac{\delta L}{\delta q} = NCF$$ **Equation 54**

$$-m_2 l(\ddot{x}\cos\theta - \dot{x}\dot{\theta}\sin\theta) + m_2 l^2 \ddot{\theta} + I\ddot{\theta} - m_2 \dot{x} l \dot{\theta}\sin\theta - m_2 gl\sin\theta + K_2\theta = T_0 - B_2\dot{\theta}$$ **Equation 55**

We assumed small vibrations and small angle changes allowing the substitution:

$\cos\theta \approx 1$ and $\sin\theta \approx \theta$

Neglecting the higher order terms, the equations reduces to:

$$(m_2 + m_1)\ddot{x}_2 - m_2 l\ddot{\theta}_2 + k_1(x - w) + B_1(\dot{x}_1 - \dot{w}) = 0$$ **Equation 56**

$$-m_2 l\ddot{x}_2 + (m_2 l^2 + I)\ddot{\theta}_2 - m_2 gl\theta + K_2\theta + B_2\dot{\theta}_1 = T_0$$ **Equation 57**

To make simplifications consider,

$$\theta_1 = \dot{\theta}$$

$$\theta_2 = \ddot{\theta}$$

$$x_1 = \dot{x}$$

$$x_2 = \ddot{x}$$

Equation 58

Where,

θ Is the angular displacement

$\dot{\theta}$ Is the angular velocity

$\ddot{\theta}$ Is the angular acceleration

x Is the linear displacement

$\dot{x}$ Is the linear velocity

$\ddot{x}$ Is the linear acceleration

$$(m_2 + m_1)x_2 - m_2 l\theta_2 + k_1(x - w) + B_1(x_1 - \dot{w}) = 0$$ **Equation 59**

$$-m_2 l x_2 + (m_2 l^2 + I)\theta_2 - m_2 g l\theta + K_2\theta + B_2\theta_1 = T_0$$ **Equation 60**

Equation 58 can be rewritten as fallowing:

$$x_2 = \frac{m_2 l}{(m_2+m_1)}\theta_2 - \frac{k_1}{(m_2+m_1)}(x - w) - \frac{B_1}{(m_2+m_1)}(x_1 - \dot{w})$$

$$x_2 = \frac{m_2 l}{(m_2+m_1)}\theta_2 - \frac{k1}{(m_2+m_1)}x - \frac{B_1}{(m_2+m_1)}x_1 + \frac{k_1}{(m_2+m_1)}w + \frac{B_1}{(m_2+m_1)}\dot{w}$$

Equation 61

Substituting equation 60 in equation 59 and simplify to get equation 63

$$m_2 l\left[\frac{m_2 l}{(m_2+m_1)}\theta_2 - \frac{k1}{(m_2+m_1)}x - \frac{B_1}{(m_2+m_1)}x_1 + \frac{k_1}{(m_2+m_1)}w + \frac{B_1}{(m_2+m_1)}\dot{w}\right] + (m_2 l^2 + I)\theta_2 - \left[m_2 g l - K_2\right]\theta + B_2\theta_1 = T_0$$

Equation 62

$$-\frac{(m_2 l)^2}{(m_2+m_1)}\theta_2 + m_2 l^2\theta_2 + I\theta_2 + \frac{m_2 l k_1}{(m_2+m_1)}x + \frac{m_2 l B_1}{(m_2+m_1)}x_1 - \frac{m_2 l k_1}{(m_2+m_1)}w - \frac{m_2 l B_1}{(m_2+m_1)}\dot{w} - \left[m_2 g l - K_2\right]\theta + B_2\theta_1 = T_0$$

Equation 63

Equation 63 can be simplifies as:

$$\left[-\frac{(m_2 l)^2}{(m_2+m_1)} + m_2 l^2 + I\right]\theta_2 = -\frac{m_2 l k_1}{(m_2+m_1)}x - \frac{m_2 l B_1}{(m_2+m_1)}x_1 + \frac{m_2 l k_1}{(m_2+m_1)}w + \frac{m_2 l B_1}{(m_2+m_1)}\dot{w} + \left[m_2 g l - K_2\right]\theta - B_2\theta_1 + T_0$$

Equation 64

Consider $\left[-\frac{(m_2 l)^2}{(m_2+m_1)} + m_2 l^2 + I\right]$ as ‘A’ for simplified representation of the equations.

$$\theta_2 = -\frac{m_2 l k_1}{A(m_2+m_1)}x - \frac{m_2 l B_1}{A(m_2+m_1)}x_1 + \frac{m_2 l k_1}{A(m_2+m_1)}w + \frac{m_2 l B_1}{A(m_2+m_1)}\dot{w} + \frac{\left[m_2 g l - K_2\right]}{A}\theta - \frac{B_2}{A}\theta_1 + \frac{T_0}{A}$$

Equation 65

$$x_2 = \left[-\frac{(m_2 l)^2 k_1}{A(m_2+m_1)^2} - \frac{k1}{(m_2+m_1)} \right] x - \left[\frac{(m_2 l)^2 B_1}{A(m_2+m_1)^2} - \frac{B_1}{(m_2+m_1)} \right] x_1 + \frac{m_2 l[m_2 gl - K_2]}{(m_2+m_1)A} \theta - \frac{m_2 l B_2}{(m_2+m_1)A} \theta_1 + \left[\frac{(m_2 l)^2 k_1}{A(m_2+m_1)^2} + \frac{k_1}{(m_2+m_1)} \right] w$$
$$+ \left[\frac{(m_2 l)^2 B_1}{A(m_2+m_1)^2} + \frac{B_1}{(m_2+m_1)} \right] \dot{w} + \frac{m_2 l T_0}{(m_2+m_1)A}$$

Equation 66

Representing equations 64 and 65 in state space representation, we arrive at

$$\begin{bmatrix} x_1 \\ x2 \\ \theta_1 \\ \theta_2 \end{bmatrix} = \begin{bmatrix} 0 & 1 & 0 & 0 \\ \left[-\frac{(m_2 l)^2 k_1}{A(m_2+m_1)^2} - \frac{k1}{(m_2+m_1)} \right] & \left[\frac{(m_2 l)^2 B_1}{A(m_2+m_1)^2} - \frac{B_1}{(m_2+m_1)} \right] & \frac{m_2 l[m_2 gl - K_2]}{(m_2+m_1)A} & -\frac{m_2 l B_2}{(m_2+m_1)A} \\ 0 & 0 & 0 & 1 \\ -\frac{m_2 l k_1}{A(m_2+m_1)} & -\frac{m_2 l B_1}{A(m_2+m_1)} & \frac{[m_2 gl - K_2]}{A} & -\frac{B_2}{A} \end{bmatrix} \begin{bmatrix} x \\ x_1 \\ \theta \\ \theta 1 \end{bmatrix}$$
$$+ \begin{bmatrix} 0 & 0 & 0 \\ \left[\frac{(m_2 l)^2 k_1}{A(m_2+m_1)^2} + \frac{k_1}{(m_2+m_1)} \right] & \left[\frac{(m_2 l)^2 B_1}{A(m_2+m_1)^2} + \frac{B_1}{(m_2+m_1)} \right] & \frac{m_2 l}{(m_2+m_1)A} \\ 0 & 0 & 0 \\ +\frac{m_2 l k_1}{A(m_2+m_1)} & \frac{m_2 l B_1}{A(m_2+m_1)} & \frac{1}{A} \end{bmatrix} \begin{bmatrix} w \\ \dot{w} \\ T_o \end{bmatrix}$$

Equation 67

The above state space representation can be used to used to obtain the transfer functions needed for evaluation using MATLAB or equations 22 and 24 can be used directly to obtain the transfer functions x(s)/w(s), θ(s)/w(s) etc. Time delays can be added to the transfer function based on experimental data and observations. Time delay of 60 milliseconds was used for frequencies below 6 Hz and time delay of 110 milliseconds was used for frequencies above 6 Hz based on experimental observations. The controller used was a gain controller. The figure below shows the muscle model with time delay element and controller in the feedback loop.

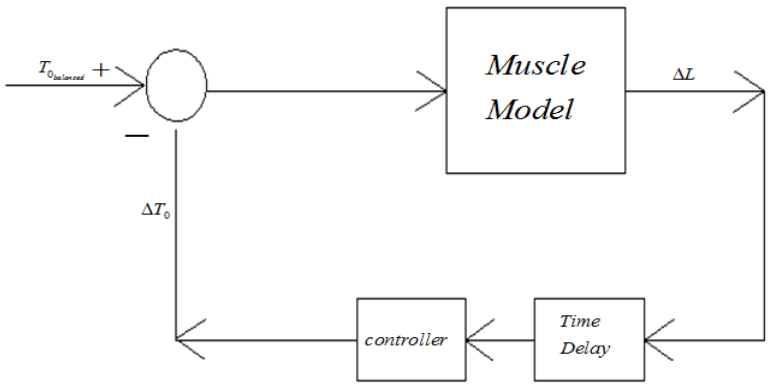

Figure 22: Muscle model with controller and time delay element in feedback loop

2.4 Input Data for the Models:

All the input parameters for the models including stiffness, damping coefficient, mass, inertia were taken from different sources. The table 2 (**Table 2**) shows the range of values for each parameter and the source from which the parameters were selected. Literature survey was done to investigate different models and parameters were selected based on the similarities in experimental and modeling conditions. The mass of head, arm and trunk were lumped into upper body mass. The mass of legs and pelvis was lumped as lower body mass. The mass of spine was added as upper body mass. The inertial of the upper body mass were based on studies from Pope, Cholewicki, and Bluthner. Lumbar spine length was based on model developed by Pope. The stiffness and damping properties of the spine were based on studies by Griffin, Pope, Rosen, and Wei. The erector spine muscle group was represented in this model and the muscle properties were based on the relationship described in the section 2.3.

Component	Value/range of values	Value Used	source
Seat Stiffness (K1) (N/m)	40000-75000	65000	Broman, Pope, Hanson [131]
Seat Damper (C1) (Ns/m)	1000	1000	Broman, Pope, Hanson [131]
Upper body mass (m1) (kg)	20	20	Broman, Pope, Hanson [131]
Lower Body Mass (m2) (Kg)	45	45	Broman, Pope, Hanson [131]
Inertia Element of Mass2 I (kgm^2)	.50	.5	Broman, Pope, Hanson [131] Cholewicki [132] Bluthner[133]
Rotational Stiffness (K) (Nm/rad)	5000-30000	25000	Broman, Pope, Hanson [131]
Rotational Damper (C) (Nms//rad)	100	100	Broman, Pope, Hanson [131]
Spine Stiffness (K2) (N/m)	5000-30000	25000	Wei And Griffin [115] Rosen and Arcan [134]
Spine Damper (C2) (Ns/m)	500-1500	1000	Wei And Griffin [115] Rosen and Arcan [134]
Lumbar Spine length l (m)	.32	.32	Broman,Pope, Hanson[131]
Muscle Length and distance from spine (cms)	3 and 6	3 and 6	Bergmark [130]

Table 2: Table showing the range of values selected for each parameter and the source

2.5 Validation of the models:

The model data was validated by comparing the predictions of the model data with the experimental data. The spine acceleration transmissibility (TF1) was also validated against the model results predicted by Padden[135]. The acceleration induced lumbar rotations (TF2) was validated based on experimental results and by comparing the results predicted by the basic

model and the model with muscle parameters included. Muscle activity due to input acceleration (TF3) and lumbar rotations induced muscle activity (TF4) were validated based on the experimental studies. One limitation with the experimental study was equipment limitation at lower frequencies. No experimental data was available for frequencies below 3 Hz. It should be noted that it is not always possible to match the experimental results with the model results because of many reasons, but all models will have a domain of validity, which defines variation of results from experiments and models.

2.6 Parametric Analysis:

Parametric analysis was conducted by varying the input parameters (individually) in 10% range to observe the sensitivity of models to changes. The spine stiffness was varied between 15 KN/m and 30 KN/m and the transmissibility functions (TF1-4) were calculated to observe the effect of altered parameters on model predictions.

2.7 Evaluation of error between the model and experimental results:

Root mean squared error and mean errors were calculated between the experimental results and model results to visualize the deviation between the experimental results. Root mean squared error is the most commonly used measure of the differences between values predicted by model and the values obtained experimentally. Mean error is the average of the error between the model and experimental results. RMSE is given by:

$$RMSE = \sqrt{\frac{\sum_{i=1}^{n} (X_m \sim X_e)^2}{n}}$$ **Equation 68**

Where X_m and X_e are the model and experimental values and n is the number of data points.

$$ME = \frac{\sum_{i=1}^{n} (X_m \sim X_e)}{n}$$ **Equation 69**

3.0 Results:

The transmissibility functions (TF1 ~ TF4) were assessed experimentally and simulated using the model. The results from experiment and model were compared to assess the validity of the model. Inter-subject variability was observed in all the transmissibility functions calculated experimentally (**Figure 49-52**) at all magnitudes and back rest conditions.

3.1 Trunk Acceleration Transmissibility Function (TF1):

TF1, the magnitude of vibration transmissibility from seatpan accelerometer to trunk accelerometer as assessed experimentally in both with and without backrest conditions. The trunk acceleration transmissibility was found to gradually reduce with the increasing in frequency. A minor peak was observed at a frequency of 6 Hz with a back-rest and a minor peak was observed at a frequency of 5 Hz without a backrest. It can be observed that the transmissibility was found to be higher in presence of backrest compared to no backrest. The average transmissibility was found to vary by 8.14% between 1 RMS and 2 RMS for with back rest condition and by 41.45% between 1 RMS and 2 RMS for with no back rest condition. TF1 was found to be similar at both 1 and 2 RMS m/s2 for both the with and the without backrest conditions, suggesting that magnitude of the vibration does not change the system dynamic behavior.

Figure 24 and Figure 25, show the plots comparing the model and the ‘without backrest’ experimental results for the trunk acceleration transmissibility. It was observed that the trunk acceleration transmissibility reduced gradually with the increase in frequency and the model results also exhibited a similar pattern. With the model it is possible to examine frequency response below that possible experimentally in this work. The model suggests that resonance

frequency of this system is likely to be lower than 2 Hz and data at lower frequencies might be useful for validating the model. Paddan et al. examined horizontal vibration transmissibility to the trunk (but not to lumbar rotation or muscle activity). As can be seen in Figures 2 and 3, this data also appears to correspond to model predictions of TF1.

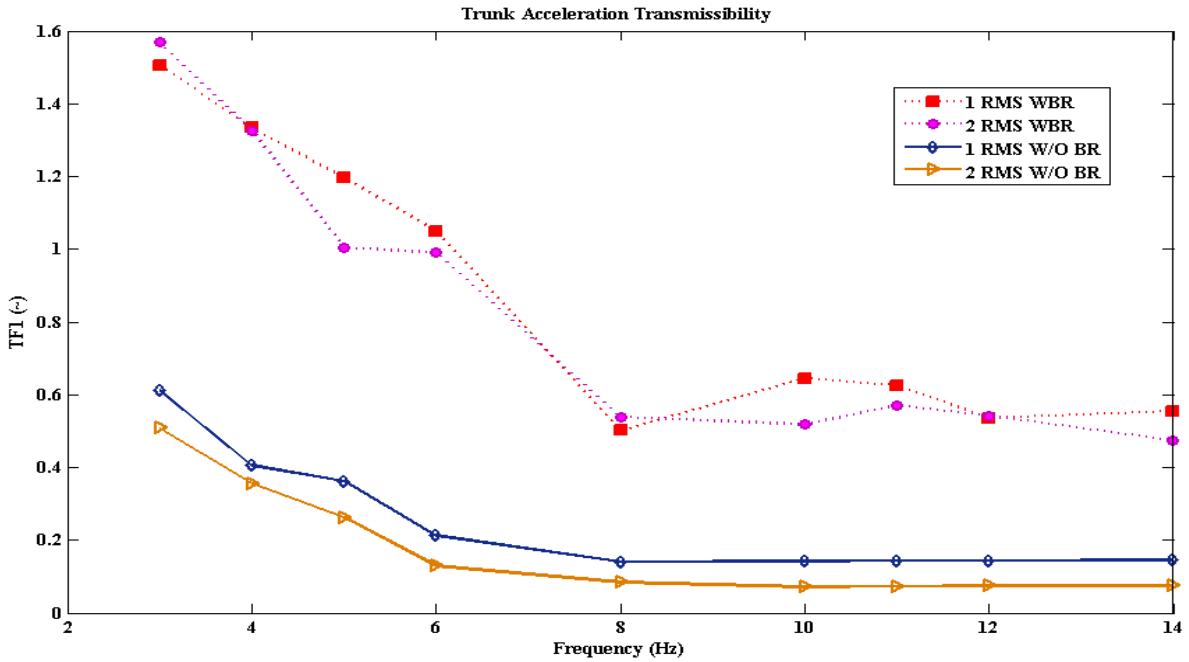

Figure 23: Trunk acceleration transmissibility plot (Experimental) with and without backrest

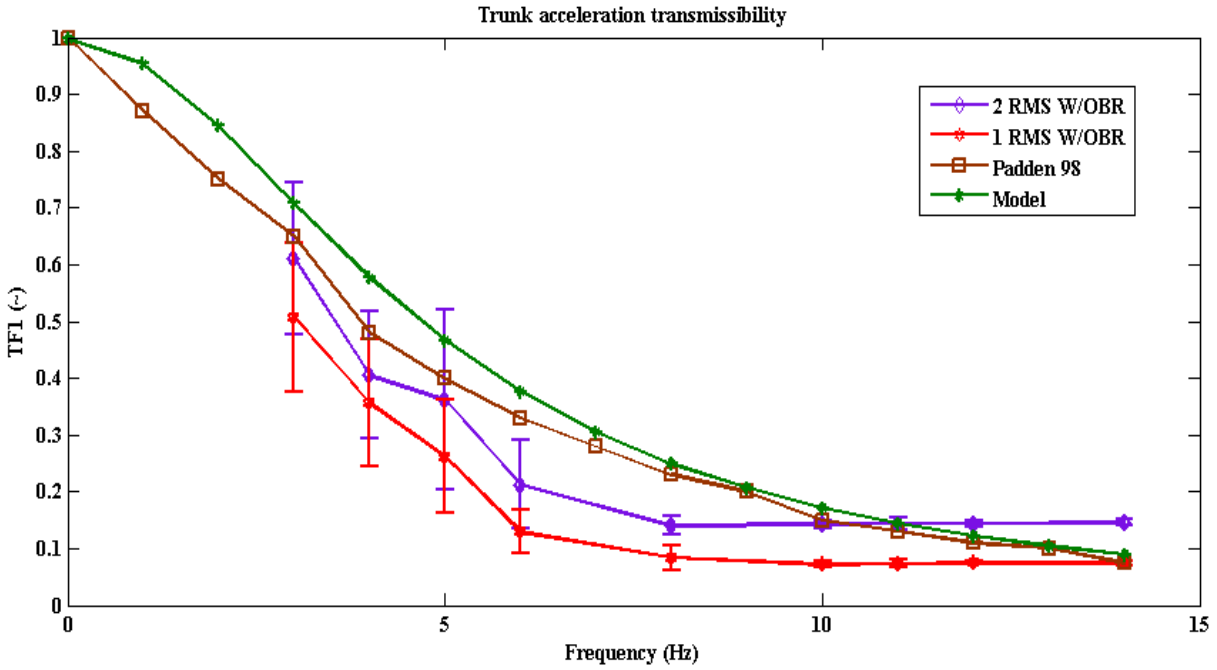

Figure 24: Trunk acceleration transmissibility plot (Experimental) without backrest with K1=65000 N/m

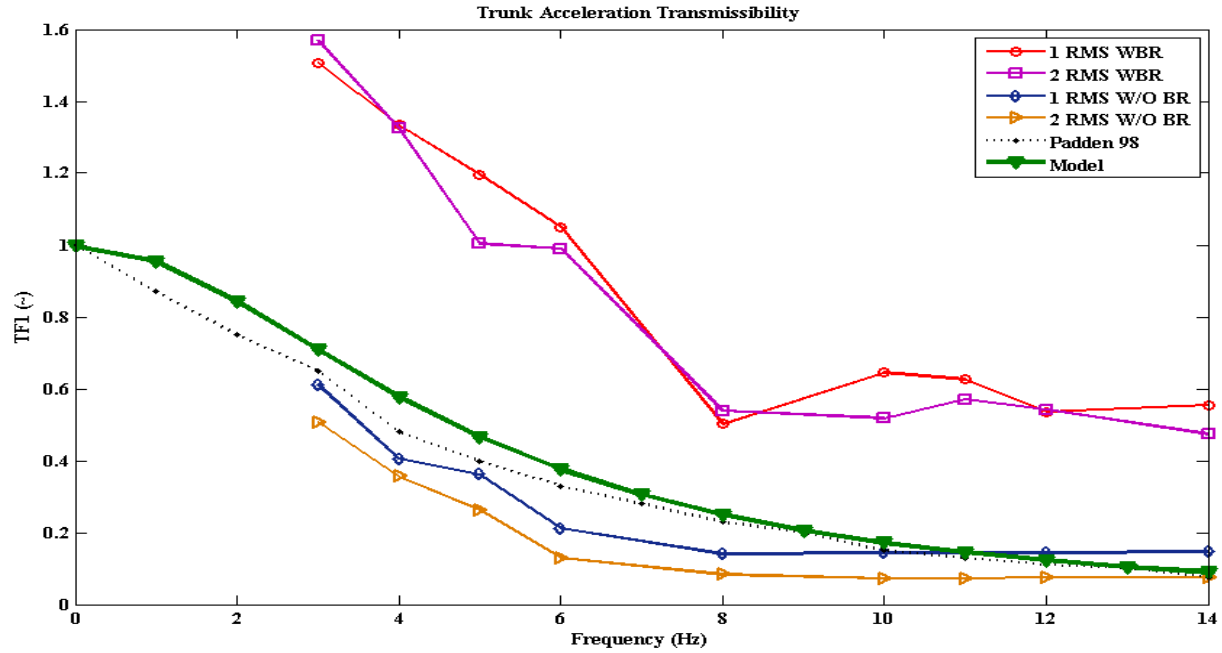

Figure 25: Trunk acceleration transmissibility plot (Experimental and model) with and without backrest with K1=65000 N/m

3.2 Vibration Induced Lumbar Rotations (TF 2):

TF2 (magnitude of vibration induced lumbar rotations relative to seatpan vibration) was found to gradually reduce with increase in frequency both with and without the presence of a backrest (Figure 26). The average transmissibility was found to vary by 8.14% between 1 RMS and 2 RMS for with back rest condition and by 41.45% between 1 RMS and 2 RMS for with no back rest condition. The average transmissibility was found to vary by 12.29% between 1 RMS and 2 RMS for with back rest condition and by 31.49% between 1 RMS and 2 RMS for with no back rest condition. It was observed that the presence of back rest was not found to have much of an impact on transmission magnitude. This suggests that while the backrest does move the thorax more (as evidenced by TF1), trunk rocking motions are unchanged, possibly due to the stiff backrest resisting rotation motions of the trunk.

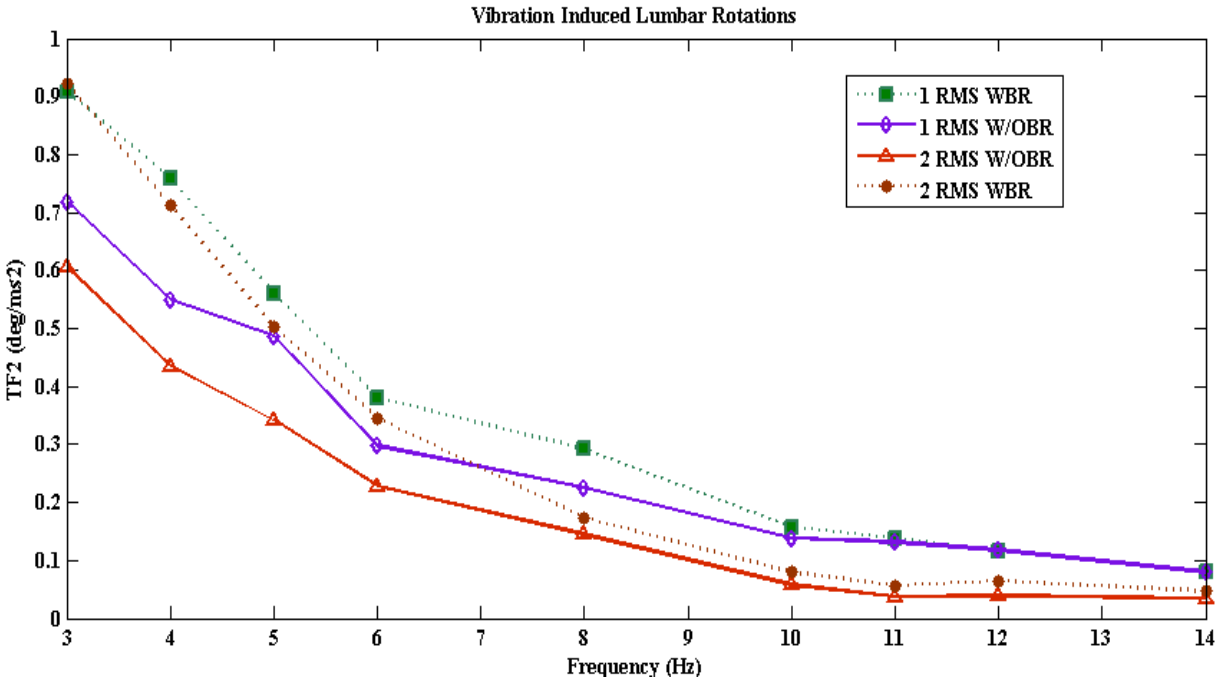

Figure 26: Vibration induced lumbar rotations plot (experimental)

Figure 27 compares the experimantal and model results for TF2 (Vibration induced lumbar rotations). Both the experimantal and model results declined with the increase in frequency. However, it was observed that the model showed a steeper decrease in transmissibility compared to gradual decrease exhibited experimentally.

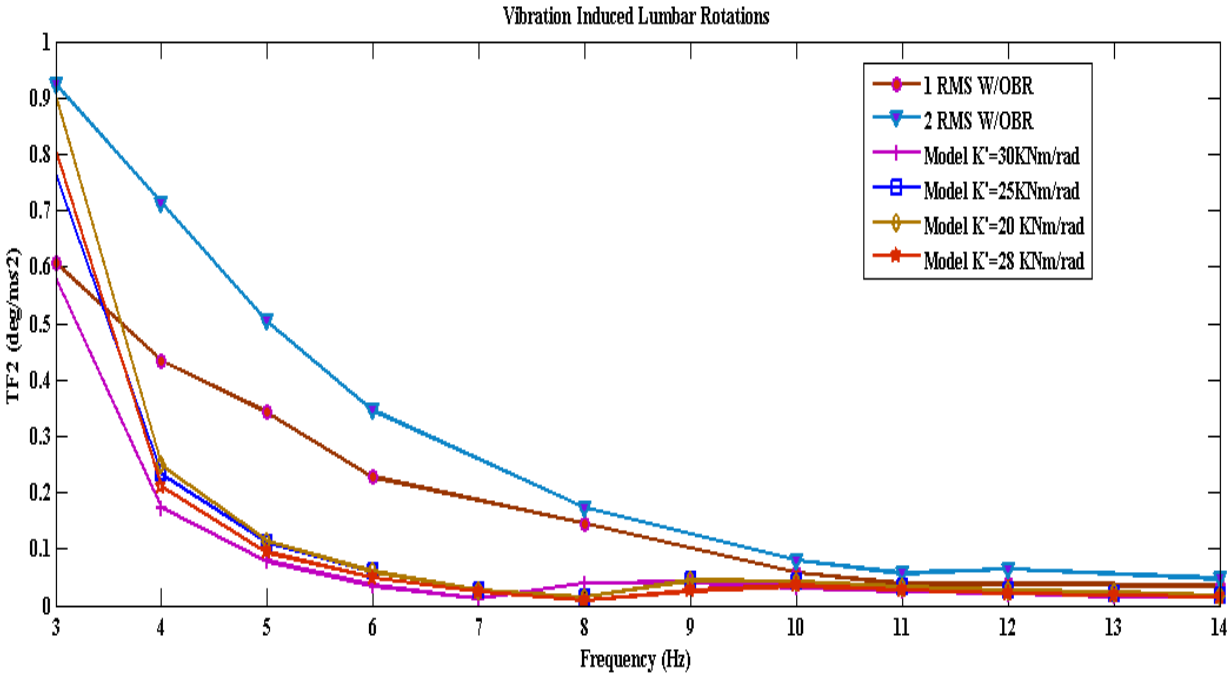

Figure 27: Vibration induced lumbar rotations plot (experimental and model) In the model the k' was varied from 20 to 30 KNm/rad

The model exhibited a peak at a frequency of about 1.5 Hz (Figure 28). It was also observed that the peak shifted towards right with the increase in spine stiffness. Because the shaker used in this experiment could only go down to 3 Hz, it was not possible to observe whether this resonant peak was also present experimentally. Figure 8 shows the patterns predicted by the basic model and the model with muscle dynamics incorporated. Both the models exhibited a resonance at a frequency of about 1.5 Hz. However the rate at which the transmissibility attenuated at lower frequencies in the model 1 was greater than observed in model 2. Figure 9 shows the model

behavior for varying spine stiffness. It was observed that with the increase in spine stiffness the transmissibility shifter a little with a small change in the resonant frequency.

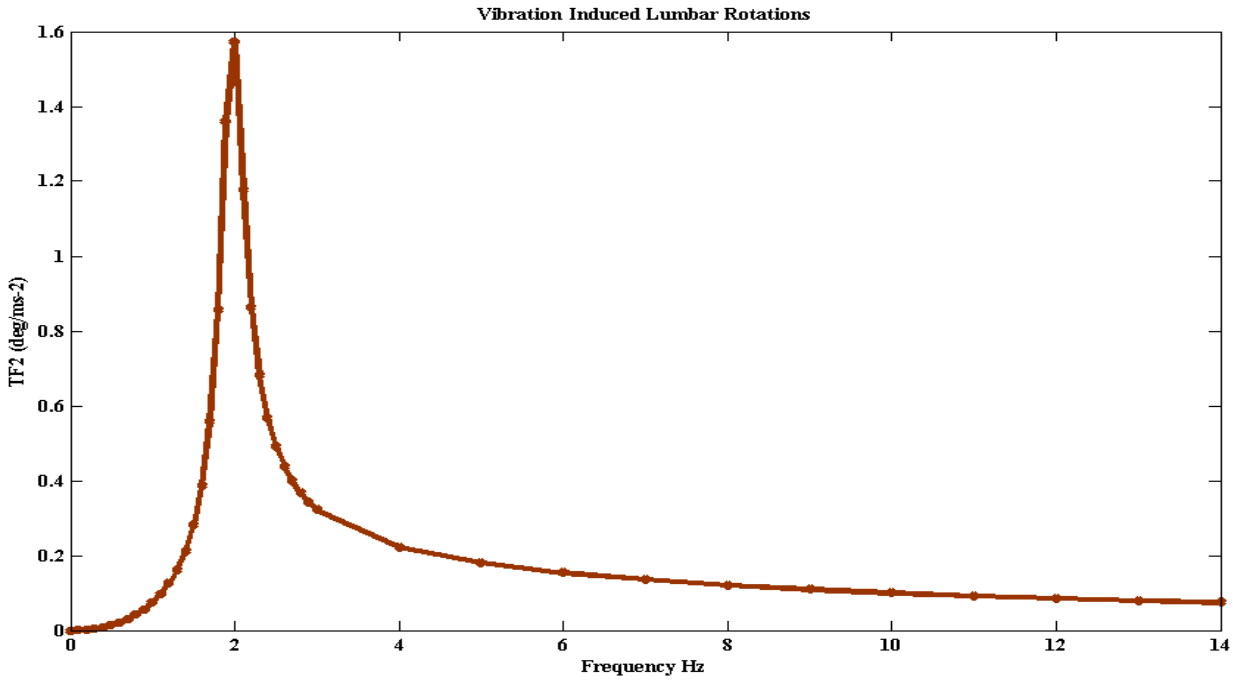

Figure 28: Vibration induced lumbar rotations (basic model) using k'= 25KN/m.

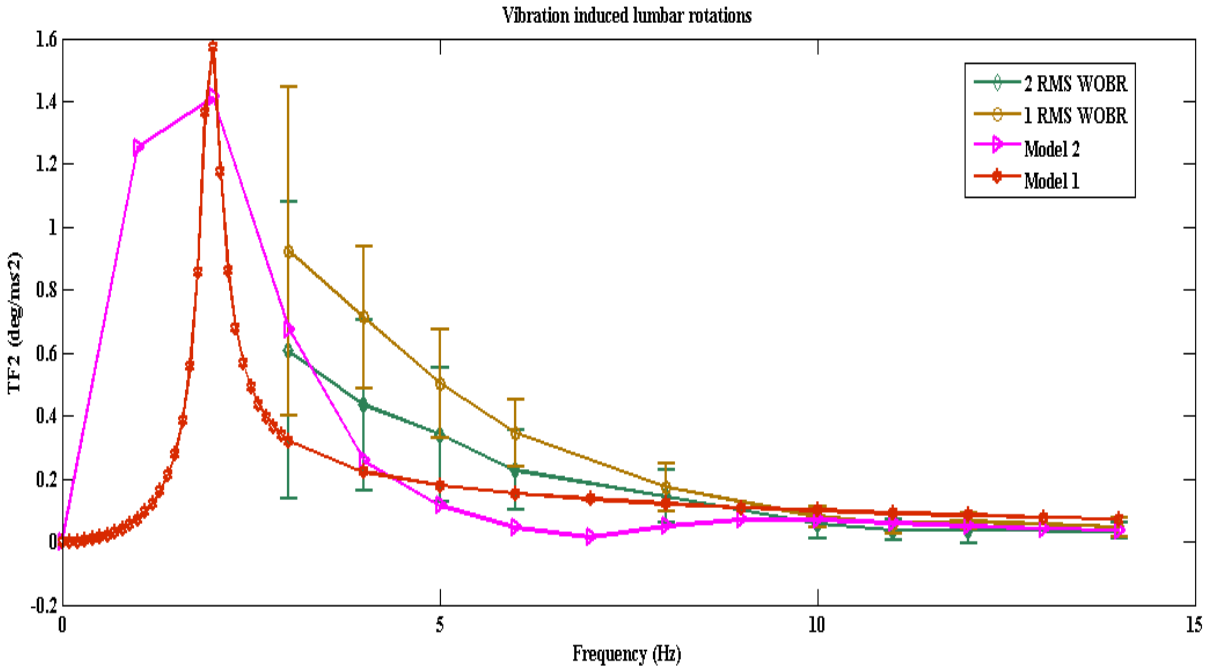

Figure 29: Vibration induced lumbar rotations model and experimental. Model 1 is the basic model and model 2 is the muscle model incorporated model

3.3 Muscle Activity due to Input acceleration (TF3):

The magnitude of muscle activity (integrated EMG normalized to MVC) relative to seat acceleration (TF3) was found to exhibit a peak at 8 Hz for 2 RMS m/s^2 and a peak at 6 Hz for 1 RMS m/s^2, with the presence of back rest. A minor peak was observed at 12 Hz and 11 Hz at 2 RMS m/s^2 and 1 RMS m/s^2 intensities respectively. Without a backrest, TF3 was found to exhibit a peak at 6 Hz for 2 RMS m/s^2 and a peak at 5 Hz for 1 RMS m/s^2. A minor peak was again observed at 12 Hz and 11 Hz at 2 RMS m/s^2 and 1 RMS m/s^2 intensities respectively. The magnitude of the minor peak was lower in comparison to the major peak observed, suggesting that the minor peak might be because of noise rather than muscle activity. However, it could also be due to resonance of the reflex system, as suggested by Abraham et al. Other than the peaks observed the magnitude reduced gradually with the increase in frequency. The average

transmissibility was found to vary by 18.97 % between 1 RMS and 2 RMS for with back rest condition and by 5.77 % between 1 RMS and 2 RMS for with no back rest condition.

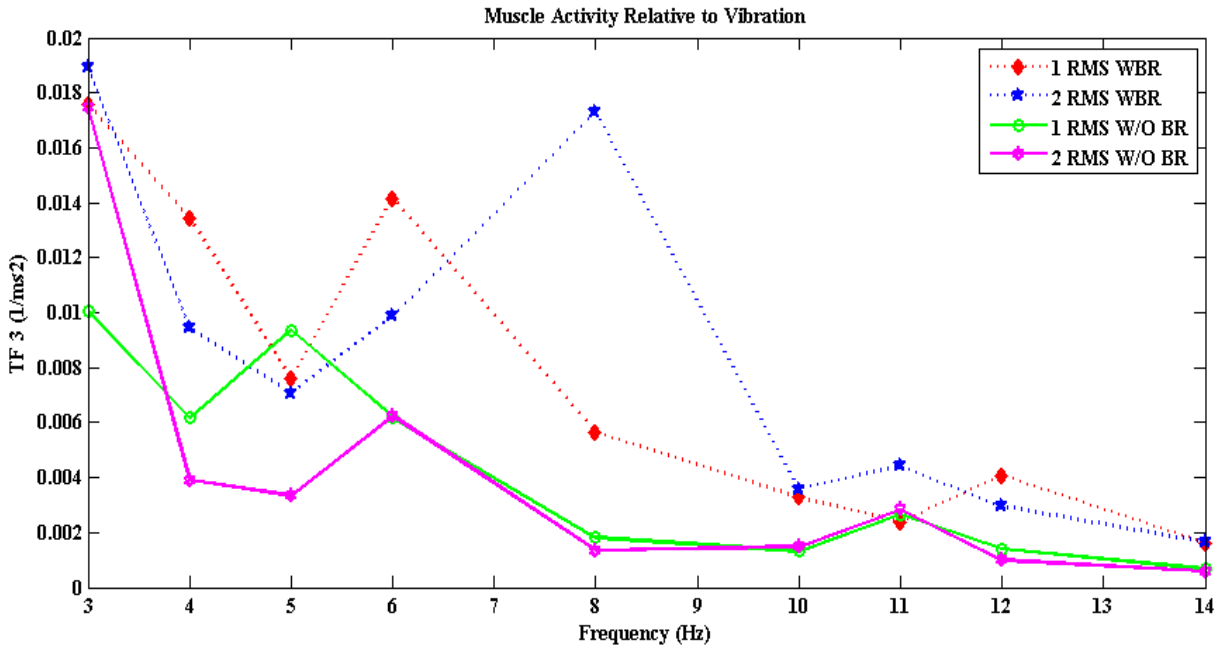

Figure 30: Muscle activity due to input acceleration (experimental)

The model with incorporated muscle and reflex dynamics was used to examine TF3. The model results were observed to follow the pattern similar to experimental results. A resonant peak was observed between the frequencies of 2 Hz and 3 Hz but no secondary was observed around 11-12 Hz. Figure 12 shows the variation of model predictions with change in muscle stiffness.

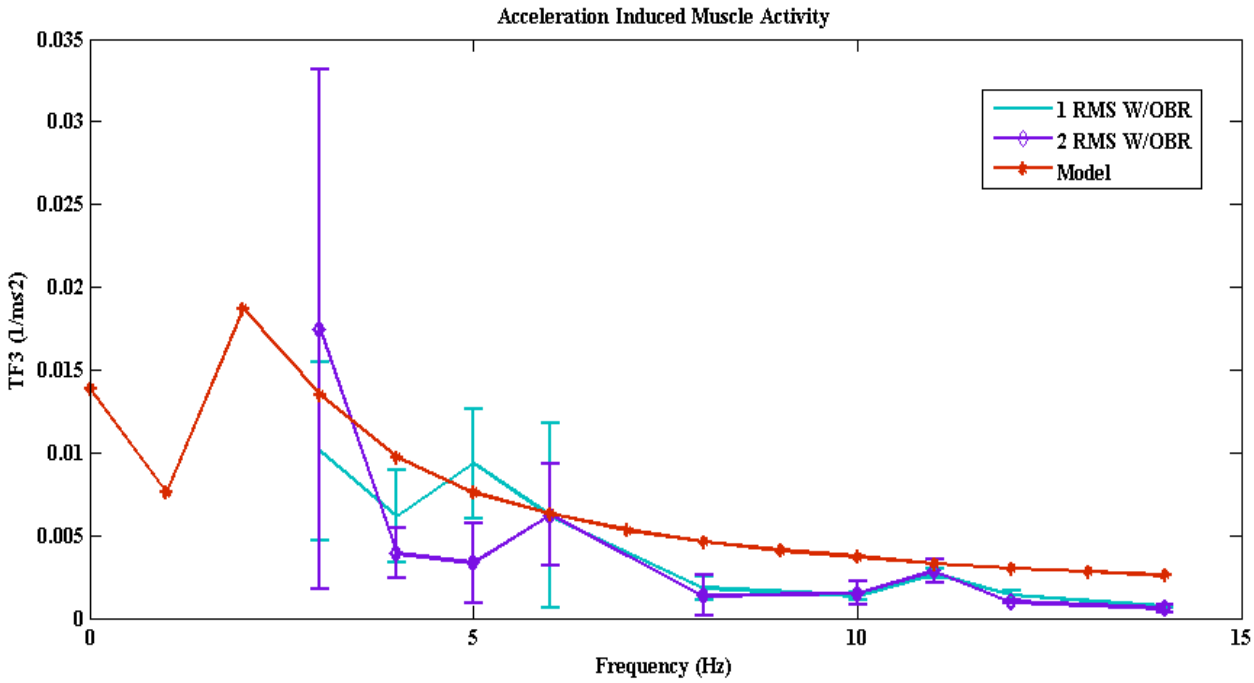

Figure 31: Vibration induced muscle activity model and experimental with k'=25 KNm/rad

3.4 Lumbar Rotations induced Muscle Activity (TF4):

The Muscle activity relative lumbar rotations or the mechano-neuromotor transmissibility (TF4) was found to be relatively constant with the increase in frequency (**Error! Reference source not found.**). A peak was observed at 8 Hz for 2 RMS with the presence of backrest. A minor peak was observed at 12 Hz for 1 RMS with back rest. In the absence of backrest condition, a minor peak was observed at 11 Hz for 1 RMS and 2 RMS intensities. The average transmissibility was found to vary by 3.84 % between 1 RMS and 2 RMS for with back rest condition and by 3.93 % between 1 RMS and 2 RMS for with no back rest condition.

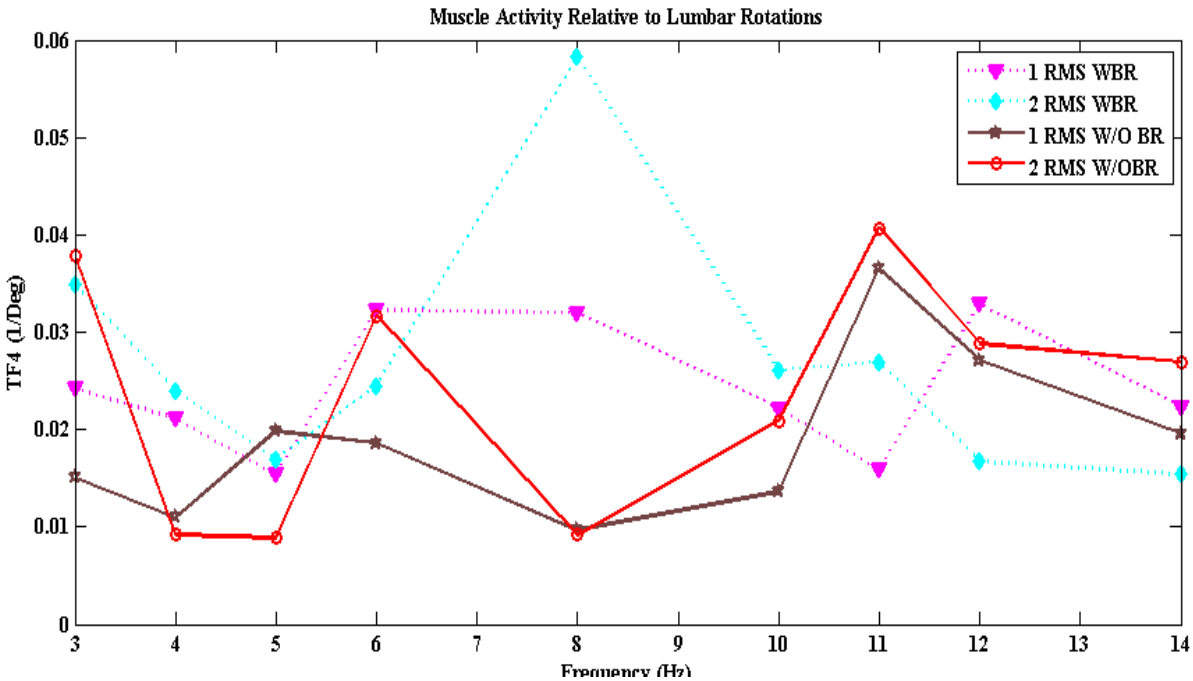

Figure 32: Lumbar rotations induced muscle activity (experimental)

The model exhibited a similar pattern exhibited by experimental studies. Transmissibility was observed to be consistent with increasing frequency with a peak at about 4 Hz. No secondary peak was observed in the model results at higher frequencies.

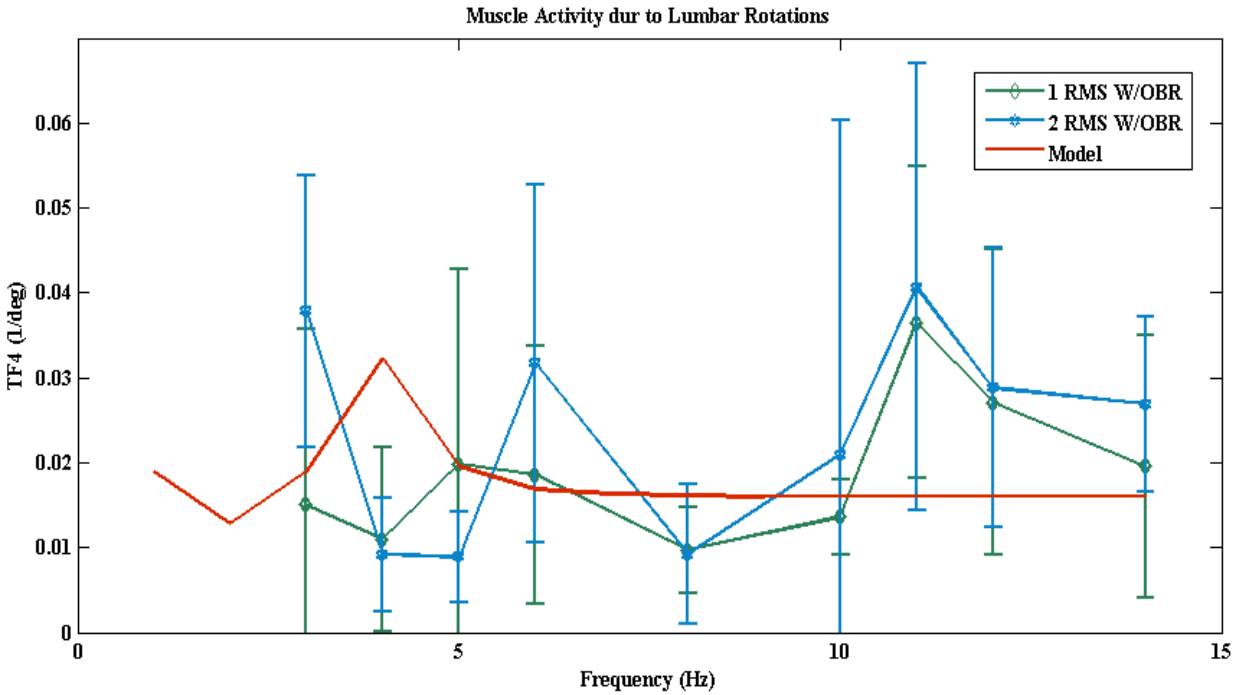

Figure 33: Lumbar rotations induced muscle activity model and experimental with k'=25KNm/rad

3.5 Parametric Analysis:

Parametric analysis was conducted by varying the input parameters (stiffness) between 15 KN/m and 30 KN/m. Trunk acceleration transmissibility (TF1) (**Figure *34*),** acceleration induced lumbar rotations (TF2) (**Figure *35***), muscle activity relative to input acceleration (TF3) (**Figure *36***), muscle activity relative to lumbar rotations (TF4) (**Figure 37**) were calculated for varying stiffness. **Figure 24**, **Figure 29**, **Figure 31**, **Figure 33** shows the variation of the experimental results from the mean values and the model predicted values. It can be observed that model response matches with the experimental results (with deviation bars). Variation of parameters

was not found to have much effect at higher frequencies (frequencies > 6 Hz). Some changes in magnitude or shift in resonance point were observed at lower frequencies (frequencies <= 6 Hz).

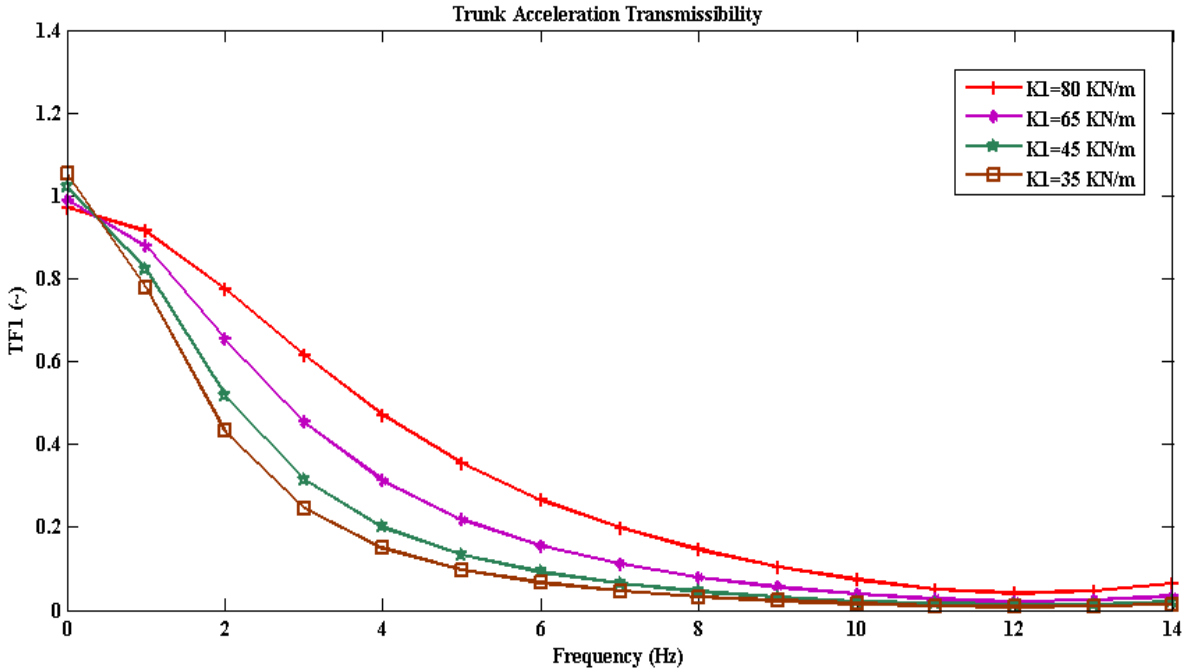

Figure 34: Trunk acceleration Transmissibility plot for varying spine stiffness (model)

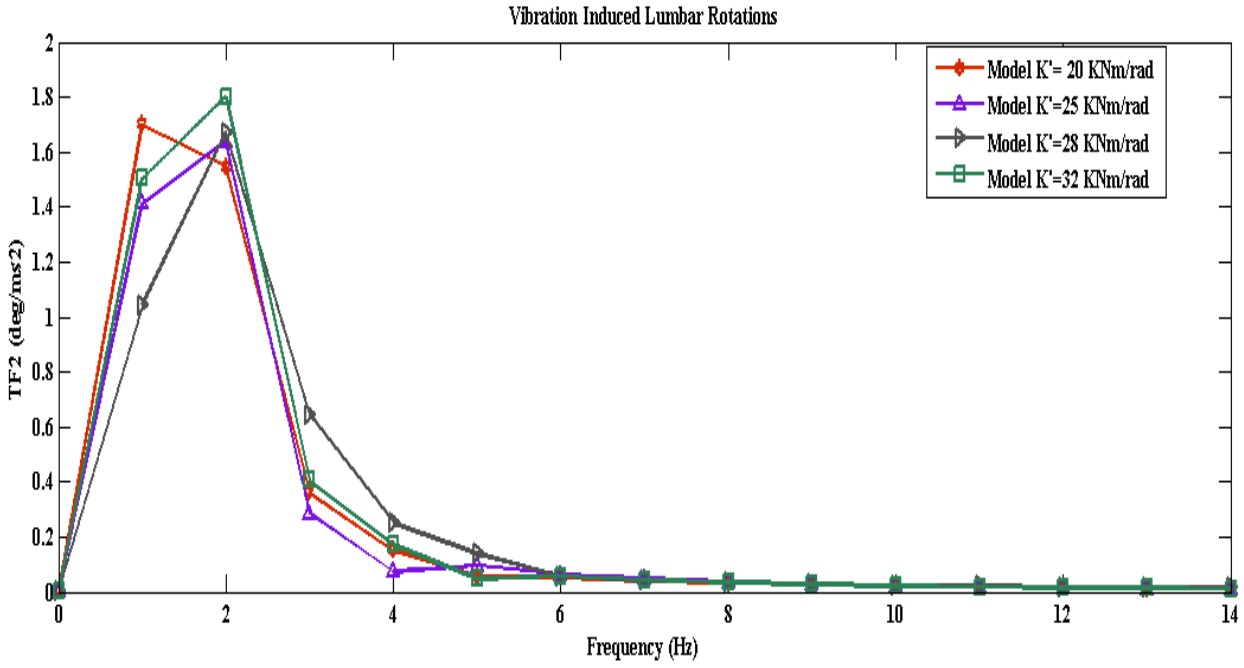

Figure 35: Vibration induced lumbar rotations for varying spine stiffness (k')

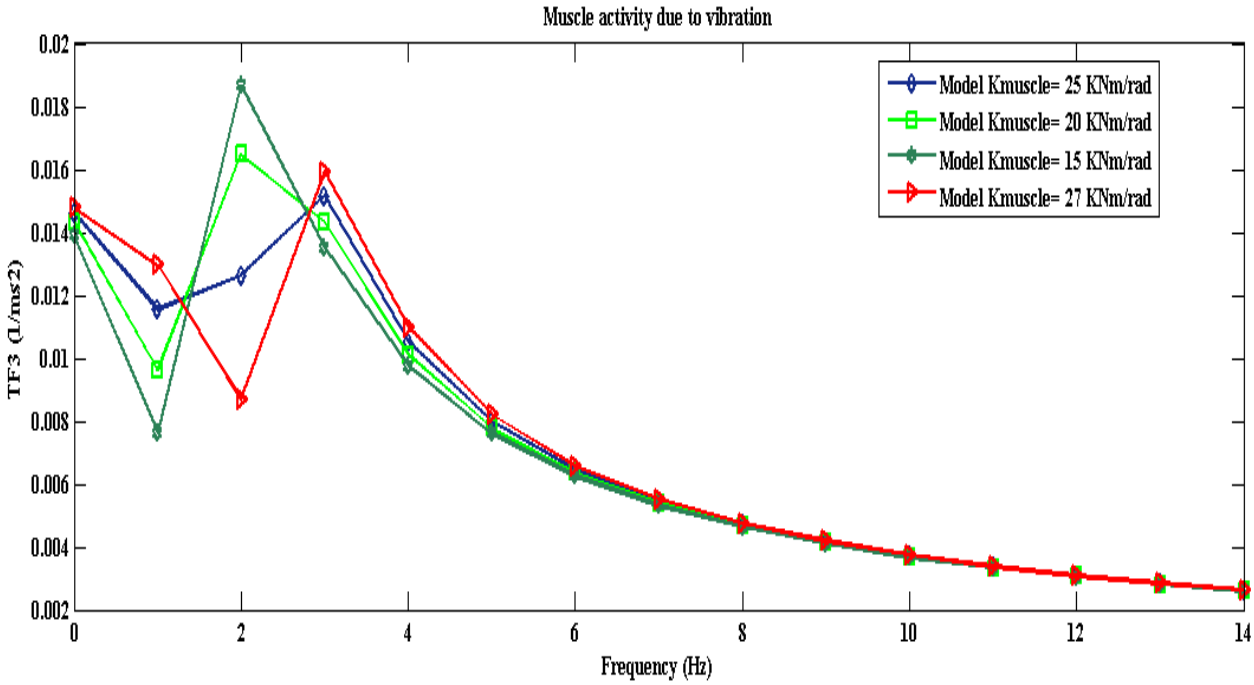

Figure 36: Vibration induced muscle activity model with varying muscle stiffness

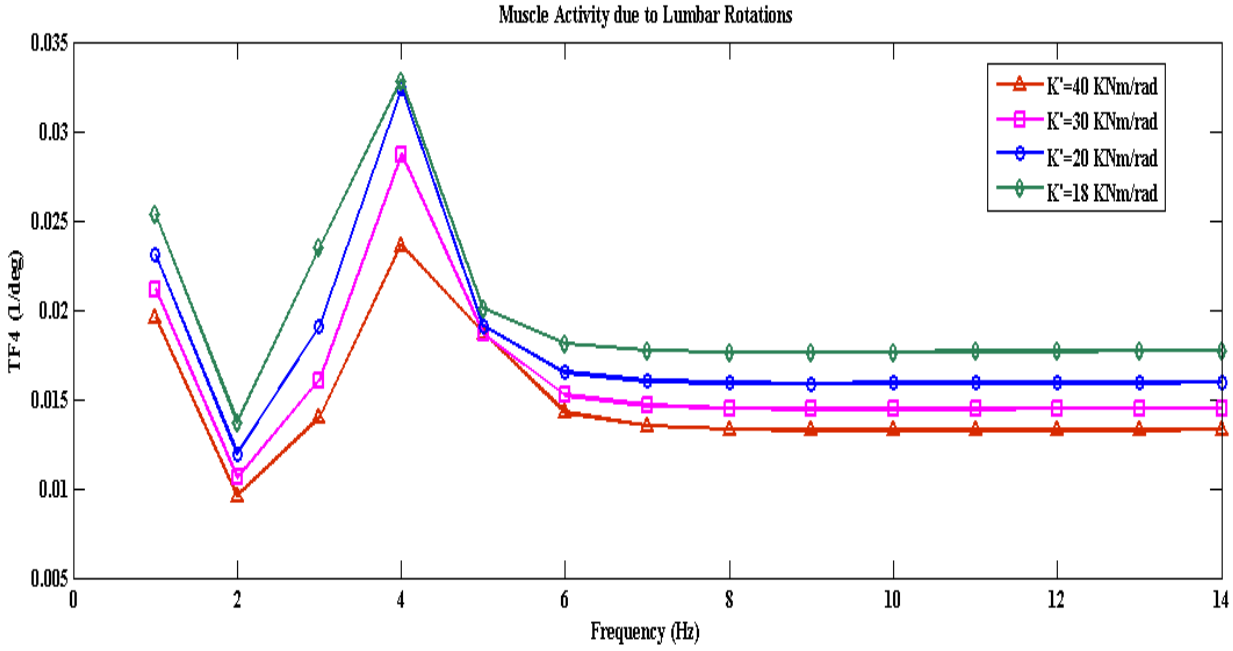

Figure 37: lumbar rotation induced muscle activity model with varying muscle stiffness

3.6 Evaluation of error between the model and experimental results:

Root mean squared error and mean errors were calculated between the experimental results and model results to visualize the deviation between the experimental results. Root mean squared error is the most commonly used measure of the differences between values predicted by model and the values obtained experimentally. Mean error is the average of the error between the model and experimental results.

3.6.1 Error between model and experimental results in TF1:

The plot below (**Figure 38**) shows the error between the values predicted by the model and experimentally obtained values for trunk acceleration transmissibility without the presence of backrest. The RMS error was found to be 0.094 at 1 RMS magnitude and .1697 at 2 RMS magnitudes. The mean errors were found to be .0804 and .1554 at 1 RMS and 2 RMS intensities respectively.

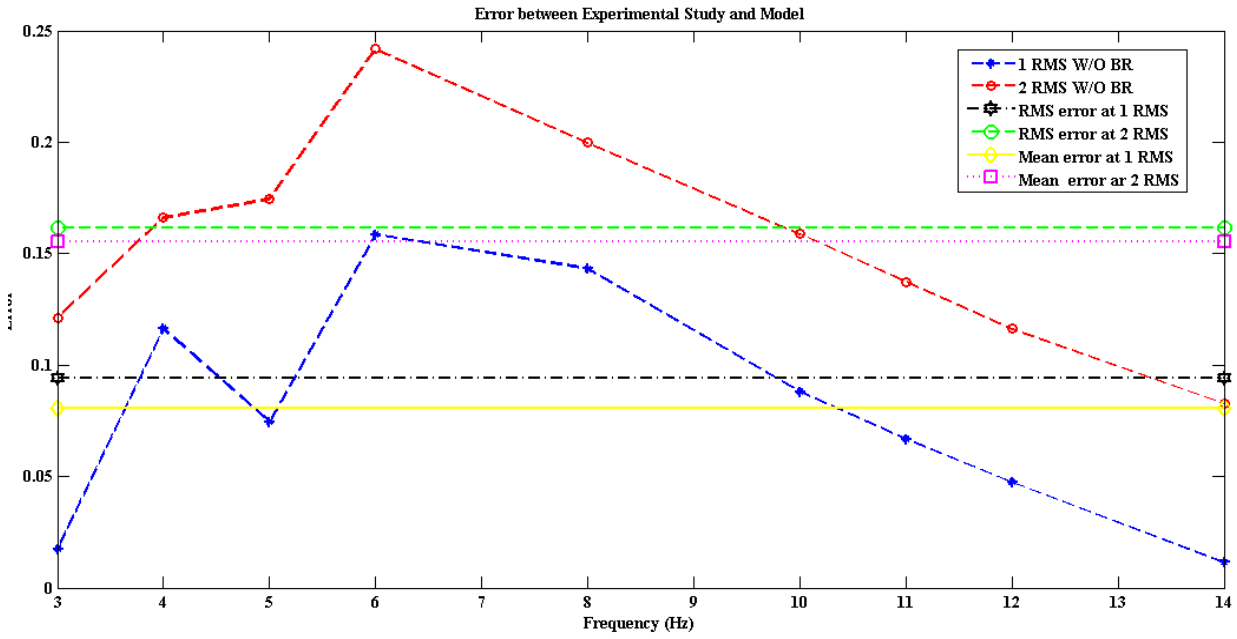

Figure 38: RMS Error for trunk acceleration transmissibility

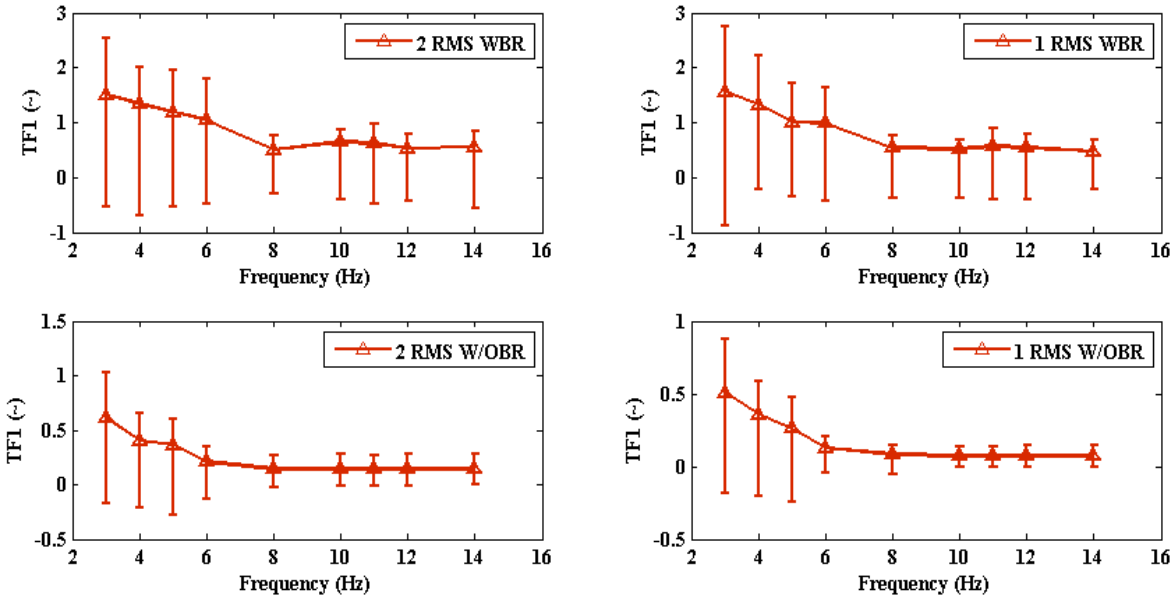

Figure 39: Deviation of experimental values for TF1

3.6.2 Error between model and experimental results in TF2:

The plot below (**Figure 40**) shows the error between the values predicted by the model and experimentally obtained values for Lumbar rotations induced due to input vibration without the presence of backrest. The RMS error was found to be 0.0894 at 1 RMS magnitude and 0.1905 at 2 RMS magnitudes. The mean errors were found to be 0.0761and 0.1347at 1 RMS and 2 RMS intensities respectively.

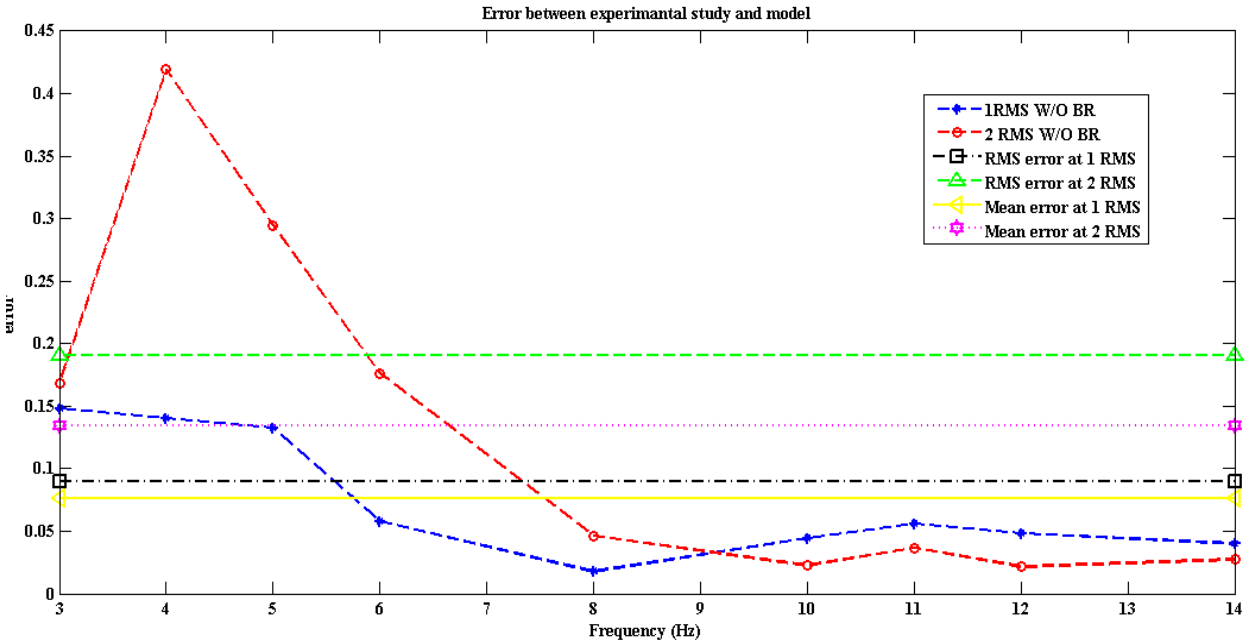

Figure 40: RMS Error for lumbar rotations due to seat pan acceleration

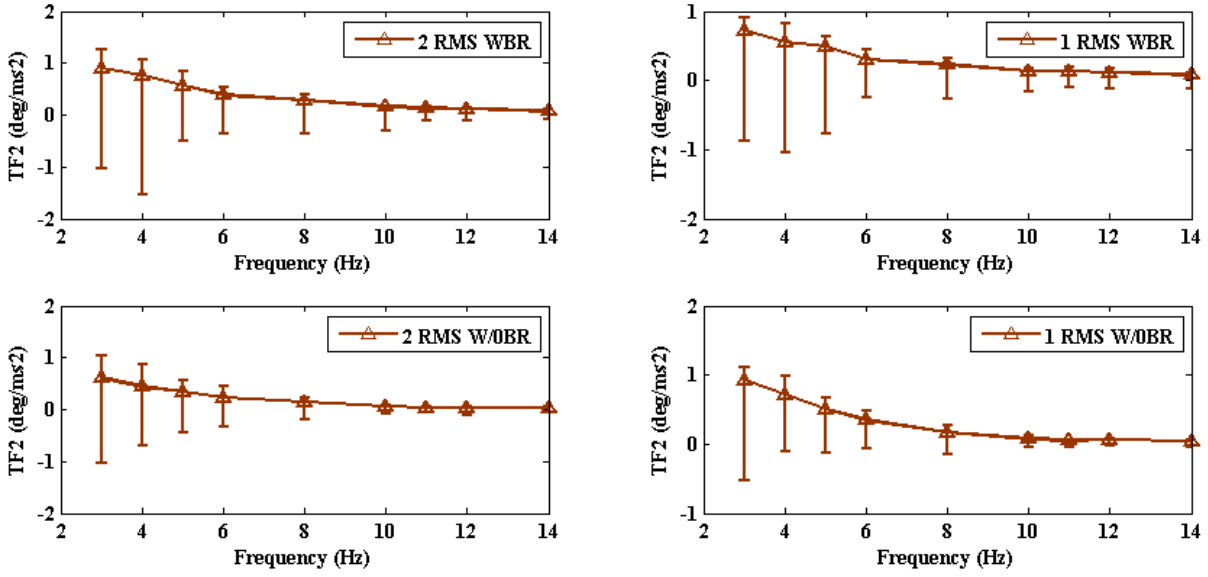

Figure 41: Deviation of experimental values for TF2

3.6.3 Error between model and experimental results in TF3:

The plot below (**Figure 42**) shows the error between the values predicted by the model and experimentally obtained values for muscle activity due to input vibration without the presence of backrest. The RMS error was found to be 0.0046 at 1 RMS magnitude and 0.0062 at 2 RMS magnitudes. The mean errors were found to be 0.0041 and 0.0056 at 1 RMS and 2 RMS intensities respectively.

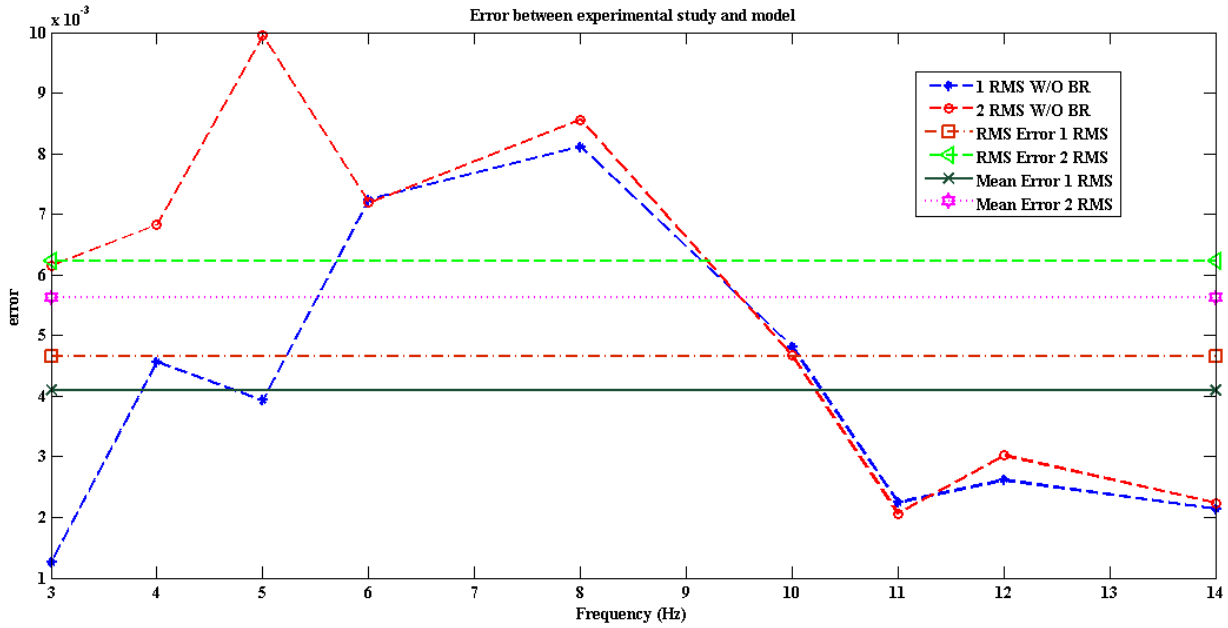

Figure 42: RMS Error for muscle activity due to seat pan acceleration

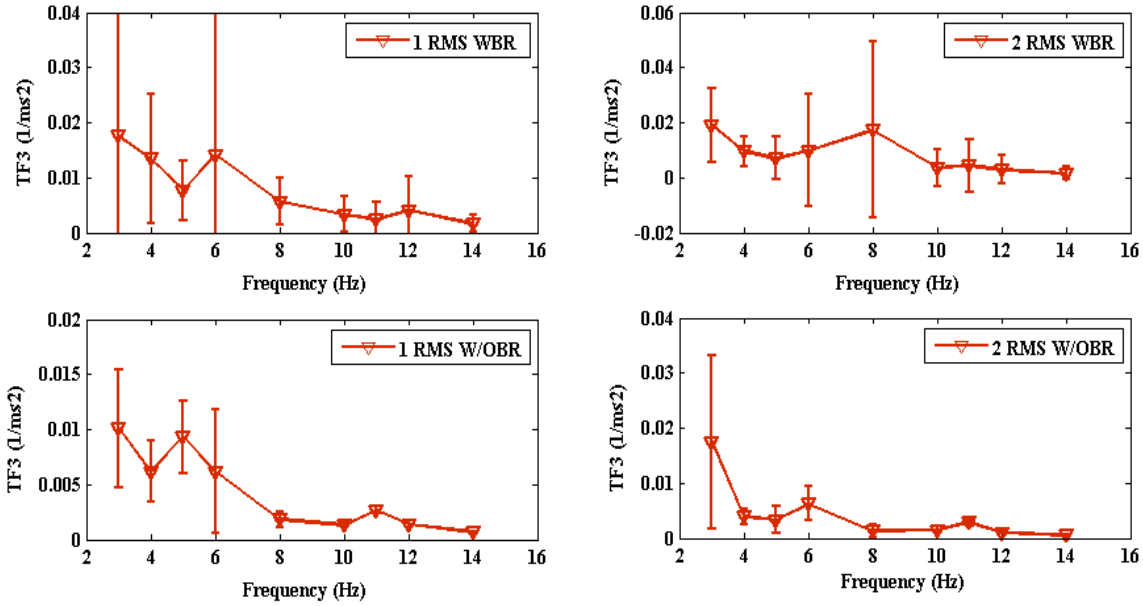

Figure 43: Deviation of experimental results for TF3

3.6.4 Error between model and experimental results in TF4:

The plot below (**Figure 44**) shows the error between the values predicted by the model and experimentally obtained values for muscle activity due lumbar rotations without the presence of backrest. The RMS error was found to be 0.0268 at 1 RMS magnitude and 0.0232 at 2 RMS magnitudes. The mean errors were found to be 0.0198 and 0.0149 at 1 RMS and 2 RMS intensities respectively.

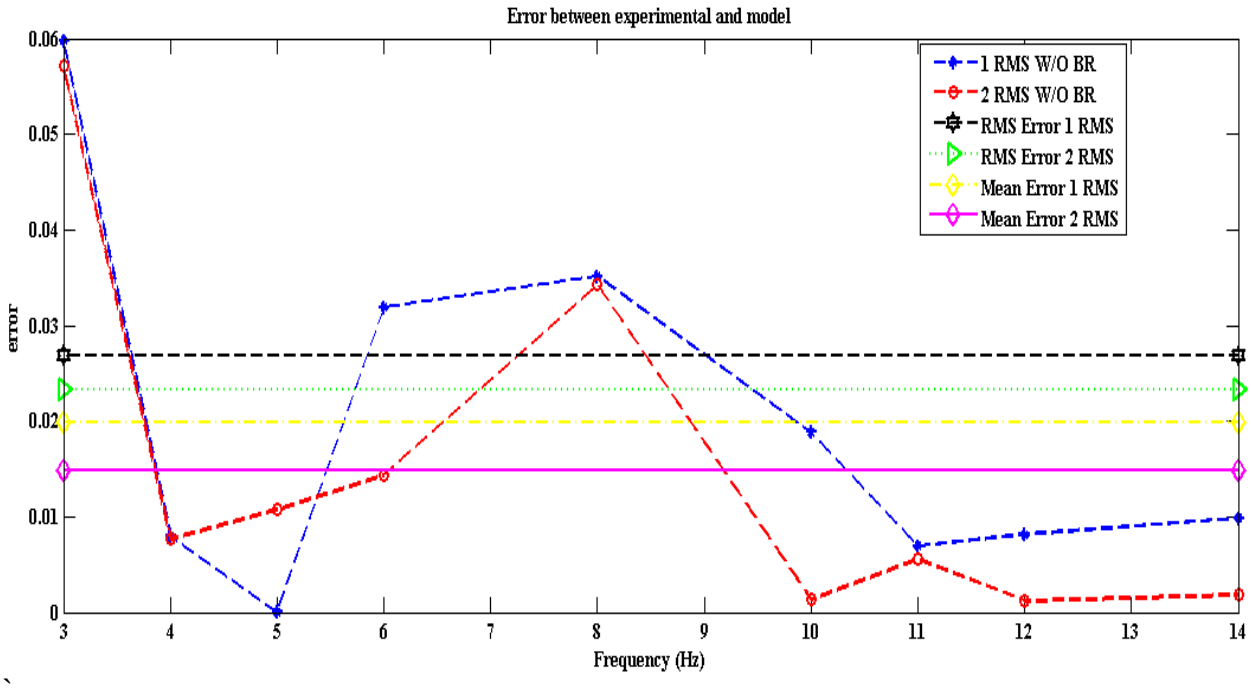

Figure 44: RMS Error for muscle activity due to lumbar rotations

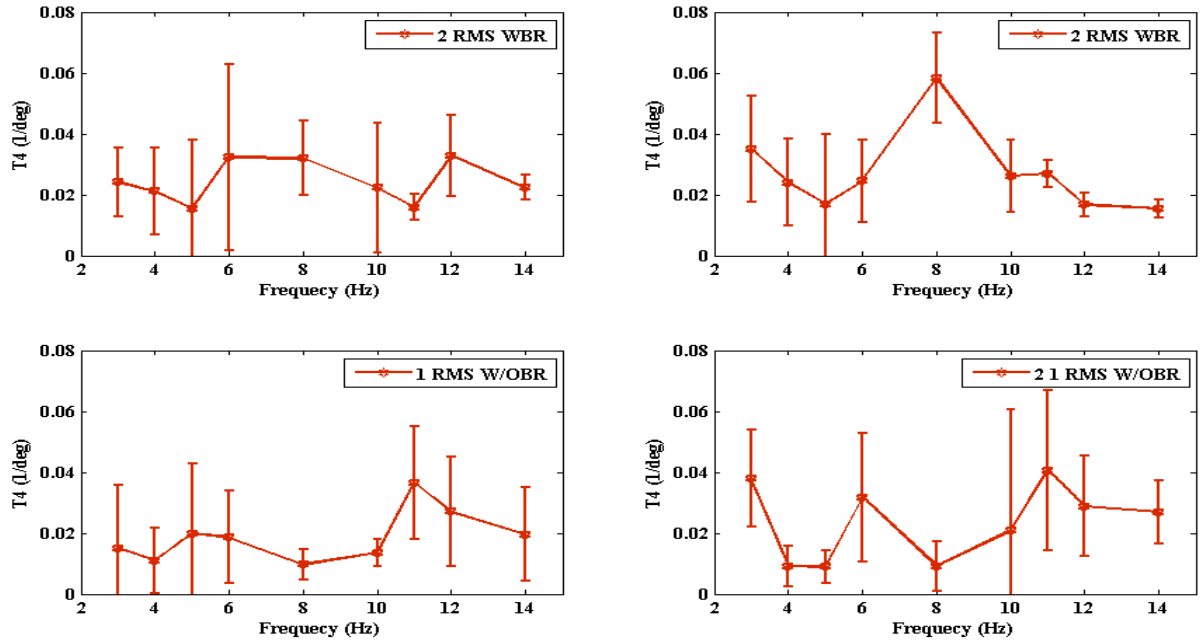

Figure 45: Deviation of experimental results for TF4

3.7 Time Delay:

Time delay was measured as offset time between the maximum input and maximum output. The average time delay between input acceleration and lumbar rotations, nEMG and input acceleration, and nEMG and lumbar rotations were calculated for all seating postures. In general time delays at 1RMS intensities were found to be higher than time delays observed at 2RMS intensities. The time delay observed between lumbar rotations and the input acceleration (lumbar rotations lagging input acceleration) (**Figure 46)** without the back rest looked consistent with a delay of about 22 ms at 3 Hz and 30 ms at 14 Hz for 1RMS intensity. The delay was about 13 ms at 3 Hz and 24 ms at 14 Hz for 2RMS intensity. In the presence of a backrest the delay was observed to decrease with increase in frequency. The average delay was about 114 ms and 156 ms at 3 Hz for 1RMS and 2 RMS intensities and about 13 ms and 73 ms at 14 Hz for 1RMS and 2RMS intensities respectively.

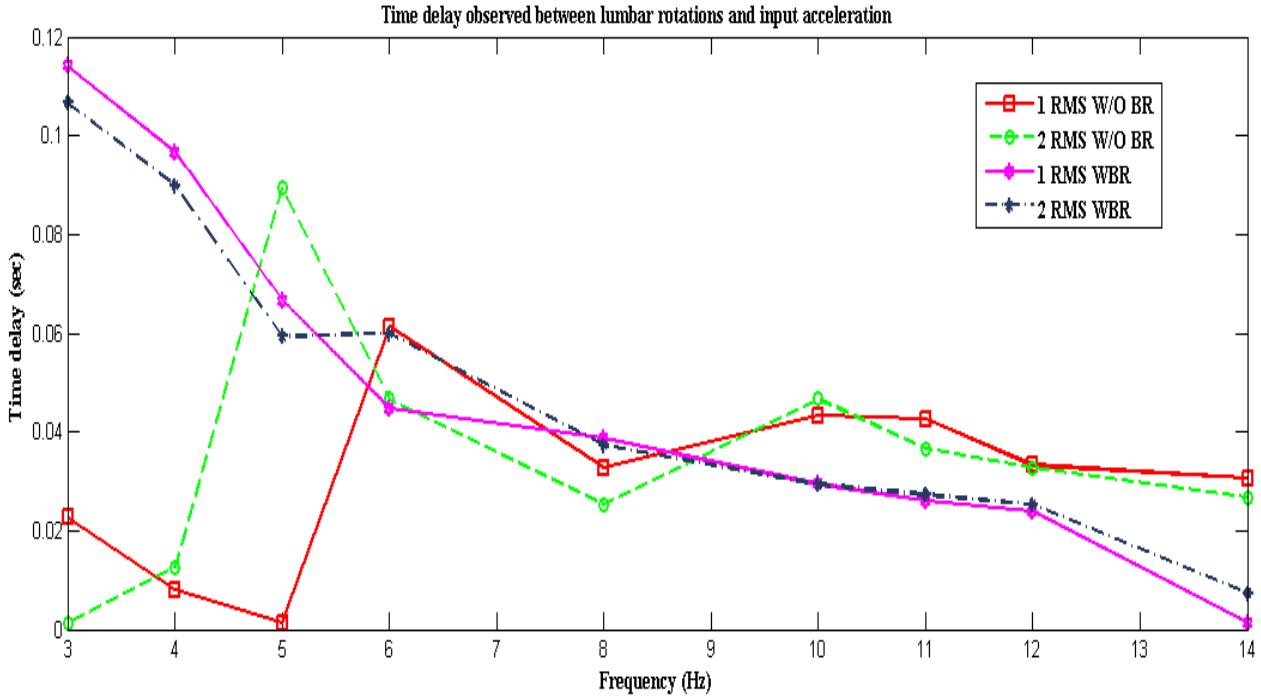

Figure 46: Time delay between lumbar rotations and input acceleration

The nEMG or the muscle activity was also observed to lag the input acceleration by about 213 ms at 3 Hz and about 44 Ms at 14 Hz for 1RMS intensity and about 161 ms at 3 Hz and about 56 ms at 14 Hz for 2RMS intensity. In the presence of backrest, a delay of 168 ms at 3 Hz and about 28 Ms at 14 Hz for 1RMS intensity and about 143 ms at 3 Hz and about 73 ms at 14 Hz for 2RMS intensity. The normal trend exhibited was reduced time delay with increase in frequency (**Figure 47**).

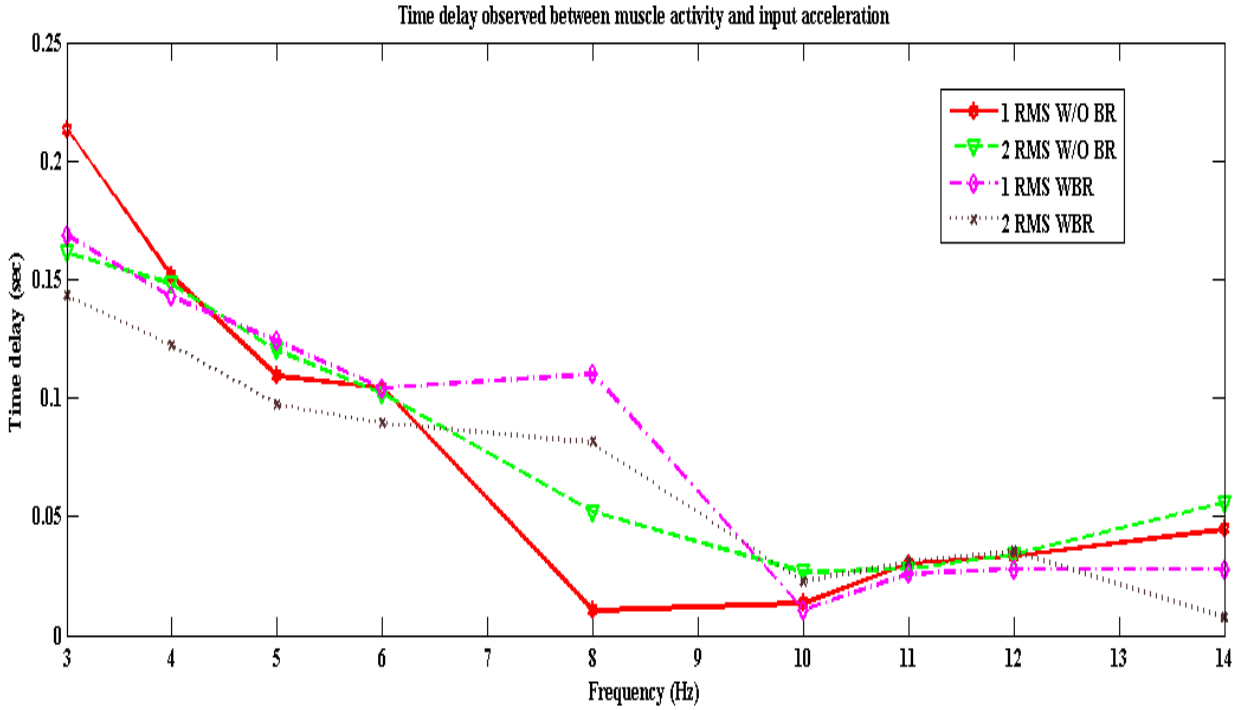

Figure 47: Time delay between muscle activity (nEMG) and input acceleration

The average time delay observed between nEMG or the muscle activity exhibited and vibration induced lumbar rotations (**Figure 48**) exhibited a gradual fall pattern with increase in frequency. The nEMG or the muscle activity was also observed to lag lumbar rotations by about 190 ms at 3 Hz and about 14 Ms at 14 Hz for 1RMS intensity and about 160 ms at 3 Hz and about 29 ms at 14 Hz for 2RMS intensity. In the presence of backrest, a delay of 250 ms at 3 Hz and about 26

Ms at 14 Hz for 1RMS intensity and about 181 ms at 3 Hz and about 26 ms at 14 Hz for 2RMS intensity. The normal trend exhibited was reduced time delay with increase in frequency.

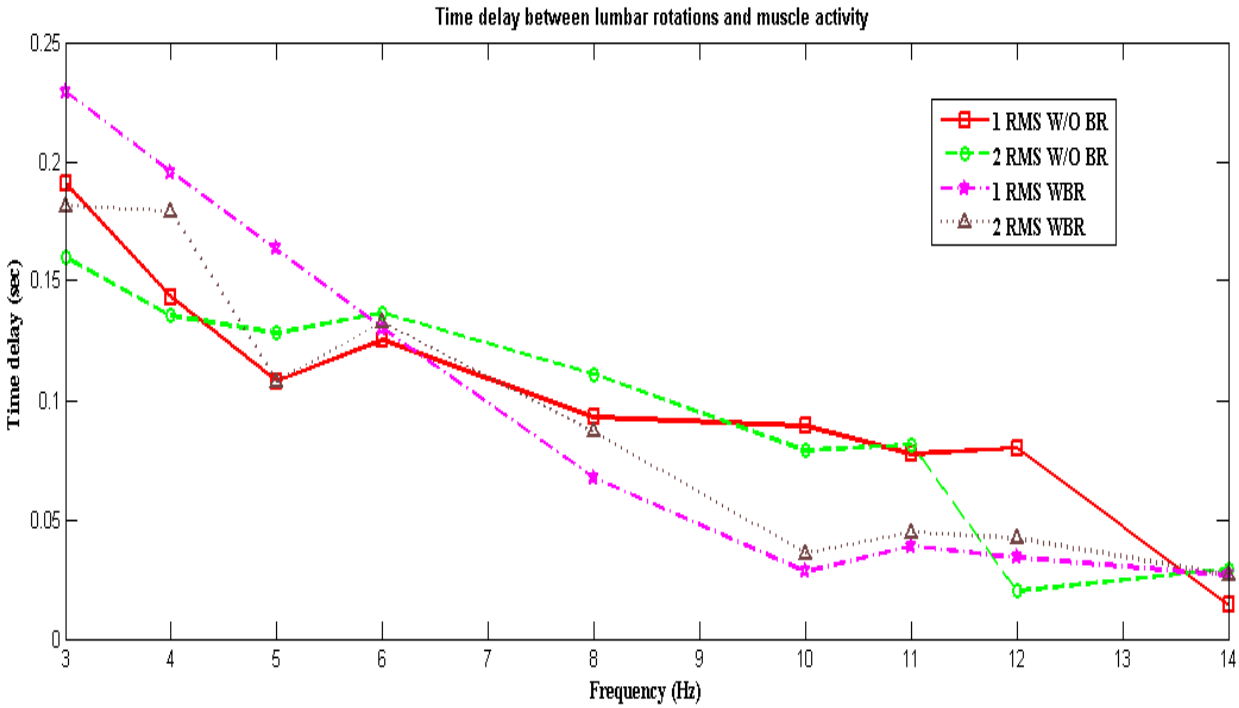

Figure 48: Time delay between lumbar rotations and muscle activity (nEMG)

3.8 Inter subject variation of transmissibility functions:

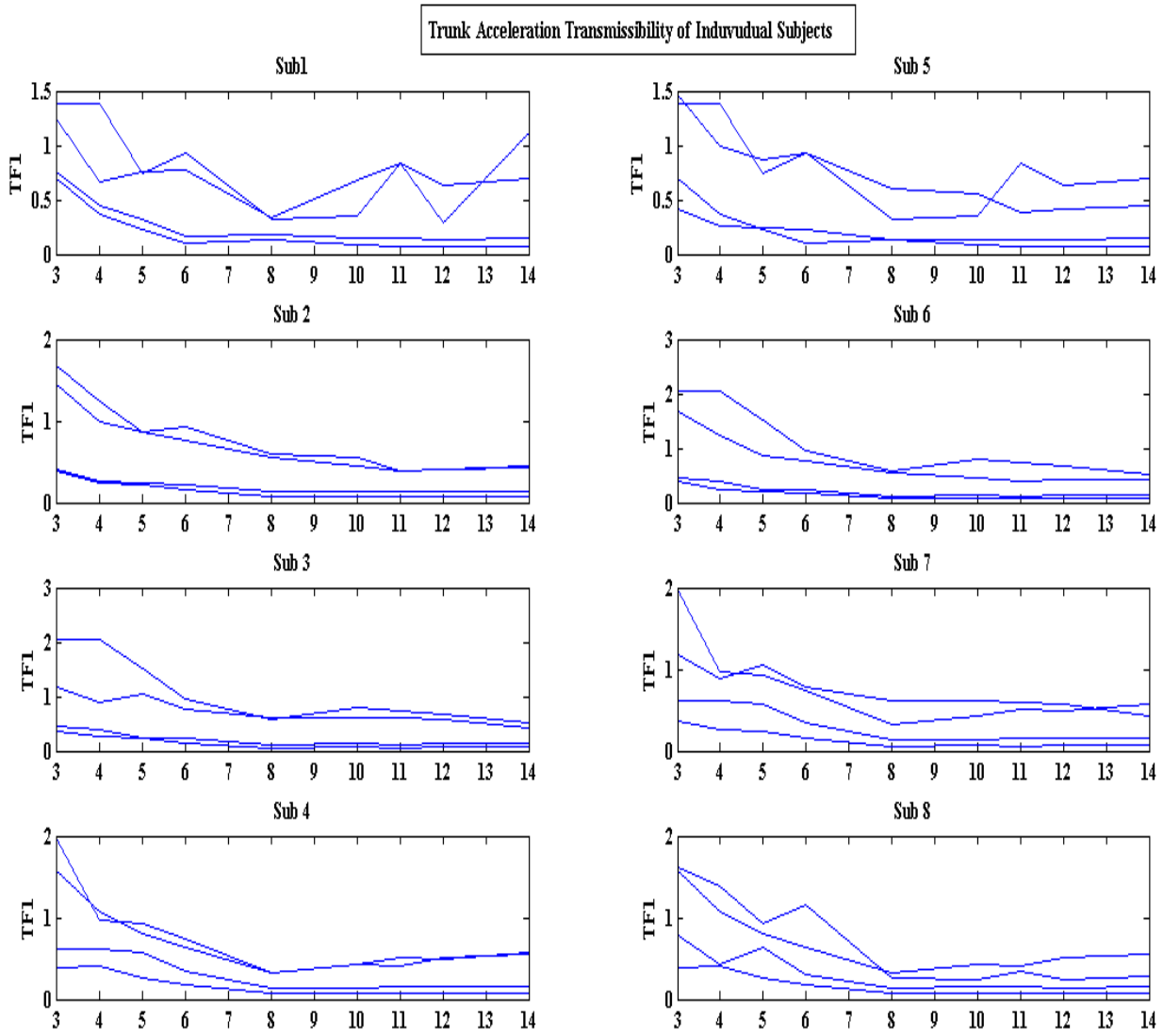

Figure 49: Trunk acceleration transmissibility plot for individual subjects

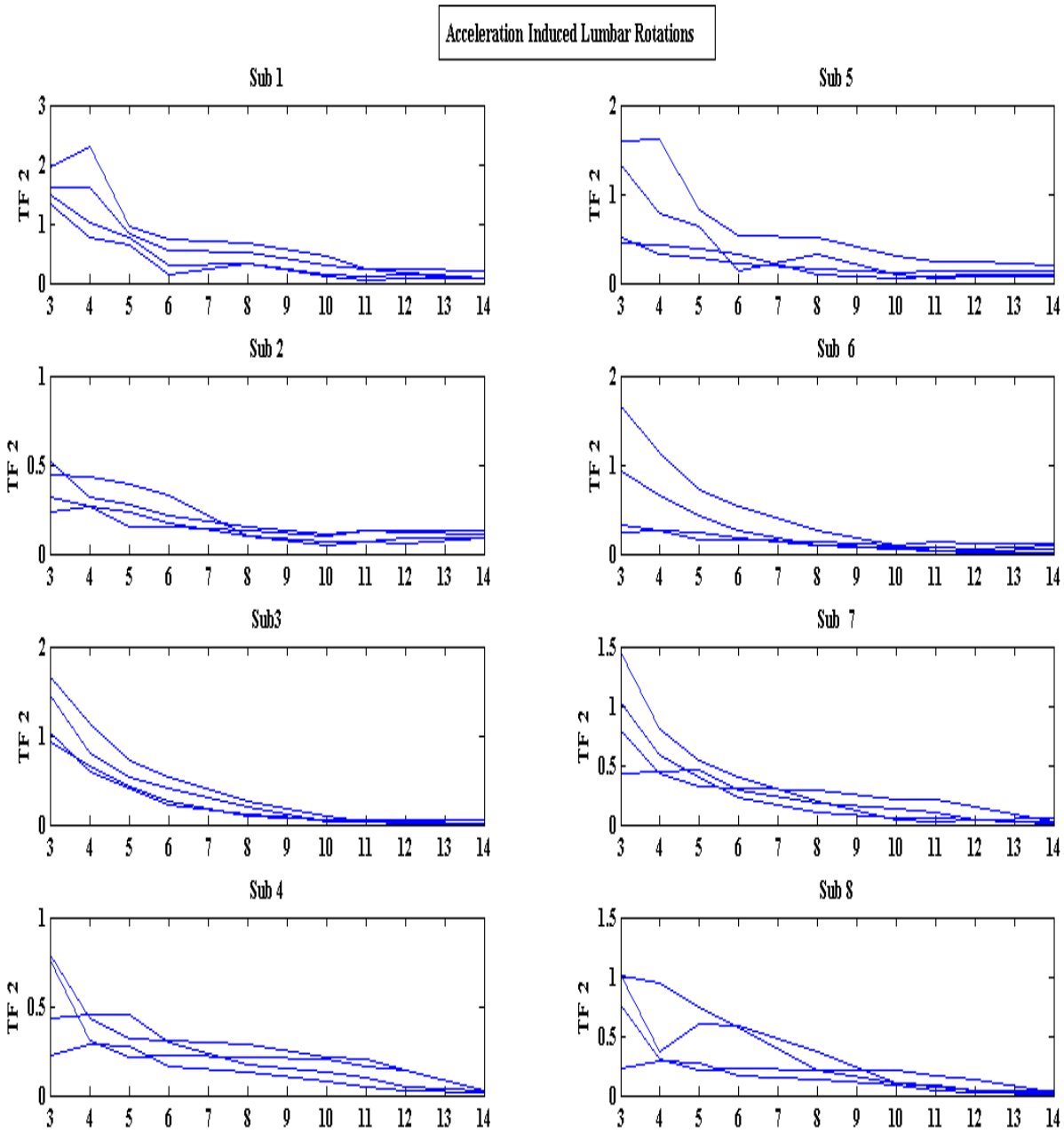

Figure 50: acceleration induced lumbar rotations plot for individual subjects

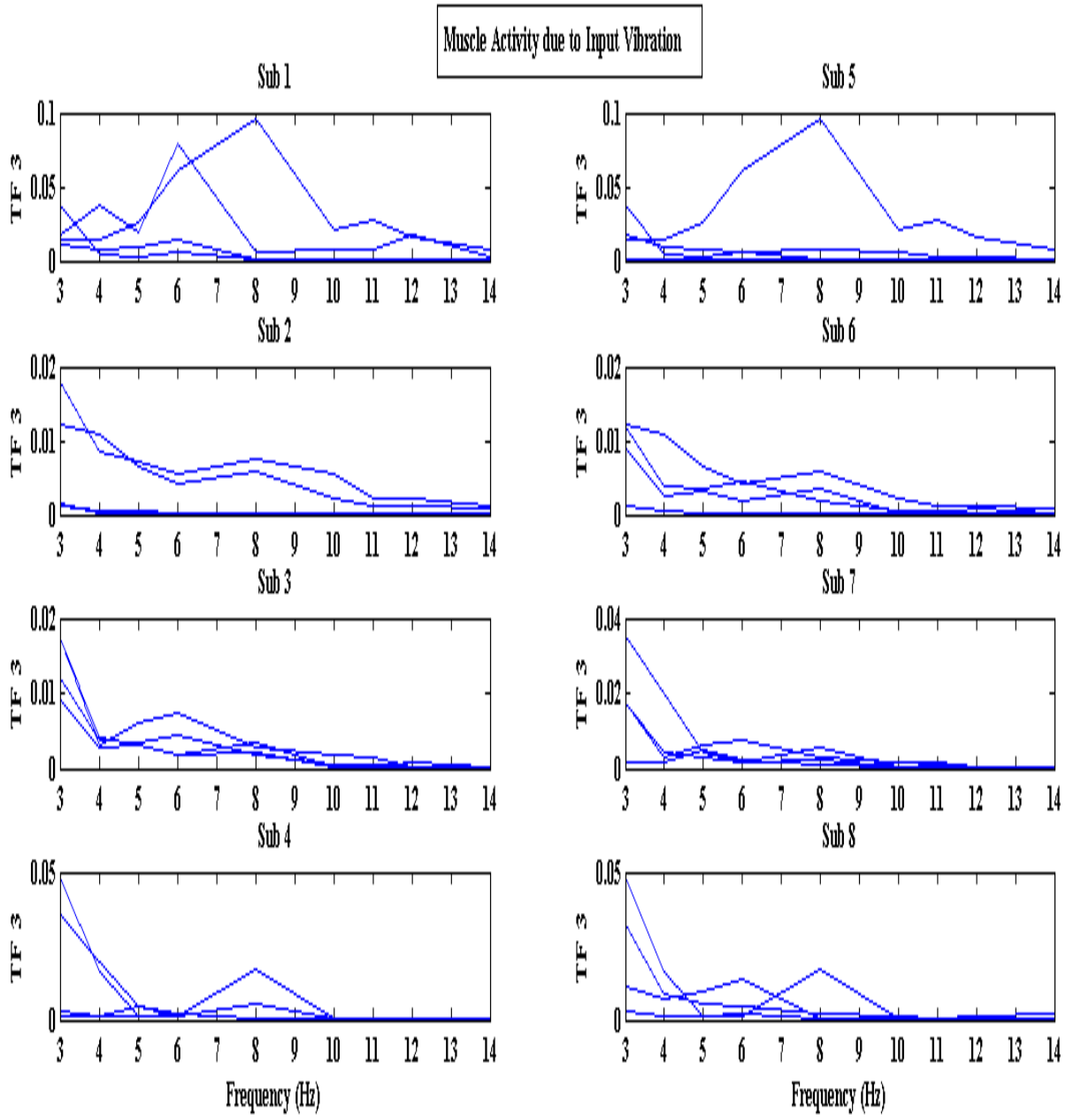

Figure 51: Muscle activity due to input acceleration plot for individual subjects

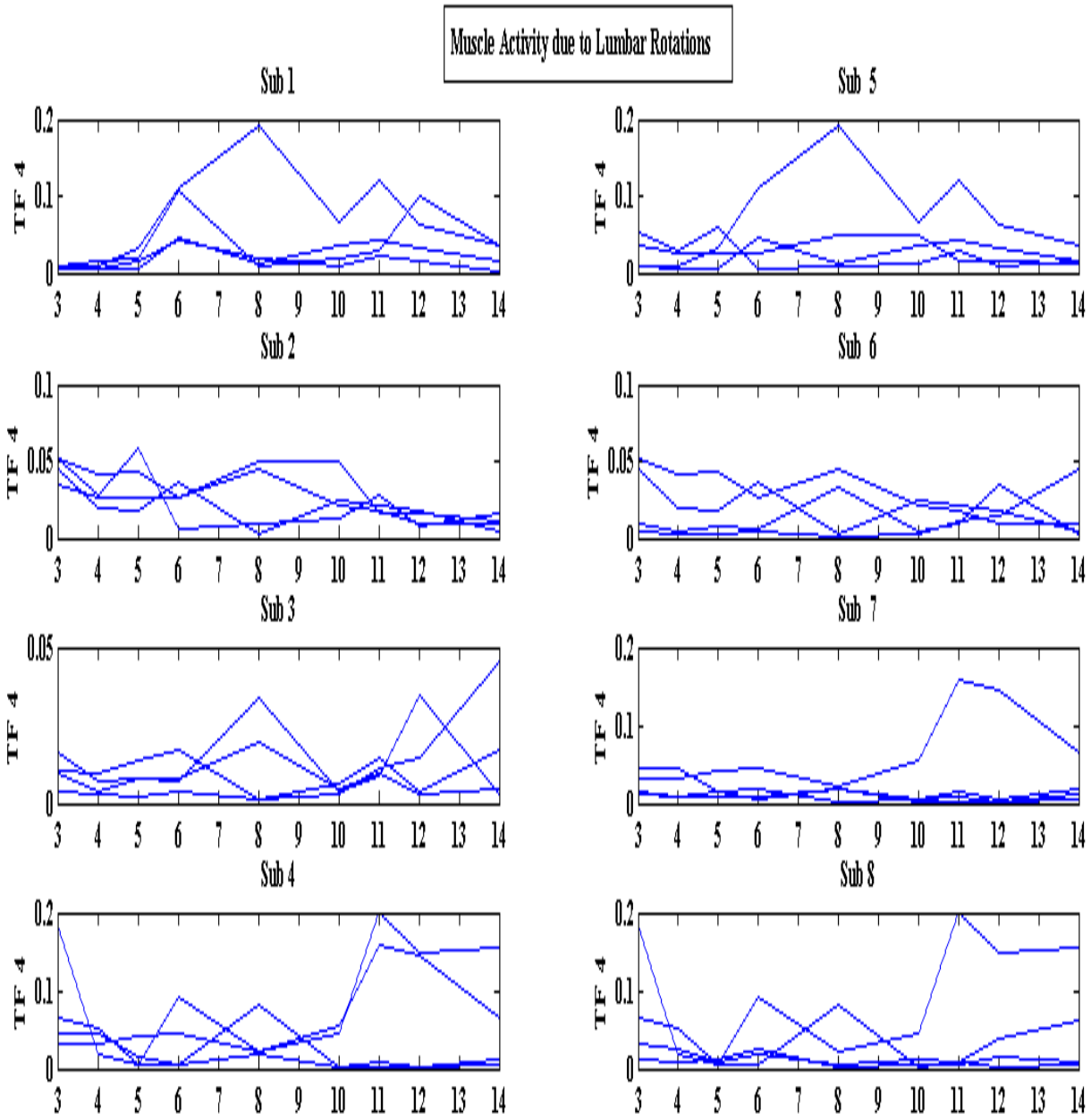

Figure 52: Muscle activity due to lumbar rotations plot for individual subjects

4. Discussion:

The specific aims of this study were to:

1. Define and experimentally measure the transmissibility functions (TF1-TF4) for horizontal set pan vibration with and without the presence of the back rest.
2. Assess transmission of fore-aft vibration to the spine rotation and erector spinae muscle activation.
3. Create a mathematical model of trunk motion, including flexion and extension in response to seatpan vibration.
4. Incorporate the muscle and reflex dynamics into the trunk motion in order to examine transmissibility of vibration to neuromotor system.
5. Study the relation between muscle activity and lumbar rotations in vibration environments.
6. Use the experimental data to validate the models of trunk motion and muscle activation.

In the present study, the transmissibility of horizontal seat pan vibration to human back was investigated with the help of a mathematical model and experimental studies for a frequency range of 3 Hz to 20 Hz. The assessment was done with by defining 4 transmissibility functions, trunk acceleration transmissibility (TF1), lumbar rotations due to input acceleration (TF2), muscle activity due to input acceleration (TF3) and muscle activity due to lumbar rotations (TF4). The time delay between the peak input and output were investigated experimentally. The experimental study was conducted with and without the presence of backrest at intensities of 1 RMS and 2 RMS. For a single muscle group (erector spine) muscle dynamics were added to the model. The results have shown that human response in vibration environment is complex and dependent on multiple variables. Understanding neuromotor transmission of whole body

vibration to the paraspinal muscles can help us understand a possible mechanism for lower back injury.

4.1 Trunk Acceleration Transmissibility (TF1)

Trunk acceleration transmissibility (TF1) was the ratio of acceleration measured at thoracic spinous process or T10 to the input horizontal seat pan vibration. The transmissibility was measured with and without the presence of back rest condition at intensities of 1 RMS and 2 RMS. The trunk acceleration transmissibility was found to decrease with increase in frequency which was consistent with the model results. A drop in trunk acceleration transmissibility from 1.6 at 3 Hz to .6 at 14 Hz and 0.6 at 3 Hz to .15 at 14 Hz was observed with and without the presence of back rest. Some insignificant peaks were observed (experimentally) in between the frequencies, but they can be attributed to the disturbances and noise in the signal.

The model exhibited a similar pattern exhibited by the experimental results with no resonance pattern between 3 Hz and 14 Hz. The model predictions were also consistent with Paddan's experimental data between 0.2 Hz to 16 Hz [135]. The limitations of electrodynamic shaker constrained the minimum experimental frequency to 3 Hz and so no resonance phenomenon was observed experimentally. The natural frequency in horizontal vibrations has been predicted to be about 2 Hz. In vertical vibration the natural frequency was found to be at about 4 Hz. The experimental and model results were consistent with literature. Paddan and Griffin [135] based on their studies concluded that horizontal seat motion results in head motion within the mid-sagittal plane. Without the presence of back rest the transmissibility of fore aft vibration was greatest at about 2 Hz. They also observed a minor peak between 6 Hz and 8 Hz. The results of head motion seemed to reduce with increase in frequency which was consistent with literature.

The model in the current study has a peak pattern below 2 Hz and a gradual decrease in transmissibility thereafter. Experimental observation of the trunk acceleration transmissibility below 3 Hz was not possible due to the limitations of the shaker.

It was observed that the presence of back rest had little effect on transmissibility to head. However in the current study it was observed that magnitude of transmissibility was found to depend of presence of back rest. The back rest used the study was a short backrest unlike the high backrest used in the current study which provided complete support in the thoracic region. The back rest condition, experiment protocol and excitation intensity can all be accounted for minor differences in transmissibilities in the two studies. The study by Barnes and Rance [136] showed the similar pattern of results in the current study and the presence of backrest induced greatest [41] back motion between 5 Hz and 10 Hz.

The trunk acceleration transmissibility measured during vertical seatpan vibration by Abraham [107, 111] showed a peak transmissibility of 1.48 and .94 at 4 Hz and the transmissibility reduced gradually thereafter with increase in frequency. With no back rest condition the transmissibility was found to be between 1.2 and 1.3 compared to a transmissibility of 0.5 to 0.6 in fore aft direction suggesting that more vibration is transmitted to lower back in vertical direction compared to horizontal direction in the frequency range of 3 Hz to 14 Hz. This attenuation can be due to soft tissues at the vibration transmission parts in the body.

4.2 Vibration Induced Lumbar Rotations TF2:

Studies have shown that vibration input in seated subjects can result in both linear and rotational movement of spine [41]. The spinal extension corresponds to anterior motion of the seat and

spinal flexions correspond to backward or posterior motion of the seat. In horizontal seat pan vibration, the fore aft movement of the thorax relative to the pelvis (which receives the input vibration) leads to the rotational movement of the spine. An electrogoniometer was used to record these anterior and posterior cycles. Based on the recordings of the electrogoniometer and the input vibration, TF2 was calculated as the ratio of lumbar rotations to input acceleration (deg/ms^-2). The magnitude of the lumbar rotations due to input acceleration was observed to reduce with increase in frequency. An average of 78% reductions in the magnitude of transmissibility was observed between 3 Hz and 14 Hz. The model also exhibited a similar pattern. The experimental results exhibited a pattern of gradual decrease in magnitude with increase in frequency. However the model showed a steep decrease in magnitude beyond 4 Hz. There was no peak or resonance pattern exhibited in the experimental study.

The model exhibited a significant peak with a magnitude greater than 1 at frequency of about 1.75 Hz. This is below 3 Hz experimental limit. It was observed that the magnitude of transmissibility shifted slightly with increase in spine stiffness. The model results were consistent with the literature. Yaw axis vibration of the body produces head vibration in all three rotational axes of the head [41]. Barnes and Rance[136] found a maximum fore-aft head response at 2 Hz when the subjects were un restrained with rapid drop at frequencies above 4 Hz. This attenuation can be attributed to the soft tissues in the vibration transmission zones in the body which reduce the linear motion and lumbar rotation.

The backrest serves as an additional input for lumbar rotations. This is because of the fact that the backrest can yields considerable interaction with the upper body. However, it was observed that the presence of backrest did not have much of impact on transmission magnitude. This suggests that while the backrest (the back rest design in the current study was such that it

restrained the posterior movement of the upper body but not the anterior movement) does move the thorax more (as evinced by TF1), trunk rocking motions are unchanged, possibly due to the stiff backrest resisting rotation motions of the trunk.

At lower frequencies the magnitude of trunk acceleration transmissibility (TF1) was greater compared to the vibration induced lumbar rotations (TF2) (significantly with the presence of backrest). This suggests that movement of thorax was greater than the movement of the pelvis at lower frequencies. The hypothesis that the cyclic movement of the spine (flexion-extension) can be diminished by the backrest was disproved at lower frequencies.

The Lumbar rotations induced by input vibration in vertical direction by Abraham showed that the transmissibility declined with increase in frequency after a peak at 4 Hz. However the magnitude of transmissibility was much smaller compared to the magnitudes observed in fore-aft vibration proving that more rotational vibration is transmitted to the lumbar spine in seated posture by fore aft vibration compared to vertical vibration [41]. If the rotations prove to be more hazardous than the extension-compression of the spine, this could lead to the conclusion that horizontal vibrations are more dangerous despite their overall high attenuation.

4.3 Vibration Induced Muscle Activity TF3:

Muscle activity was quantified using electromyography (EMG). The ratio of normalized, integrated electromyography (nEMG) to the input vibration was used to enumerate the vibration induced muscle activity. The peak to peak nEMG exhibited peaks at 8 Hz and 6 Hz for intensities 2 RMS and 1 RMS with the presence of backrest, and at 6 Hz and 5 Hz for intensities 2 RMS and 1 RMS without the presence of backrest. A significant dip was observed between 4 Hz and 5 Hz at all intensities and backrest conditions. The magnitude at peaks observed were

smaller than or equal to the magnitude at 3 Hz. Minor peaks were observed between 10 Hz and 13 Hz frequencies. The model predictions were similar to experimental predictions at lower frequencies with a peak observed at about 2.5 Hz. However no secondary peak was observed in the model predictions as found in experimental results. The magnitude of the secondary peaks was lower compared to the major peaks, suggesting that the minor peak might be because of noise rather than muscle activity. However it could also be due to resonance of reflex system as suggested by Abraham et al[111] The muscle could be acting as a biomechanical feedback element and opposing trunk forces as suggested by Seroussi et al[137]. Abraham's experiment in vertical direction showed a resonant peak between 4-6 Hz which was a result of greater muscle activity at the regions of trunk resonance. With the variation the muscle stiffness in the model the slight shift is resonance peak was observed.

4.4 Muscle Activity due to Lumbar Rotations TF4:

The response of erector spine muscle group to vibration induced, lumbar rotations was found to be relatively constant with a peak at 8 HZ for 2 RMS (ms^-2) with the presence of backrest**.** . A minor peak was observed at 12 Hz for 1 RMS with back rest. In the absence of backrest condition, a minor peak was observed at 11 Hz for 1 RMS and 2 RMS intensities. The model exhibited a very similar pattern with a resonant peak at about 4 Hz. No secondary peaks were exhibited by the model as observed in the experimental study. The minor peaks observed at higher frequencies might be because of internal resonance of the neuromuscular system. It should also be considered that the vibration transmission at higher frequencies is attenuated so the lumbar rotations and the EMG activity recorded are more susceptible to noise. It can be

observed that TF2 and TF3 show a similar transmissibility pattern. If the lumbar rotations were to influence muscle activity directly, then TF4 should have been an almost constant line over the range of frequency. However minor peaks were observed suggesting that there might be some other additional factors influencing the muscle activity. Abraham[111] suggested that the additional factors might include modes of reflex activation outside the lumbar rotation or internal resonance of the neuromotor feedback loop due to delay in the circuit timing (nonlinear frequency response). When a activated muscle experiences a length change by an external source, a reflex can be activated resulting in a increased activation of the muscle [137]. This is stretch reflex. It is this reflex which was incorporated in this model. The cyclic variation of the EMG with vibration can cause the repetitive muscle activation from this stretch reflex activation [137]. Abraham's study in vertical direction showed a peak 4 Hz to 6 Hz and at 10 Hz. It was suggested that the peak at 4 to 6 Hz was due to effect of axial vibration transmission or the effect of response feedback loops such as voluntary control. The secondary peak was attributed to internal resonance of the neuromuscular system[111]. The secondary peak in our current study could also be attributed to internal resonance of neuromuscular system although noise signals artifact is also possible. The parametric study of muscle stiffness showed an increase in magnitude but no shift in peak resonance was observed.

4.5 Time Delay:

Time delay was measured as offset time between the maximum input and maximum output. The nEMG or the muscle activity was also observed to lag the input acceleration by about 213 ms at 3 Hz and about 44 Ms at 14 Hz for 1RMS intensity and about 161 ms at 3 Hz and about 56 ms at 14 Hz for 2RMS intensity. In the presence of backrest, a delay of 168 ms at 3 Hz and about 28

Ms at 14 Hz for 1RMS intensity and about 143 ms at 3 Hz and about 73 ms at 14 Hz for 2RMS intensity. The average time delay observed between nEMG or the muscle activity exhibited and vibration induced lumbar rotations exhibited a gradual fall pattern with increase in frequency. The nEMG or the muscle activity was also observed to lag lumbar rotations by about 190 ms at 3 Hz and about 14 Ms at 14 Hz for 1RMS intensity and about 160 ms at 3 Hz and about 29 ms at 14 Hz for 2RMS intensity. In the presence of backrest, a delay of 250 ms at 3 Hz and about 26 Ms at 14 Hz for 1RMS intensity and about 181 ms at 3 Hz and about 26 ms at 14 Hz for 2RMS intensity. It should be noted that at higher frequencies the magnitude of lumbar rotations and nEMG were small, making more room for noise and other disturbances. Also the sensitivity of the goniometer was relatively low. As a result, the time delays determined experimentally might be prone to some error. Based on the hypothesis that vibration induced lumbar rotations induces the muscle activity, it can be suggested that there is a transition from voluntary to reflex-modulated erector spinae muscle response. Voluntary feedback systems are associated with longer time delays compared to monosynaptic reflexes[126]. Abraham's study in vertical direction also showed the time delays in a similar pattern. In the model time delay of 60 ms was used for lower frequencies (<= 6 Hz) and a time delay of 110 ms was used for frequencies greater than 6 Hz.

4.6 Limitations and Future Work:

There were a number of limitations in this work. First the rigid backrest data was collected but not modeled in this current study. Also experiments were conducted using a high rigid backrest condition. Other back rest orientations (low backrest, inclined backrest) should be investigated. Second, due to the limitations with the electrodynamic shaker, experimental studies were not investigated at lower frequencies (< 3Hz). Experimental investigations below 3 Hz would be

helpful for further predictions. In the model single muscle group was represented. Erector spine muscle group was represented in this model. There is a need to include multiple muscle groups. Internal and external obliques, rectus abdomens, hip muscles are few groups that can be included. Finally the model examines fore-aft vibration. A vertical vibration model needs to be developed for further investigations. Response for random or mixed frequencies should also be investigated experimentally. Further studies should investigate to see if muscle properties change with duration of exposure and posture.

4.7 Conclusions:

Transmissibility of fore-aft vibration to the low back experimentally and in the model was found to be consistent with previous literature. The mechanical model of trunk dynamics was found to have similar transmissibility and lumbar rotations as were observed experimentally. Vibration induced muscle activity and mechano-neuromotor transmission due to lumbar rotations were assessed and represented in the model. Muscle activity in fore-aft vibration was found to correspond to lumbar rotation with delays that suggest a transition from voluntary to reflex-modulated erector spinae muscle response. Understanding the transmission of vibration to neuromotor system is very important and helps in assessing a possible mechanism for lower back injury. Even though the model developed in the study is a simple model with a single muscle group incorporated, it is very important to understand the fundamentals before we can increase the complexity of the model. Human body modeling is complicated. The numbers of parameters involved are huge. There is also always inter-subject variation.

5. References:

[1] H. C. Boshuizen, et al., "Self-reported back pain in tractor drivers exposed to whole-body vibration," Int Arch Occup Environ Health, vol. 62, pp. 109-15, 1990.

[2] M. Bovenzi, "Health risks from occupational exposures to mechanical vibration," Med Lav, vol. 97, pp. 535-41, May-Jun 2006.

[3] E. Johanning, et al., "Whole-body vibration exposure in subway cars and review of adverse health effects," J Occup Med, vol. 33, pp. 605-12., 1991.

[4] S. Lings and C. Leboeuf-Yde, "Whole-body vibration and low back pain: a systematic, critical review of the epidemiological literature 1992-1999," Int Arch Occup Environ Health, vol. 73, pp. 290-7, Jul 2000.

[5] C. Tuzun, et al., "Low back pain and posture," Clin Rheumatol, vol. 18, pp. 308-12, 1999.

[6] G. B. Andersson, "Epidemiologic aspects on low-back pain in industry," Spine, vol. 6, pp. 53-60., 1981.

[7] W. L. Cats-Baril, The economics of spinal disorders, 1991

[8] M. Bovenzi and C. T. Hulshof, "An updated review of epidemiologic studies on the relationship between exposure to whole-body vibration and low back pain (1986-1997)," Int Arch Occup Environ Health, vol. 72, pp. 351-65, Sep 1999.

[9] P.-U. A. Punnett L, Nelson DI, Fingerhut MA, Leigh J, Tak S, Phillips S., "Estimating the global burden of low back pain attributable to combined occupational exposures," American Journal of Industrial Medicine, vol. 48, pp. 459-469, American Journal of Industrial Medicine 2005.

[10] F. Biering-Sorensen, "Physical measurements as risk indicators for low-back trouble over a one-year period," Spine, vol. 9, pp. 106-19, 1984.

[11] M. J. D. MacDonald, MPH; Sorock, Gary S. PhD; Volinn, Ernest PhD; Hashemi, Lobat MS; Clancy, "A Descriptive Study of Recurrent Low Back Pain Claims," Journal of Occupational & Environmental Medicine, vol. 39, pp. 35-43, 1997.

[12] S. Crown, "PSYCHOLOGICAL ASPECTS OF LOW BACK PAIN," British Society for Rheumatology, vol. 17, pp. 114-24, 1978.

[13] A. Magora, "Investigation of the relation between low back pain and occupation. VII. Neurologic and orthopedic condition," Scand J Rehabil Med, vol. 7, pp. 146-51, 1975.

[14] M. Magnusson, et al., "[Vibrations as the cause of low back pain disorders. Professional drivers are at risk]," Lakartidningen, vol. 92, pp. 1711-2., 1995.

[15] M. L. Magnusson, et al., "European Spine Society--the AcroMed Prize for Spinal Research 1995. Unexpected load and asymmetric posture as etiologic factors in low back pain," Eur Spine J, vol. 5, pp. 23-35, 1996.

[16] M. T. Manley, et al., "The load carrying and fatigue properties of the stem-cement interface with smooth and porous coated femoral components," J Biomed Mater Res, vol. 19, pp. 563-75, 1985.

[17] D. P. Manning, et al., "Body movements and events contributing to accidental and nonaccidental back injuries," Spine, vol. 9, pp. 734-9, 1984.

[18] S. J. Bigos, et al., "A prospective study of work perceptions and psychosocial factors affecting the report of back injury [published erratum appears in Spine 1991 Jun;16(6):688]," Spine, vol. 16, pp. 1-6, 1991.
[19] S. J. Bigos, et al., "Back injuries in industry: a retrospective study. III. Employee-related factors," Spine, vol. 11, pp. 252-6, 1986.
[20] D. K. Damkot, et al., "The relationship between work history, work environment and low-back pain in men," Spine, vol. 9, pp. 395-399, 1984.
[21] A. L. Backman, "Health survey of professional drivers," Scandinavian journal of work, environment, and health, vol. 9, pp. 36-41, 1983.
[22] J. W. Frymoyer, et al., "Risk factors in low-back pain. An epidemiological survey," J Bone Joint Surg Am, vol. 65, pp. 213-8., 1983.
[23] J. W. Frymoyer, et al., "Epidemiologic studies of low-back pain," Spine, vol. 5, pp. 419-23., 1980.
[24] A. B. P. D. C. CALDWELL, CHRISTOPHER, "Diagnosis and Treatment of Personality Factors in Chronic Low Back Pain," CALDWELL, ALEX B. PH.D.; CHASE, CHRISTOPHER, vol. 129, pp. 141-149, November/December 1977 1977.
[25] S. K. M. Tyson A.C. Beach, Jack P. Callaghan, "The effects of a continuous passive motion device on myoelectric activity of the erector spinae during prolonged sitting at a computer workstation," Work (Reading, Mass.), vol. 20, 01/01/2003 2002.
[26] M. H. Pope, K.L. Goh, and M.L. Magnusson,, "Annual Review of Biomedical Engineering," SPINE ERGONOMICS, vol. 4, pp. 49-68, 2002.
[27] M. L. Magnusson, et al., "Are occupational drivers at an increased risk for developing musculoskeletal disorders?," Spine, vol. 21, pp. 710-7., 1996.
[28] G. R. Hazard, "Continuous Passive Lumbar Spinal Motion: The BackCycler® System for Preventing Low Back Discomfort, Stiffness and Fatigue During Sitting," Society of Automotive Engineers,, 2000.
[29] D. D. Seidel . H., "Selected health risks caused by long-term, whole-body vibration," American Journal of Industrial Medicine, vol. 23, 1992.
[30] M. Bovenzi, "Low back pain disorders and exposure to whole-body vibration in the workplace," Semin Perinatol, vol. 20, pp. 38-53, Feb 1996.
[31] M. Bovenzi, "Health effects of mechanical vibration," G Ital Med Lav Ergon, vol. 27, pp. 58-64, Jan-Mar 2005.
[32] M. Fritz, "Simulating the response of a standing operator to vibration stress by means of a biomechanical model," J Biomech, vol. 33, pp. 795-802., 2000.
[33] M. H. Pope, Hansson, T.H., "Vibration of the spine and low back pain," Clinical Orthopaedics and Related Research, vol. 279, pp. 49-59, 1992.
[34] M. H. Pope and T. H. Hansson, "Vibration of the spine and low back pain," Clin Orthop Relat Res, pp. 49-59, Jun 1992.
[35] M. H. Pope, et al., "The effect of vibration on back discomfort and serum levels of von Willebrand factor antigen: a preliminary communication," Eur Spine J, vol. 3, pp. 143-5, 1994.
[36] M. H. Pope, et al., "The role of the musculature in injuries to the medial collateral ligament," J Bone Joint Surg [Am], vol. 61, pp. 398-402, 1979.
[37] M. H. Pope, et al., "The upper extremity attenuates intermediate frequency vibrations," J Biomech, vol. 30, pp. 103-8, 1997.

[38] M. H. Pope, et al., "Kappa Delta Award. Low back pain and whole body vibration," Clin Orthop, pp. 241-8., 1998.
[39] M. H. Pope, et al., "The response of the seated human to sinusoidal vibration and impact," J Biomech Eng, vol. 109, pp. 279-84., 1987.
[40] M. H. Pope, et al., "A review of studies on seated whole body vibration and low back pain," Proc Inst Mech Eng [H], vol. 213, pp. 435-46, 1999.
[41] M. J. Griffin, Handbook of human vibration. London, England: Academic Press Limited, 1990.
[42] S. Kitazaki and M. J. Griffin, "Resonance behaviour of the seated human body and effects of posture," J Biomech, vol. 31, pp. 143-9, 1998.
[43] Y. Matsumoto and M. J. Griffin, "Non-linear characteristics in the dynamic responses of seated subjects exposed to vertical whole-body vibration," J Biomech Eng, vol. 124, pp. 527-32, Oct 2002.
[44] G. S. Paddan and M. J. Griffin, "The transmission of translational seat vibration to the head--I. Vertical seat vibration," J Biomech, vol. 21, pp. 191-7, 1988.
[45] C. T. Hulshof, et al., "Evaluation of an occupational health intervention programme on whole-body vibration in forklift truck drivers: a controlled trial," Occup Environ Med, vol. 63, pp. 461-8, Jul 2006.
[46] S. Lings and C. Leboeuf-Yde, "[Whole body vibrations and low back pain]," Ugeskr Laeger, vol. 160, pp. 4298-301, Jul 13 1998.
[47] M. K. Patil and M. S. Palanichamy, "A mathematical model of tractor-occupant system with a new seat suspension for minimization of vibration response," Appl Math Modeling, vol. 12, pp. 63-71, 1988.
[48] M. S. Mansfield J.Neil, "The apparent mass of the seated human exposed to single-axis and multi-axis whole-body vibration," Journal of Biomechanics, vol. 40, 2006.
[49] L. Li, et al., "Whole body vibration alters proprioception in the trunk," International Journal of Industrial Engineering, vol. 38, pp. 792-800, 2008.
[50] B. L. Hagberg. M., "The association between whole body vibration exposure and musculoskeletal disorders in the Swedish work force is confounded by lifting and posture," Journal of Sound and Vibration, vol. 298, pp. 492-498, 2006.
[51] A. F. Abercromby, et al., "Vibration exposure and biodynamic responses during whole-body vibration training," Med Sci Sports Exerc, vol. 39, pp. 1794-800, Oct 2007.
[52] N. Alem, "Application of the new ISO 2631-5 to health hazard assessment of repeated shocks in U.S. Army vehicles," Ind Health, vol. 43, pp. 403-12, Jul 2005.
[53] H. C. Boshuizen, et al., "Long-term sick leave and disability pensioning due to back disorders of tractor drivers exposed to whole-body vibration," Int Arch Occup Environ Health, vol. 62, pp. 117-22, 1990.
[54] A. P. Cann, et al., "Predictors of whole-body vibration exposure experienced by highway transport truck operators," Ergonomics, vol. 47, pp. 1432-53, Oct 22 2004.
[55] K. M. Cornelius, et al., "Postural Stability after Whole-Body Vibration Exposure," International Journal of Industrial Ergonomics, vol. 13, pp. 343-351, Jun 1994.
[56] C. Delecluse, et al., "Strength increase after whole-body vibration compared with resistance training," Med Sci Sports Exerc, vol. 35, pp. 1033-41, Jun 2003.
[57] C. T. Haas, et al., "The effects of random whole-body-vibration on motor symptoms in Parkinson's disease," NeuroRehabilitation, vol. 21, pp. 29-36, 2006.

[58] A. Sullivan and S. M. McGill, "Changes in spine length during and after seated whole-body vibration," Spine, vol. 15, pp. 1257-60, Dec 1990.
[59] S. Turbanski, et al., "Effects of random whole-body vibration on postural control in Parkinson's disease," Res Sports Med, vol. 13, pp. 243-56, Jul-Sep 2005.
[60] C. L. Zimmermann and T. M. Cook, "Effects of vibration frequency and postural changes on human responses to seated whole-body vibration exposure," Int Arch Occup Environ Health, vol. 69, pp. 165-79, 1997.
[61] V. K. Gade and S. E. Wilson, "Variations in reposition sense in the lumbar spine with torso flexion and moment load," in American Society of Mechanical Engineers Summer Bioengineering Conference, Key Biscayne, FL, 2003.
[62] M. J. Griffin and M. W. Brett, "Effects of fore-and-aft, lateral and vertical whole-body vibration on a head-positioning task," Aviat Space Environ Med, vol. 68, pp. 1115-22., 1997.
[63] M. J. Griffin, et al., "Vibration and comfort. I. translational seat vibration," Ergonomics, vol. 25, pp. 603-630, 1982.
[64] N. J. Mansfield and M. J. Griffin, "Non-linearities in apparent mass and transmissibility during exposure to whole-body vertical vibration," J Biomech, vol. 33, pp. 933-41, 2000.
[65] G. M. Mansfield NJ, "Difference thresholds for automobile seat vibration," Applied Ergonomics, vol. 31, pp. 255-261, 2000.
[66] B. R. Ronnestad, "Comparing the performance-enhancing effects of squats on a vibration platform with conventional squats in recreationally resistance-trained men," J Strength Cond Res, vol. 18, pp. 839-45, Nov 2004.
[67] P. M. Bongers, et al., "Long-term sickness absence due to back disorders in crane operators exposed to whole-body vibration," Int Arch Occup Environ Health, vol. 61, pp. 59-64, 1988.
[68] P. M. Bongers, et al., "Back disorders in crane operators exposed to whole-body vibration," Int Arch Occup Environ Health, vol. 60, pp. 129-37, 1988.
[69] M. Cardinale and C. Bosco, "The Use of Vibration as an Exercise Intervention," Exercise and Sport Sciences Reviews, vol. 31, pp. 3-7, 2003.
[70] M. Cardinale and J. Rittweger, "Vibration exercise makes your muscles and bones stronger: fact or fiction?," J Br Menopause Soc, vol. 12, pp. 12-8, Mar 2006.
[71] D. Adamo, et al., "Vibration-induced muscle fatigue, a possible contribution to musculoskeletal injury," European Journal of Applied Physiology, vol. 88, pp. 134-140, 2002.
[72] S. O. Vøllestad NK, "Biochemical correlates of fatigue. A brief review," European Journal for applied physiology and occupational physiology, vol. 57, pp. 336-347, 1988.
[73] D. G. Wilder, et al., "The biomechanics of lumbar disc herniation and the effect of overload and instability," J Spinal Disord, vol. 1, pp. 16-32, 1988.
[74] D. G. Wilder, et al., "Vibration and the human spine," Spine, vol. 7, pp. 243-54., 1982.
[75] G. B. a. D. F. J. Rittweger, "Acute physiological effects of exhaustive whole-body vibration exercise in man," Institute of Physiology, Freie UniversitaÈ t Berlin, Arnimallee, Berlin1999.
[76] V. J. Romaiguère P, Pagni S., "Effects of tonic vibration reflex on motor unit recruitment in human wrist extensor muscles.," Brain Research, vol. 602, pp. 32-40, 1993.

[77] S. Torvinen, et al., "Effect of 4-min vertical whole body vibration on muscle performance and body balance: a randomized cross-over study," Int J Sports Med, vol. 23, pp. 374-9, Jul 2002.
[78] D. Cochrane, et al., "Acute whole-body vibration elicits post-activation potentiation," European Journal of Applied Physiology, vol. 108, pp. 311-319, 2010.
[79] J. A. Feagin, Jr. and K. L. Lambert, "Mechanism of injury and pathology of anterior cruciate ligament injuries," Orthop Clin North Am, vol. 16, pp. 41-5, 1985.
[80] A. G. Feldman and M. I. Latash, "Inversions of vibration-induced senso-motor events caused by supraspinal influences in man," Neuroscience Letters, vol. 31, pp. 147-151, 1982.
[81] A. G. Feldman and M. L. Latash, "Inversions of vibration-induced senso-motor events caused by supraspinal influences in man," Neurosci Lett, vol. 31, pp. 147-51, 1982.
[82] M. A. Adams, et al., "Personal risk factors for first-time low back pain," Spine, vol. 24, pp. 2497-505, 1999.
[83] M. A. Adams, et al., "Sustained loading generates stress concentrations in lumbar intervertebral discs," Spine, vol. 21, pp. 434-8, 1996.
[84] J. C. Iatridis, Weidenbaum, M., Setton, L.A., Mow, V.C., "Is the Nucleus Pulposus a Solid or a Fluid? Mechanical Behaviors of the Nucleus Pulposus of the Human Intervertebral Disc," Spine, vol. 21, pp. 1174-1184, 1996.
[85] M. Solomonow, et al., "Biomechanics of increased exposure to lumbar injury caused by cyclic loading: Part 1. Loss of reflexive muscular stabilization," Spine, vol. 24, pp. 2426-34, 1999.
[86] M. Solomonow, et al., "Mechanoreceptors and reflex arc in the feline shoulder," J Shoulder Elbow Surg, vol. 5, pp. 139-46, 1996.
[87] M. Solomonow, et al., "EMG-force model of the elbows antagonistic muscle pair. The effect of joint position, gravity and recruitment," Am J Phys Med, vol. 65, pp. 223-44, 1986.
[88] M. Solomonow, et al., "Biomechanics and electromyography of a common idiopathic low back disorder," Spine, vol. 28, pp. 1235-48, Jun 15 2003.
[89] L. Kazarian, "Creep characteristics of the human spinal column," Orthop Clin North Am, vol. 6, pp. 3-18, 1975.
[90] U. Klingenstierna and M. H. Pope, "Body height changes from vibration," Spine, vol. 12, pp. 566-8, Jul-Aug 1987.
[91] T. S. Keller, et al., "Validation of the force and frequency characteristics of the activator adjusting instrument: effectiveness as a mechanical impedance measurement tool," J Manipulative Physiol Ther, vol. 22, pp. 75-86., 1999.
[92] T. S. Keller, et al., "Mechanical behavior of the human lumbar spine. I. Creep analysis during static compressive loading," J Orthop Res, vol. 5, pp. 467-78, 1987.
[93] G. P. Slota, et al., "Effects Of Seated Whole-Body Vibration On Seated Postural Sway " in North American Congress on Biomechanics, Ann Arbor, MI, 2008.
[94] S. M. L. Bryan L. Riemann., "The Sensorimotor System, Part I: The Physiologic Basis of Functional Joint Stability," Journal of Athletic Training, vol. 37, pp. 71-79, 2002.
[95] S. Brumagne, et al., "The role of paraspinal muscle spindles in lumbosacral position sense in individuals with and without low back pain," Spine, vol. 25, pp. 989-94., 2000.

[96] S. Brumagne, et al., "Proprioceptive weighting changes in persons with low back pain and elderly persons during upright standing," Neurosci Lett, vol. 366, pp. 63-6, Aug 5 2004.
[97] S. D. Cook, et al., "Upper extremity proprioception in idiopathic scoliosis," Clin Orthop, pp. 118-24, 1986.
[98] J. P. Roll and J. P. Vedel, "Kinaesthetic role of muscle afferents in man, studied by tendon vibration and microneurography," Exp Brain Res, vol. 47, pp. 177-90, 1982.
[99] M. Arashanapalli and S. E. Wilson, "Vibration alters proprioception and dynamic low back stability," in XXth Congress of the International Society of Biomechanics and 29th Annual Meeting of the American Society of Biomechanics, Cleveland, Ohio, 2005.
[100] L. Q. Zhang, et al., "In vivo human knee joint dynamic properties as functions of muscle contraction and joint position," J Biomech, vol. 31, pp. 71-6, 1998.
[101] M. S. Palanichamy, et al., "Minimization of the vertical vibrations sustained by a tractor operator, by provision of a standard-type tractor seat suspension," Ann Biomed Eng, vol. 6, pp. 138-53, 1978.
[102] J. Griffin. Michael, "The validation of biodynamic models," Clinical biomechanics (Bristol, Avon), vol. 16, pp. S81-S92, 2001.
[103] Y. Matsumoto and M. J. Griffin, "DYNAMIC RESPONSE OF THE STANDING HUMAN BODY EXPOSED TO VERTICAL VIBRATION: INFLUENCE OF POSTURE AND VIBRATION MAGNITUDE," Journal of Sound and Vibration, vol. 212, pp. 85-107, 1998.
[104] T. E. Fairley and M. J. Griffin, "The apparent mass of the seated human body: vertical vibration," J Biomech, vol. 22, pp. 81-94, 1989.
[105] R. R. Coermann, "THE MECHANICAL IMPEDANCE OF THE HUMAN BODY IN SITTING AND STANDING POSITION AT LOW FREQUENCIES,," Hum Factors., pp. 227-53, Oct 1962.
[106] J. Sandover, Dupuis, H., "A Reanalysis of Spinal motion During Vibration," Ergonomics, vol. 30, pp. 975-985, 1987.
[107] P. M. Abraham and S. E. Wilson, "Whole body vibration and neuromuscular response," in ASME Summer Bioengineering Conference, Amelie Island, Florida, 2006.
[108] P. M. Abraham and S. E. Wilson, "Effects of a lumbar belt on neuromotor transmission of whole body vibration," in American Society of Mechanical Engineers International Mechanical Engineering Congress and Exposition, Seattle, WA, 2007.
[109] M. Demic and J. Lukic, "Investigation of the transmission of fore and aft vibration through the human body," Applied Ergonomics, vol. 40, pp. 622-629, 2009.
[110] "ISO 2631 Internation Standard," vol. 2nd edition, 1997.
[111] P. Abraham, "Whole body vibration neuromotor transmissibility," Mechanical Engineering, University of Kansas, Lawrence, 2006.
[112] W. K. T. Shier.D.R., Applied Mathematical Modelling A Multidisciplinary approch: CHAPMAN & HALL/CRC.
[113] J. G. Michael, "The validation of biodynamic models," Clinical biomechanics (Bristol, Avon), vol. 16, pp. S81-S92, 2001.
[114] M. Zoghi-Moghadam, et al., "Biodynamics model for operator head injury in stand-up lift trucks," Computer Methods in Biomechanics and Biomedical Engineering, vol. 11, pp. 397 - 405, 2008.

[115] G. J. WEI. L., "The prediction of seat transmissibility from measures of seat impedance," Journal of sound and vibration, vol. 214, pp. 121-137, 1998.
[116] Mertens.H., "Nonlinear behavior of sitting humans under increasing gravity.," Aviat Space Environ Med., vol. 49 part 2, pp. 287-98, 1978.
[117] R. Muksian and C. D. Nash Jr, "A model for the response of seated humans to sinusoidal displacements of the seat," Journal of Biomechanics, vol. 7, pp. 209-215, 1974.
[118] N. Nawayseh and M. J. Griffin, "Non-linear dual-axis biodynamic response to vertical whole-body vibration," Journal of Sound and Vibration, vol. 268, pp. 503-523, 2003.
[119] R. Muksian and C. D. Nash Jr, "On frequency-dependent damping coefficients in lumped-parameter models of human beings," Journal of Biomechanics, vol. 9, pp. 339-342, 1976.
[120] N. J. Mansfield and J. M. Marshall, "Symptoms of musculoskeletal disorders in stage rally drivers and co-drivers," Br J Sports Med, vol. 35, pp. 314-20, Oct 2001.
[121] G. Legnani, et al., "A model of an electro-goniometer and its calibration for biomechanical applications," Medical Engineering & Physics, vol. 22, pp. 711-722, 2000.
[122] G. A. Mirka, "The quantification of EMG normalization error," Ergonomics, vol. 34, pp. 343-52, Mar 1991.
[123] J. M. Winters, "How detailed should muscle models be to understand multi-joint movement coordination?," Human Movement Science, vol. 14, pp. 401-442, 1995.
[124] J. M. Winters and L. Stark, "Muscle models: what is gained and what is lost by varying model complexity," Biol. Cybern., vol. 55, pp. 403-420, 1987.
[125] J. M. Winters and L. Stark, "Estimated mechanical properties of synergistic muscles involved in movements of a variety of human joints," J Biomech, vol. 21, pp. 1027-41, 1988.
[126] T. McMahon, Muscles, reflexes, and locomotion. Princeton, NJ: Princeton University Press, 1984.
[127] A. J. van den Bogert, et al., "Human muscle modelling from a user's perspective," J Electromyogr Kinesiol, vol. 8, pp. 119-24, Apr 1998.
[128] T. S. BUCHANAN, et al., "Estimation of Muscle Forces and Joint Moments Using a Forward-Inverse Dynamics Model," Medicine & Science in Sports & Exercise, vol. 37, pp. 1911-1916 10.1249/01.mss.0000176684.24008.6f, 2005.
[129] C. Ettore, "Hill-Based Model as a Myoprocessor for a Neural Controlled Powered Exoskeleton Arm -Parameters Optimization," in International Conference on Robotics and Automation, Barcelona, Spain, April 2005, 2005.
[130] A. Bergmark, "Stability of the lumbar spine: a study in mechanical engineering," Acta Orthopaedica Scandinavica, vol. 230, pp. 1-54, 1989.
[131] H. Broman, et al., "A mathematical model of the impact response of the seated subject," Med Eng Phys, vol. 18, pp. 410-9, 1996.
[132] J. Cholewicki, et al., "Postural control of trunk during unstable sitting," J Biomech, vol. 33, pp. 1733-1737, 2000.
[133] R. Bluthner, et al., "Examination of the myoelectric activity of back muscles during random vibration - methodical approach and first results," Clinical Biomechanics, vol. 16, pp. S25-S30, 2001.
[134] A. M. Rosen Jacob, "Modeling the Human Body/Seat System in a Vibration Environment," Journal of Biomechanical Engineering, vol. 125, 2003.

[135] G. S. Paddan and M. J. Griffin, "The transmission of translational seat vibration to the head--II. Horizontal seat vibration," J Biomech, vol. 21, pp. 199-206, 1988.
[136] G. R. Barnes and B. H. Rance, "Transmission of angular acceleration to the head in the seated human subject," Aerosp Med, vol. 45, pp. 411-6, Apr 1974.
[137] R. E. Seroussi, et al., "Trunk muscle electromyography and whole body vibration," Journal of Biomechanics, vol. 22, pp. 219-221, 223-229, 1989.